Solar Protection in Buildings

Part 2: 2000 - 2002

Editors
Maria Wall
Helena Bülow-Hübe

Division of Energy and Building Design
Department of Construction and Architecture
Lund Institute of Technology
Lund University, 2003
Report EBD-R--03/1

Lund University

Lund University, with eight faculties and a number of research centres and specialized institutes, is the largest establishment for research and higher education in Scandinavia. The main part of the University is situated in the small city of Lund which has about 101 000 inhabitants. A number of departments for research and education are, however, located in Malmö. Lund University was founded in 1666 and has today a total staff of 5 530 employees and 34 000 students attending 60 degree programmes and 850 subject courses offered by 89 departments.

Department of Construction and Architecture

The Department of Construction & Architecture is part of Lund Institute of Technology, the technical faculty of Lund University. The main mission of the Department of Construction & Architecture is to pursue research and education on topics related to the built environment. Some of the topics of interest are: restoration and maintenance of buildings, construction management, design processes, construction, energy efficiency, climatization and design of ventilation and heating systems, demolition, disposal and re-use of building materials.

These topics are treated from both a Swedish and an international perspective and collaboration between actors from mutidisciplinary fields of competence forms a particularly important aspect of research and education at the Department. The Department is divided into 6 sub-departments or divisions: Architectural Conservation & Restoration, Building Services, Computer Aided Architectural Design, Construction Management, Energy & Building Design, and Housing Development & Management.

Division of Energy and Building Design

Reducing environmental effects of construction and facility management is a central aim of society. Minimising the energy use is an important aspect of this aim. The recently established division of Energy and Building Design belongs to the department of Construction and Architecture at the Lund Institute of Technology in Sweden. The division has a focus on research in the fields of energy use, passive and active solar design, daylight utilisation and shading of buildings. Effects and requirements of occupants on thermal and visual comfort are an essential part of this work. Energy and Building Design also develops guidelines and methods for the planning process.

Solar Protection in Buildings

Part 2: 2000 – 2002

edited by:

Maria Wall
Helena Bülow-Hübe

in cooperation with:

Marie-Claude Dubois
Bengt Hellström
Håkan Håkansson
Björn Karlsson
Hasse Kvist
Urban Lundh

Key words

Solar protection, solar shading, windows, buildings, energy demand, heating, cooling, measurements, calorimetric, solar energy transmission, shading coefficient, calculation, design aid, solar simulator, comfort

Layout: Hans Follin, LTH, Lund
Cover Photo: Front: Grand Hotel, Lund. Maria Wall
Back: Ingvar Kamprad Design Centre, Lund. Helena Bülow-Hübe
Translation: L J Gruber BSc(Eng) CEng MICE MIStructE

Printed by KFS AB, Lund 2003

Report No EBD-R--03/1
Solar protection in buildings. Part 2, 2000 - 2002.
Department of Construction and Architecture, Lund University, Lund

ISSN 1651-8128
ISBN 91-85147-00-1

Lund University, Lund Institute of Technology
Department of Construction and Architecture
P.O. Box 118
SE-221 00 LUND
Sweden

Telephone: +46 46 - 222 73 52
Telefax: +46 46 - 222 47 19
E-mail: ebd@ebd.lth.se
Home page: www.byggark.lth.se

Research project home page: http://www.byggark.lth.se/shade/shade_home.htm

Abstract

Commercial buildings with large glazed surfaces may easily suffer from overheating problems or large peak cooling loads. Solar shading devices can significantly reduce these cooling loads, improve thermal comfort and reduce potential glare problems. Also in moderately glazed buildings, shading devices may to a great extent improve conditions. Due to lack of relevant data as to how well sunshades protect buildings, the Solar Shading Project at Lund University was initiated. Phase 1 of the project focused on exterior shading devices, and was completed in 1999. Now phase 2 is completed and includes both interpane and interior devices.

The work consists of measurements of the performance of a large selection of solar shadings available on today's market, in order to provide comparable g-values measured under similar conditions. The work also includes development of detailed calculation models, and development of ParaSol, a user-friendly design tool. Parametric studies of energy use in offices and studies of the effect on daylight quality were also carried out but reported earlier in the project.

The developed detailed calculation models include both interpane and internal shading devices. Calculation models for external shading devices were developed during the first phase of the project.

Results from outdoor measurements in Lund, Sweden, showed on average 4-5% higher total transmittance (g-value) than results from the developed calculation models. The average g-value for each group of measured shading devices was 0.3 for external products, 0.5 for interpane products and 0.6 for internal products. Thus, on average, external products are twice as good as internal products in reducing peak cooling loads. However, note that other aspects, such as daylight, are also very important. Some products yielding low g-values admit almost no daylight into the room and totally obstruct the view out, two of the main reasons for having a window.

A solar simulator for measurements under standard conditions was developed. This enables study of conditions different from those at the latitude of Lund. Extensive developments have been carried out in order

to achieve reliable measuring methods. The shading devices measured in the solar laboratory showed reasonable agreement with the developed calculation models. The differences were in general within ± 4%.

Further developments and validations need to be carried out especially regarding convective heat transfer, which could have a large influence on both measurements and calculation results for internal shading devices.

As a design aid the computer tool ParaSol has been developed. With this tool it is possible to determine the solar transmittance properties of arbitrary combinations of glazing systems and shading devices. It also enables simulation of peak heating and cooling loads and annual heating and cooling demands for an office module. Thermal comfort can also be studied. The program handles exterior shading devices in combination with internal or interpane sunshades. Different strategies for controlling sunshades as well as an air conditioning unit to heat or cool the inlet air are also included.

Contents

Acknowledgements

This research was conducted with grants from the Swedish Research Council for Environment, Agricultural Sciences and Spatial Planning (FORMAS), The Swedish Energy Agency (STEM), and the Swedish Solar Control Association (SSF). We are very grateful for their support.

We also wish to thank the reference group for their cooperation, which was completely altruistic since we had no finance available for their assistance. The reference group consisted of Conny Rolén, FORMAS; Peter Pertola/Tomas Berggren, STEM; Siv Averud/Mattias Klasson, SSF; Marie Hult/Marja Lundgren, White Arkitekter; Martin Storm, Swedish Board of Housing, Building and Planning; Kenneth Falck, Norwegian Solar Protection Association; Ida Bryn, Erichsen & Horgen AS, Norway and Karsten Duer/Svend Svendsen, DTU, Denmark.

Apart from the above mentioned, we would also like to thank the company Bengt Dahlgren AB for the good advice they gave regarding the ParaSol development. Special thanks also to architect Andreas Fieber, Energy and Building Design, who helped with the illustrations for the ParaSol software.

1 Introduction

Commercial buildings with large glazed surfaces may easily suffer from overheating problems or large peak cooling loads. Solar shading devices can significantly reduce these cooling loads, improve thermal comfort and also reduce potential glare problems. Due to lack of relevant data as to how well sunshades protect buildings against unwanted insolation, the solar shading project was initiated in 1997 at Lund University, Lund, Sweden.

Phase 1 of the Solar Shading Project included only exterior shading devices, and was completed in 1999. A first version of the software ParaSol for exterior shading devices was released in 2000. A full report on Phase 1 activities is found in (Wall & Bülow-Hübe, 2001). Phase 2 was completed in 2002 and included both interpane and interior devices. This report constitutes the final report on the whole project.

The work within the Solar shading project consisted of a number of "work packages" which are: measurements of the performance of sunshades; development of calculation models; development of a user-friendly software tool, ParaSol; parametric studies of energy use in offices; and studies of the effect on daylight quality. Figure 1.1 illustrates the work packages and the links between them.

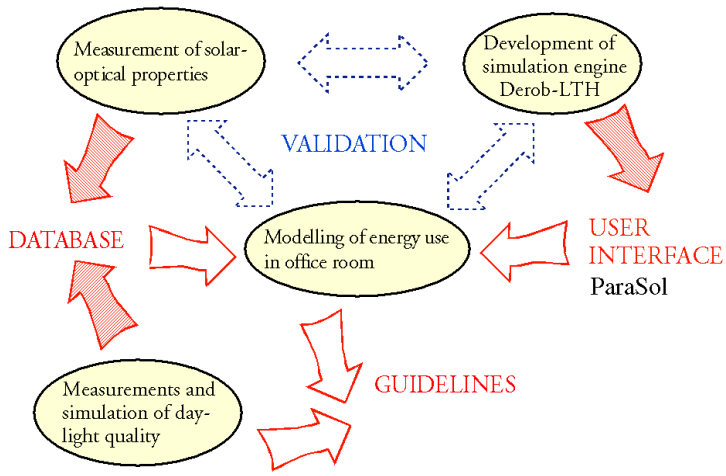

Figure 1.1 Overview of the Solar Shading Project.

One of the first goals of the project was to measure the solar transmission properties of a large selection of solar shadings available on today's market, in order to provide comparable *g*-values measured under similar conditions. The project has specifically targeted common types of shading devices which are applicable both in new construction and in refurbishing. The products have been divided into three groups: external shading devices, devices between panes (interpane devices), and internal shading devices. Results from the extensive measurement programme are given in Chapter 2.

During the project a solar simulator for measurements during standard conditions has been developed. An indoor measurement facility also provides freedom from the vicissitudes of the weather, which in the climate of Lund can make you wait long for a sunny day… Results from the extensive calibration work and measurements are given in Chapter 3.

In order to disseminate the knowledge gained to a broader audience, i.e. architects, HVAC-engineers and the solar shading industry, the computer tool ParaSol has been developed within the project. With this tool it is possible to determine the solar transmittance properties of arbitrary combinations of glazing systems and shading devices. It also enables the user to simulate peak heating and cooling loads and annual heating and cooling demands for an office module with one wall and one window facing the external climate. The program can handle exterior shading devices in combination with internal or interpane sunshades. The math-

ematical models which needed to be developed and implemented in the simulation engine are described in Chapter 4, while the tool itself is described in Chapter 5.

Comparisons between measurements (both outdoors in the twin-boxes and indoors in the solar simulator) and simulations are discussed in chapter 6.

The daylight issues which were included in the second phase of the project have been reported earlier, and are therefore not included in this report. See Dubois (2001, a, b, c) and Bülow-Hübe (2001).

Guidelines in Swedish will be developed as a separate project during 2003, in collaboration with architects and consultants.

2 Outdoor measurements

Helena Bülow-Hübe and Urban Lundh

A shorter version of this was presented at EPIC 2002 AIVC, Lyon 23-26 Oct 2002 (Bülow-Hübe, H. & Lundh, U., 2002)

2.1 Introduction

One aim of the Solar Shading project has been to measure the solar transmission properties of a large selection of solar shading devices available on today's market, in order to provide comparable g-values measured under similar conditions. The measurements have been divided into three groups: external shading devices, devices between panes (interpane devices), and internal shading devices. Phase 1 of the Solar Shading Project included measurements on exterior shading devices only, and was completed in 1999. A full report on Phase One activities is found in (Wall & Bülow-Hübe, 2001). Phase 2 was completed in 2002 and included both interpane and interior devices. This chapter summarizes Phase 1 and Phase 2 field measurement results.

2.2 Method

The measurements were performed in two well insulated boxes, placed in a room at about 20°C. The boxes had a double glazed unit (1.17 m × 1.17 m) which was in contact with the sun and the outdoor climate through a window in the south wall of the building, see Figures. 2.1 & 2.2.

A sealed insulated glass unit (4 mm – 12 mm – 4 mm, clear float) was used for external and internal shading products. For interpane products a double-glazed unit was used (4 mm – 30 mm – 4 mm, clear float), which corresponds to a coupled window, typical of older Swedish buildings. The boxes were placed in Lund at 55.7°N.

Figure 2.1 *Twin-boxes equipped with Italian awnings (left), and external venetian blinds (right).*

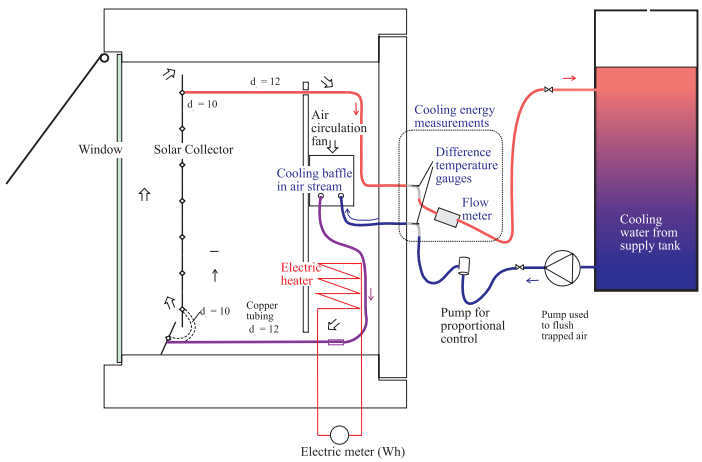

Figure 2.2 *Hot box and measuring system.*

A solar absorber (Sunstrip fins) was placed behind the window. The air between the absorber and the window, as well as the water in the pipes of the absorber, was temperature controlled with cooling and electrical heating. The air was held at around 20°C, approximately the same as for the room where the boxes were located, and was blown along the absorber to reduce the heat resistance between the air and the absorber. For the total

solar energy transmittance, the temperature difference between the box and the outdoor air, multiplied by the window U-value (from night measurements), was used. The heat balance for the box is:

$$Q_{sun} = Q_{cool} - Q_{el.heat} + Q_{window} + Q_{room} + Q_{capacity} \qquad \text{(Eqn. 2.1)}$$

where Q_{sun} is the total transmitted solar energy, Q_{cool} and $Q_{el.heat}$ are the measured cooling and heating energies, Q_{window} is the measured and calculated heat losses through the window, Q_{room} is the measured and calculated heat losses from the box to the room, and finally $Q_{capacity}$ is a correction term for the heat capacity of the box with respect to changes in the box temperature during the measurement period.

During the night Q_{sun} is zero. This is used to calibrate the boxes. Equation 2.1 is used to calculate Q_{sun}, the total solar energy transmitted through sunshade and window. The total solar transmittance of this system is denoted g_{system}, which is calculated by dividing Q_{sun} by the product of global solar radiation on the window, I_G, and the area of the window, A_w:

$$g_{system} = \frac{Q_{sun}}{I_G \cdot A_w} \qquad \text{(Eqn. 2.2)}$$

The solar energy transmittance for a certain sunshade can be calculated in different ways. The simplest way is to assume that the total transmittance is the product of the transmittance for the different parts of the system, and thus solving the g-value of the sunshade as:

$$g_{sunshade} = \frac{g_{system}}{g_{window}} \approx \quad \text{“shading coefficient”} \qquad \text{(Eqn. 2.3)}$$

As the window is double glazed, $g_{sunshade}$ is the same as the shading coefficient which is sometimes used in connection with sunshades. The $g_{sunshade}$-value depends slightly on the type of window used. In Sweden, a double pane window is normally used as a reference for the shading coefficient. However, some countries use a single clear glazing as reference. The *g*-value is therefore a more straightforward measure of the solar transmittance.

The transmittance of the window, g_{window}, can be either measured or calculated. It is easiest to use one box to measure the transmittance of the sunshade and the other to measure the transmittance of only the window. This is particularly advantageous when there is cloud or haze which makes the solar radiation vary at random. All the results set out below are based

on 5 minute means which have been smoothed with a moving average over 50 minutes. In all cases, the global solar radiation on the facade was greater than 100 W/m^2.

The values reported below all apply to the hour with the highest solar altitude, i.e. at around 12 o'clock standard time. The estimated maximum measuring error was ± 5% of the calculated transmittance, but was not less than ± 1%. However, the measurements have been performed throughout the year, and the effect of varying solar altitudes has not been corrected for.

2.2.1 External shading devices

Measurements reported here relate to: Two awnings, two Italian awnings, two external venetian blinds, three screen fabrics, one horizontal slatted baffle, and a number of solar control films laminated on the external side of the glazing system. The two awnings (and the Italian awnings) were of the same type and geometry, but one had a light coloured fabric (off-white) and the other a dark blue fabric. The awnings were tested in two positions, fully and partially extended. The external venetian blinds were silver coloured with slats 50 and 80 mm wide . Both blinds were tested fully lowered with the slats in two positions: horizontal and with slats at 45° to the window. More details about the products and the measurements are given in (Wall & Bülow-Hübe, 2001).

2.2.2 Interpane shading devices

The shading devices mounted between two clear panes were: venetian blinds (28 mm metal slats), two pleated curtains, two roller blinds (Texienne) and one screen fabric. Three different blind colours (blue, white and metal) and also several slat angles were studied. The two roller curtains tested were both of a light colour.

2.2.3 Internal shading devices

The internal shading devices were mounted close to the inner side of the window. The products tested were venetian blinds, pleated curtains, roller blinds (both fabrics and solar control films), one screen fabric and several solar control films applied directly on the inner pane. Several of the internal shading devices were identical to those measured between panes. The reflectance and transmittance of the fabrics and films were also measured with a spectrophotometer at Uppsala University.

2.3 Results

Results from all measurements are presented in three tables: Table 2.1 for external, Table 2.2 for interpane and Table 2.3 for internal products respectively. The tables show measured values for g_{window} and g_{system}, evaluated at 12 o'clock on sunny days, and the calculated value $g_{sunshade}$. In order to get an indication of the corresponding angle of incidence, or solar altitude, the month when the measurement took place is also noted.

Figure 2.3 summarizes the results of the g-value measurements for the three product groups external, interpane and internal shading devices. Although a large variation within each group is evident, external products generally have lower g-values than interpane and internal products. The regression line indicates that the average g-value ($g_{sunshade}$) is 0.29 for external, 0.48 for interpane and 0.62 for internal shading devices.

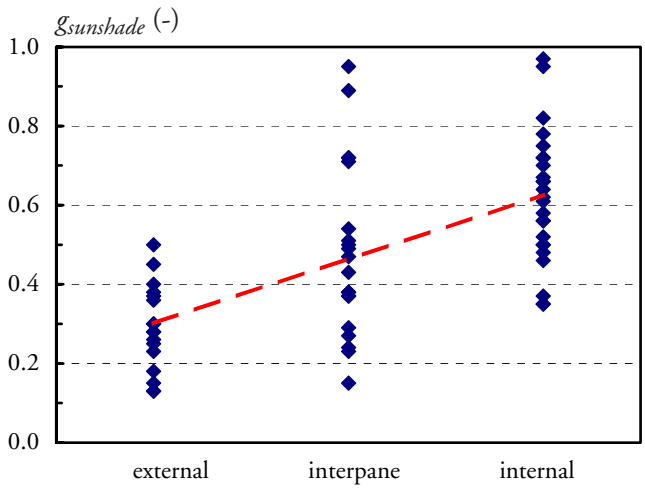

Figure 2.3 *Summary of all measurements of $g_{sunshade}$ for external, interpane and internal shading devices respectively.*

Since some of the products are applicable as both interpane and internal devices, ten of them were measured in both positions, see Figure 2.4. For these products, $g_{sunshade}$ is on average 0.23 units lower for interpane than for internal placement. Some further comparisons with simulations and solar simulator measurements are presented in chapter 6.

Table 2.1 Field measurements, external solar shading devices.

Product (type and name)	$g_{sunshade}$ (-)	g_{window} (-)	g_{system} (-)	Measuring month
Awnings				
Dark blue (NCS 7030-R70B), fully extended	0.18	(0.67)	0.12	June
Dark blue (NCS 7030-R70B), partially extended	0.30	(0.60)	0.18	June
Light beige (NCS 0502-Y), fully extended	0.45	(0.58)	0.26	June
Light beige (NCS 0502-Y), partially extended	0.40	(0.58)	0.23	June
Italian awnings				
Dark blue (NCS 7030-R70B), fully extended	0.13	(0.54)	0.07	September
Dark blue (NCS 7030-R70B), partially extended	0.70*	(0.59*)	0.41*	September
Light beige (NCS 0502-Y), fully extended	0.30	(0.57)	0.17	September
Light beige (NCS 0502-Y), partially extended	0.75*	(0.57*)	0.43*	September
External venetian blinds				
Width 50 mm, slat angle 0°	0.28	(0.61)	0.17	July
Width 50 mm, slat angle 45°	0.15	(0.53)	0.08	August
Width 80 mm, slat angle 0°	0.25	(0.56)	0.14	July
Width 80 mm, slat angle 45°	0.13	(0.54)	0.07	August
Fabric screens				
Hexcel 21136 Satine Blanc 101	0.27*	(0.67*)	0.18*	April
Hexcel 21136 Satine Sable 109	0.13*	(0.69*)	0.09*	March
Ferrari Soltis 92 1045	0.04*	(0.63*)	0.02*	May
Horizontal slatted baffle	0.23	(0.61)	0.14	May
Roller shutters				
Type 1			0.03	June
Type 2			0.03	June
Solar control films (on glass)				
Type 1	0.38	(0.66)	0.25	July
Type 2	0.28	(0.71)	0.20	August
Sun stop N20B KYNAR PS	0.36	0.73	0.26	October
Sun stop R20 KYNAR PS	0.26	0.73	0.19	October
Sun stop R30 PS XT	0.37	0.71	0.26	January
Sun stop XIR PS SR	0.50	0.73	0.37	March

* only primary transmission.

(0.xx) calculated value, may be uncertain since small values lead to large errors

Table 2.2 Field measurements, solar shading devices between panes

Product (type and name)	$g_{sunshade}$ (-)	g_{window} (-)	g_{system} (-)	Measuring month
Venetian blinds				
Blue, slat angle 0°	0.72	0.74	0.53	March
Blue, slat angle 45°	0.49	0.78	0.38	February
Blue, slat angle 80°	0.43	0.75	0.32	February
White, slat angle 0°	0.72	0.75	0.54	March
White, slat angle 45°	0.38	0.74	0.28	March
White, slat angle 80°	0.24	0.73	0.18	March
Metallic, slat angle -80°	0.37	0.76	0.28	September
Metallic, slat angle -60°	0.54	0.78	0.42	February
Metallic, slat angle -45°	0.89	0.76	0.68	September
Metallic, slat angle -30°	0.95	0.77	0.73	September
Metallic, slat angle 0°	0.71	0.72	0.51	August
Metallic, slat angle 30°	0.51	0.75	0.38	September
Metallic, slat angle 45°	0.37	0.68	0.25	August
Metallic, slat angle 60°	0.29	0.77	0.22	September
Metallic, slat angle 80°	0.23	0.77	0.18	September
Fabric screen				
Hexcel 21136 Satine Sable 109	0.27	0.73	0.20	March
Pleated curtains				
Off white	0.50	0.68	0.34	May
Metallized	0.38	0.68	0.26	May
Roller blinds (Texienne)*				
H925-90, white/white (dense), double coated	0.15	0.68	0.10	May

* The fabric colour is indicated as follows: ”room facing side”/”outdoor facing side” whenever the fabric had two distinct sides. A visual characterisation of the fabric is given in parenthesis (e.g. dense).
H = Haglunds

Table 2.3 Field measurements, internal solar shading devices

Product (type and name)	$g_{sunshade}$ (-)	g_{window} (-)	g_{system} (-)	Measuring month
Venetian blinds				
Blue, slat angle 0°	0.97	0.73	0.71	November
Blue, slat angle 45°	0.75	0.66	0.50	June
White, slat angle 0°	0.82	0.68	0.56	July
White, slat angle 45°	0.66	0.68	0.45	July
White, slat angle 80°	0.50	0.74	0.37	October
Metallic, slat angle 0°	0.95	0.68	0.65	August
Metallic, slat angle 45°	0.58	0.69	0.40	August
Pleated curtains				
Off white	0.61	0.74	0.45	April
Metallized	0.67	0.72	0.48	May
Fabric screen				
Hexcel 21136 Satine Sable 109	0.50	0.71	0.36	February
Roller blinds*				
LS Ombra, white/metal (semi transparent)	0.64	0.70	0.45	May
LS Optic, white/metal (dense)	0.37	0.70	0.26	May
H542-98, black/metal (semi transparent)	0.72	0.68	0.49	June
H981-95, grey/silver (rather dense)	0.52	0.67	0.34	June
H925-90, white/white (dense), double coated	0.35	0.68	0.24	July
H927-95, grey-white patterned/white (dense)	0.35	0.66	0.23	July
H500-90, white (rather thin), uncoated	0.56	0.66	0.37	July
H500-54, dark (rather thin), uncoated	0.78	0.67	0.53	July
Solar control film on glass				
Sun stop R 20 PS SR	0.48	0.73	0.35	November
Sun stop R 30 PS XT	0.62	0.69	0.43	May
Sun stop XIR PS SR	0.72	0.75	0.54	March
Solar control film – roller blinds				
Sun stop Roller blind Gold	0.56	0.71	0.40	March
Sun stop Roller blind Bronze	0.70	0.70	0.48	March
H991-91, Roller blind Silver grey	0.46	0.76	0.35	November
H992-25, Roller blind Bronze	0.66	0.76	0.50	November

* The fabric colour is indicated as follows: ”room facing side”/”outdoor facing side” whenever the fabric had two distinct sides. A visual characterisation of the fabric is given in parenthesis (e.g. dense).
H = Haglunds LS = Ludvig Svensson

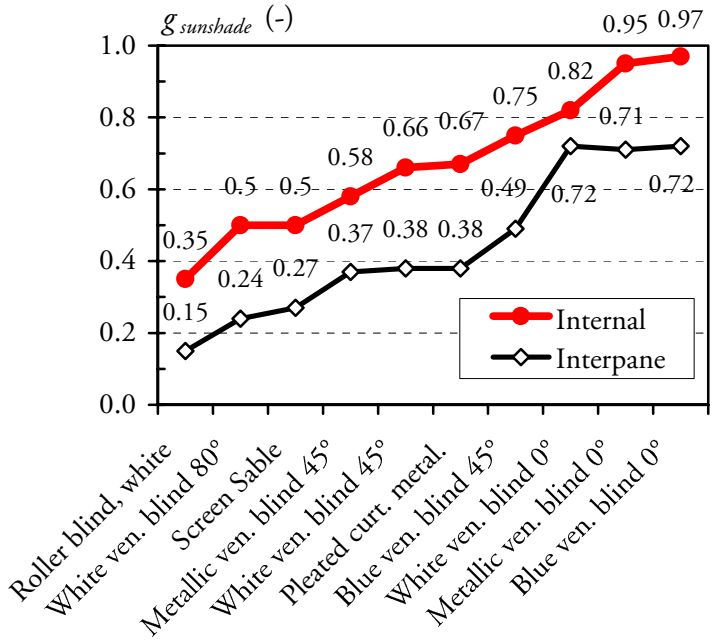

Figure 2.4 *Effect of position of shading device on $g_{sunshade}$ for some interpane and internal products of various colours and slat angles.*

The effect of slat angle and colour on $g_{sunshade}$ for venetian blinds is shown in Figures 2.5a and b. Both figures show a strong dependence on the slat angle, while the effect of the colour is much smaller. The difference seen between colours at equal slat angles may also be due to slightly varying solar altitudes, since the measurements were performed throughout the year.

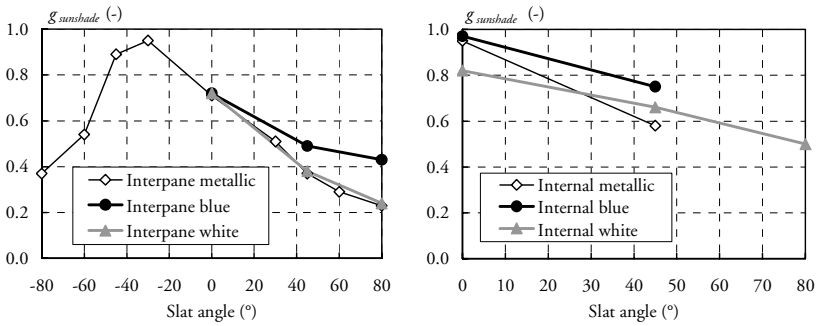

Figure 2.5a, b *Effect of slat angle on $g_{sunshade}$ for venetian blinds mounted between panes (a, left) and internally mounted (b, right). Zero degrees is equal to horizontal slats, 80° is fully closed, and a negative angle means that the outer parts of the slats are turned upwards.*

In order to obtain a low $g_{sunshade}$ for internal solar shading devices, it is important that the fabric used has a light colour, i.e. a high solar reflectance, R_{sol}. This is demonstrated for six roller blind fabrics in Figure 2.6. However, it must be kept in mind that the two products with the lowest g-values also have a very low visual transmittance, T_{vis}, of the order of 3-4 per cent, thus admitting very little daylight to the room behind. The product yielding the highest $g_{sunshade}$ (a dark blue roller curtain) also admits very little daylight to the room (T_{vis} < 1%), see Table 2.4. Here, the high g-value is a result of a high solar absorptance (about 80%). The product which provided the most daylight was a white roller curtain (T_{vis} = 38%), and its $g_{sunshade}$ was 0.56.

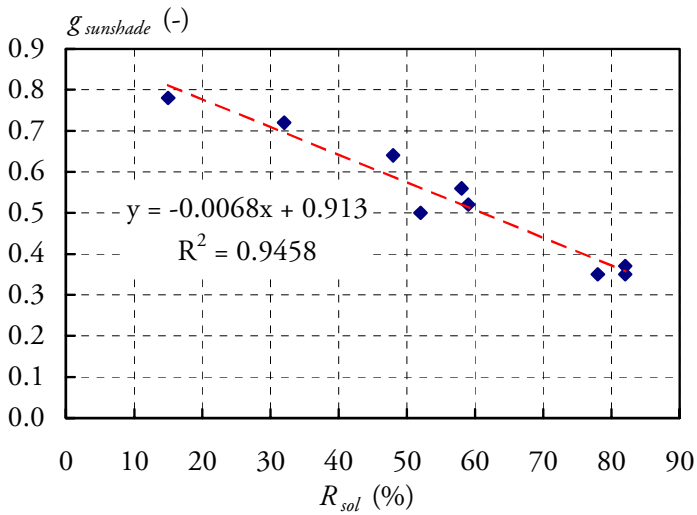

Figure 2.6 *Relationship between $g_{sunshade}$ and solar reflectance, R_{sol}, of some internally mounted roller curtains.*

Table 2.4 Results from optical measurements of some fabrics. T_{vis} is the visual transmittance (380 - 780 nm), T_{sol} the solar transmittance (300 - 2500 nm), R_{sol} the solar reflectance. The g-value of the sunshade when internally mounted is also shown.

Product	T_{vis}	T_{sol}	R_{sol}	$g_{sunshade}$, internally mounted
LS Ombra, white thread	0.40	0.41	0.48	0.64
LS Optic, white thread	0.04	0.04	0.82	0.37
H 981-95	0.03	0.05	0.59	0.52
H 542-98	0.18	0.19	0.32	0.72
H 925-90	0.04	0.06	0.82	0.35
H 927-95	0.03	0.05	0.78	0.35
H 500-90	0.37	0.37	0.58	0.56
H 500-54	0.00	0.04	0.15	0.78
Screen Hexcel Sable	0.11	0.12	0.52	0.50

2.4 Discussion and conclusions

Naturally, external sunshades have a much greater potential to reduce cooling loads and unwanted solar gains, since the absorbed heat is mostly dissipated to the outdoor air. For internal products it is essential to try to reflect the short wave solar radiation, since the heat absorbed in the sunshade contributes to room overheating. This is quite elementary physics, and these results are also confirmed by the measurements. However, depending on colour, slat angle position etc, there is a large variation in measured g-values within each product group of external, interpane and internal sunshades. For internal shading devices it is demonstrated that the reflectance of the fabric is the most important parameter in obtaining low g-values. This is contrary to external shading devices where we have previously shown that for example dark awnings (with low reflectance and high absorptance) provide lower g-values than light ones (Wall & Bülow-Hübe, 2001). In selecting shading products one should also pay attention to the transmitted daylight and the effect on the view out. The internal products yielding low g-values admit almost no daylight into the room, and totally obstruct the view out, two of the main reasons for having a window.

2.5 Summary

Solar shading devices can significantly improve thermal comfort and reduce cooling loads and potential glare problems in highly glazed buildings. An extensive measurement programme covering external shading devices, products placed between two panes (interpane devices), and internal shading devices has been conducted between 1997 and 2002. Measurements of the total solar energy transmittance (g-value) have been performed using a double hot-box arrangement placed in a real climate. One box was equipped with the solar shading device, while the box with a bare window was used as a reference. Thus, the g-value of each product ($g_{sunshade}$) has been estimated as g_{system}/g_{window}.

In general, external shading devices have a larger potential to reduce cooling loads since the absorbed solar heat is mostly dissipated to the outdoor air. Interpane products have a slightly higher g-value and internal products show the highest g-values. This is demonstrated within the project, although the variation in each group is large. The average g-value within each group ($g_{sunshade}$) was 0.3 for external products, 0.5 for

interpane products and 0.6 for internal products. Thus, on average, external products are twice as good as internal products in reducing peak cooling loads.

3 Solar laboratory

3.1 Objective and features

A solar simulation installation has been constructed so that solar transmission for sunshades, windows and solar heating components may be measured in a more standardized and consistent manner. Measurements can be made for different angles of incidence and not only for those that are encountered outdoors in Lund. The maximum obtainable solar altitude is 72°, see Figure 3.1.

It is a special feature of this solar simulation installation that the beam of light is as parallel as possible. One of the reasons for this is to make it possible for measurements to be made on sunshades with marked angle dependent characteristics like awnings and venetian blinds. Concentrating solar collectors are also distinctly angle dependent.

Solar simulation is carried out at full scale to make conditions as realistic as possible. In any case it is almost impossible for most sunshades to be scaled down.

3.2 Description of the solar simulator components

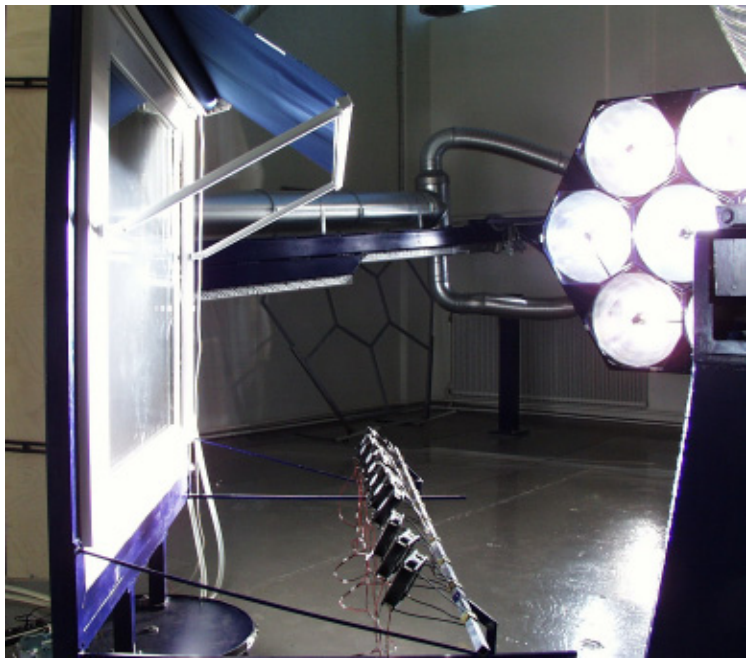

Figure 3.1 *Solar laboratory with lamp cluster and box for calorimeter measurement on window with sunshade.*

3.2.1 Generation of solar angles

Making the object of measurement rotatable around a vertical axis generates the horizontal angle between the sun and the façade. Mounting the entire lamp arrangement on two moving arms generates the angle of the sun above the horizon, the solar altitude. Both these rotations are centred around a point in the centre of the window opening. Since the studied window is kept vertical at all times, the air flow patterns at boundary layers and gaps are not changed in comparison with the window that is simulated.

3.2.2 The reflector arrangement

The simulator light source is based on seven parabolic reflectors in a honeycomb pattern. The diameter of the reflectors is 0.8 m. The lamps are fitted with a small reflector in the centre, Figure 3.2. The function of this small reflector is to throw a large proportion of the light from the solid angle to the front, which is not covered by the large reflector, back into focus in the lamp so it can be utilized by the main reflector and in this way be made parallel.

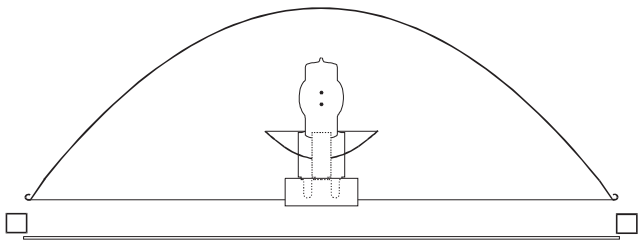

Figure 3.2 *Cross-section of a main parabolic reflector including the lamp with a small reflector.*

3.2.3 Lamps

The lamps are 2.5 kW Philips discharge lamps. This model is called MSR by the manufacturer, which denotes Metal halide Short arch Rare earth. The current in the lamps is controlled by inductive ballast and a thyristor unit.

The front of the lamp arrangement is covered with panes of UV-reducing glass to remove harmful radiation. These glass panes also assist in directing the hot air from the lamps to be evacuated with a fan through a duct system.

3.2.4 Calorimeter box

The exploded drawing in Figure 3.3 shows the object of measurement mounted on a calorimeter box. The calorimeter plate is placed close to the window for tests on external and interpane sunshades. The measuring situation is well defined since there are no secondary uncooled surfaces that are heated to excessive temperatures. For measurements on interior sunshades, the calorimeter plate can be retracted.

The calorimeter box has cores of extruded EPX styrofoam plastic. The rear cover is a sandwich construction with a surface layer of 0.5 mm aluminium sheeting. The inner sheet covers only the area that abuts on

the inside volume so as to avoid thermal bridges. The front surface of the main frame of the box consists of 10 mm plywood. The inner surface is made of only 3 mm plywood to keep down the thermal mass. The window is held in position by a wooden frame at the front. This frame makes the depth of the recess at the front 12 mm. The frame is screwed to the box by reinforcing fixings of Ø 12 wooden blocks that are glued to the plastic core. A frame of rectangular steel hollow section reinforces the outer edge of the box. This reinforcing frame is in its turn fixed to the rotatable support.

In the walls of the box, thermopiles are placed to measure the flow of heat due to the difference in temperature between the inside of the box and the surroundings. The pairs of thermocouples are spread out in positions representative of their individual part of the heat flow.

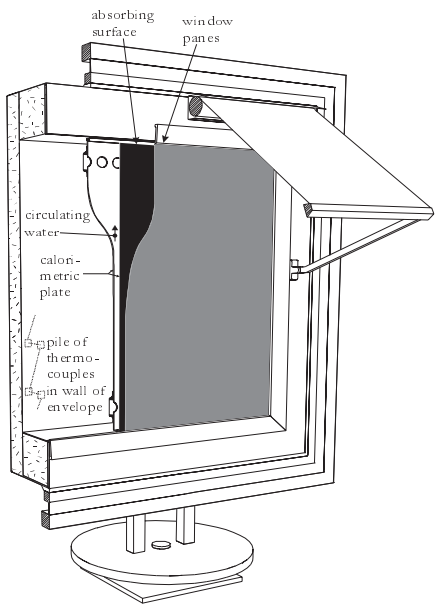

Figure 3.3 *Exploded drawing of calorimeter box with calorimeter plate, window and sunshade.*

3.2.5 Calorimeter plate

In the basic measuring arrangement , the calorimeter plate is placed only a short distance away from the inner pane of the window. In this configuration the gap of stagnant air represents the convective heat transfer between a window and a room. The distance used is 8 mm and it is therefore important that the front surface of the calorimeter plate is flat.

The first calorimeter plate used was made of two 1 mm thick aluminium plates glued together with acrylic resin with spacers of 3 × 20 mm aluminium bars at a distance of 200 mm. Since the whole plate had to be glued in one stage the mounting pressure was distributed over the whole plate after the second aluminium plate was applied. The resin was probably not viscous enough to match the pressure used (totalling 200 kg) to obtain a good quality result, since the spacers proved not to be fully covered by resin. This could be the reason for some later failures. Another reason could be corrosion of the aluminium by the water. Corrosion additive for automotive purposes was later used.

Later, calorimeter plates made of glass panes were used. Satisfactory bonding was achieved by using silicon sealant of the viscous type. An extra advantage of using a transparent material is that the glue adhesion can be inspected and the removal of trapped air can be observed.

The calorimeter plate used most often was made from two 4 mm glass panes. A lighter version was also made with only 1.7 mm thick panes and a 2 mm gap. This plate contained 4 l of water. Not surprisingly this delicate plate broke but only after more than 120 hours of use and gave valuable information about the performance of the temperature control. The spacing strips of glass were 12 mm wide and placed 110 mm apart. The spacing strips and the seal at the edge of the plate takes up about 10% of the area of the two types of glass plates, and the heat transfer for glass is not so high. Therefore the temperature is locally higher at this part of the calorimeter plate on exposure. This results in an unnecessarily high average temperature at the surface and a time delay of the measured effect.

Based on the experience gained, a well functioning calorimeter plate with a compromise between stiffness, heat transfer and corrosion could be as follows: A glass pane for stiffness and flatness covered on the front side by a relatively thin copper plate with thin spacers of copper.

The exit on the top of the plate is mounted in such a way as to give the water sufficient speed to carry away trapped air. In a wide tube with low flow rate, air and water have a tendency to separate . A hose of 16 mm inner diameter proved not too wide to carry away entrained?? air downwards at the used water flow of 0.08 l/s. The front absorbing surface is spray-painted with a (heat-resistant) matt, black paint from Silpoxkemi AS, Denmark.

3.2.6 Cooling arrangement

A stainless storage tank of 315 l volume is used to provide cooling water of stable temperature. A compressor with a coaxial evaporator of 2 kW rating is used. A pump with filter forces water through the evaporator. The evaporator is fitted with a frost protection device. The warmer water from the calorimeter plate is discharged at the top of the tank to facilitate stratification. This warmer water is gradually mixed with the rest of the volume by the circulation pump. The inlets and outlets are separate for the compressor loop and the loop to the calorimeter plate to avoid disturbances to the control that operates with small pressure differences. The cooling tank is positioned lower than the calorimeter plate to avoid buoyancy-driven unintended circulation.

The temperature difference between the on and off states of the cooling compressor is kept very small to avoid disturbances to the temperature control of the calorimeter plate. The control switch for the compressor did not allow a smaller difference of the setting than 1°C between on and off. A smaller temperature difference is achieved by placing a small heater close to the thermostat probe. The heater is on when the compressor is off.

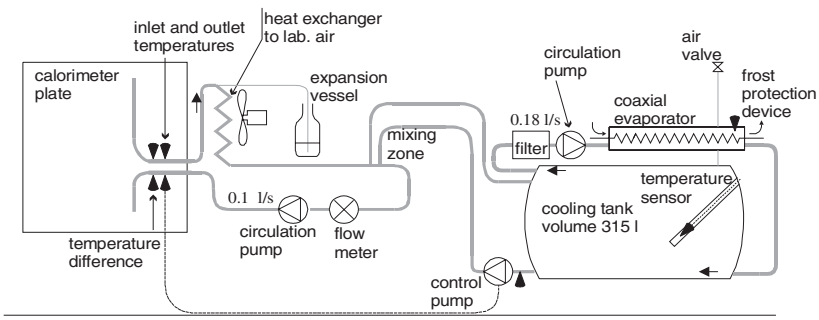

Figure 3.4 Layout of cooling arrangement.

3.2.7 Simulation of surface convective heat transfer

For tests on exterior and interpane sunshades the calorimeter plate is normally positioned 8 mm behind the rear pane. In this narrow gap the air is basically stagnant and has a convective heat transfer corresponding to a value usually assumed for an internal surface.

The convective heat transfer between a room and an inside flat sunshade, for instance a curtain, can in the same way be simulated by placing the calorimeter plate 8 mm behind the curtain. With such an arrangement, the volume between the curtain and the rear pane becomes closed. Consequently only an inside sunshade that has a tight fit to the window can be simulated with this arrangement.

In order to simulate the exterior convective heat transfer, ten small axial fans are mounted on a bar in front of the window. The row of fans is placed sufficiently low not to shade the window. The arrangement is seen in Figure 3.1. The fan motors are brushless DC motors, which can be controlled collectively by varying the power supply. The nominal rating of a fan is 24 V 5 W, 170 m^3/h. Normally 12 V is used.

Tests to determine the external convective heat transfer on the window were conducted under dark conditions and at small excess temperatures. A single pane was used. The heat flow through the pane was calculated from the temperature difference between the calorimeter plate and the glass pane. With this heat flow and the temperature difference between the window and the laboratory air, the external convective heat transfer coefficient was estimated.

For the normal 12 V setting for the fans a convective heat transfer coefficient, h_c = 10 W/(m^2 K), was calculated. An increased power supply to the fans of 24 V resulted in a surprisingly small difference, h_c = 13 W/(m^2 K).

In the ParaSol simulations, the value h_c = 15 W/(m^2 K) is used. In the ParaSol calculation of a standardized g-value at normal incidence the value h_c = 8 W/(m^2 K) is used, while for the U-value, h_c = 15 W/(m^2 K) is used. The last two values are taken from a draft for the international standard ISO/DIS 15099.

A rather low convective heat transfer coefficient is normally assumed for g-value estimates to enable them to be used for peak cooling load purposes. For U-value calculation purposes under dark conditions, the convective heat transfer coefficient is normally assumed substantially higher, to be used for estimating peak heating loads.

A test without the fans was also conducted. This gave a convective heat transfer coefficient, h_c = 3.9 W/(m^2 K). The temperature difference, DT, was 3.2°C. One rough estimate of the heat transfer coefficient for natural convection for a vertical wall in a normal room is $h_c = C \cdot (DT)^{0.25}$, C = 2. The measured value gives C = 2.9. This value is slightly high, but the laboratory had some circulating air from ventilation during the measurement.

In 3.3.9 a number of measurements of the influence on g-values due to wind on external sunshades are shown.

3.3 Measuring procedures and calibration

3.3.1 Temperature control

Temperatures of the water at the inlet and the outlet of the calorimeter plate are measured with fast thermocouple sensors. The lengths of their terminals are adjusted so that an equal resistance is attained. It is then possible to get an average temperature reading between the two by connecting them in parallel. If this average temperature is controlled to be constant, the disturbance due to the thermal inertia of the calorimeter plate is equal to zero. A slightly better result with less oscillation was achieved by controlling the inlet temperature only. In the later tests, control of the inlet temperature was used.

A control flow with cooling water is regulated by a pump and mixed into the loop of circulating water in the calorimeter plate. A direct current motor by magneto coupling powers the pump. In principle, the rate of water flow varies linearly with the voltage applied to the motor. One consideration is that the connection to the loop must be such that the high flow rate through the calorimeter plate does not induce flow in the control flow.

The control works according to the PID-principle. An accurate temperature control gives the opportunity to reduce the duration of the test, as less averaging time is needed for reducing the influence from oscillations.

The well-insulated box with its double pane window has a relatively long time constant for passive thermal equalization of a temperature difference to the surroundings. If a large flow of cooling water is circulated to the surroundings, it gives a much shorter time constant because the flow results in a higher thermal conductance. Ideally, the PID-parameters should be changed over the duration of a test to adjust to large variations in the control flow. One way to get a higher conductance to the surrounding air is to mount an external heat exchanger in the circulation loop in the box. Such a heat exchanger also reduces the effect of a disturbance which can reappear periodically in the circulation loop. Such a heat exchanger has been tested as is shown in Figure 3.4. A radiator from a car with an integral fan was used. A better control with smaller oscillations was achieved, especially at the start of a test and at high angles of incidence when only a small cooling control flow is needed. The effect of the heat exchanger can largely be bypassed by just shutting off the fan.

The box is temperature controlled by cooling water only. An electric heater inside a silicone rubber tube in the box is supplied with a regulated voltage to give a constant base heat of 100 W. Such a heater makes it possible to regulate the temperature in the box to be the same as, or a little higher than, that of the surroundings.

The temperature setting for the calorimeter plate is close to that of the air in the laboratory for a normal test. For the normal test the temperature of the water in the cooling tank is set at 3 to 4°C lower.

One indication of the performance of the regulator is the temperature variations over time. For the lightest calorimeter plate, regulation on the incoming water and heat exchanger to the laboratory air, the variations in the control temperature over time were typically 0.04°C. This variation was calculated as standard deviation during the course of the whole test. With the calorimeter plate of higher thermal inertia the variations in temperature were higher.

A decisive test of the performance of the regulator is the response to a large step in the load. For most of the tests, an additional ten minutes of measurements have been logged after a step from full perpendicular irradiation to no irradiation. This gives an indication of the regulating performance and also an indication of the amount of heat stored in the box and the window components.

The following example gives an estimate of the size of the temporary error caused by deviation in the controlled temperature. The conditions in the example are a step change from full power in irradiation to zero, in a reference test without shading device. The light calorimeter plate was used and the inlet temperature was the controlled one. The time from the step change to fully recovered temperature was recorded to 230 s. The average deviation from the set temperature during this time was 0.154°C including a short peak of 0.3°C. The recorded step in power was 1000 W. The volume flow of circulating water was 0.087 l/s. With this flow and the average deviation in temperature, the temporary erroneous effect due to the temperature deviation during this short time can be calculated to 56 W.

It should be pointed out that the previous calculation example only accounts for the energy lag of the circulating water due to non-ideal control. For instance, erroneous power measurement due to an incorrect or non-representative temperature reading is not included. Many more components than the water in the calorimeter plate are involved in thermal inertia, e.g. the walls of the plate, inner box walls and glass panes.

In order to cool the lamps, air is extracted from the lamp housing. This air can either be sent to the outside or recirculated into the laboratory, controlled by valves. This makes it possible to regulate the temperature in the laboratory if the outside air is sufficiently cool.

3.3.2 Calorimeter measurement

In order to achieve a measurement of high accuracy of the difference in temperature between in and out-flowing water through the envelope of the calorimeter box, a thermopile with many pairs of thermocouples is used.

The thermocouples are made from Ø 0.08 mm thermocouple wire that is protected by being glued between two 0.1 mm sheets of glass (microscope cover slide). The sheets made in this way are mounted through longitudinal slots in two glass tubes. External disturbances to temperature measurement are negligible since thermal conduction along the approx. 0.4 mm thick sheets (radially in the tube) is low compared with the convective surface of heat transfer at the surface of the sheets that are exposed to the flowing water. The number of thermocouple pairs and the Seeback constant of the thermocouples therefore exclusively determine the output voltage from the difference temperature measurement. The difference temperature sensor need not necessarily be calibrated and can therefore be replaced without calibration.

The water flow rate must also be measured in order to get a calorimeter measurement. An inductive flow meter is used. This type of sensor is based on the Hall effect and gives a correct reading even if the measuring cross section is altered. An inductive flow meter is therefore rather immune to the building up of deposits.

A test to validate the performance of the calorimetric measurement was conducted by reducing the circulating flow of water. If both the difference temperature measurement and the flow measurement give a proportional reading, the same amount of heat should be registered. A difference of around 1% was registered as an average of a whole test, which was about the same repeatability as for a normal test. The flow rate was reduced from 0.08 to 0.046 l/s in the test.

3.3.3 Light intensity

The lamps are provided with a thyristor dimming unit. Despite this, the light is not fully stable and the intensity also varies over the life span of a lamp. There is a need for a simple way to measure the light that falls on to the measured object without blocking the light too much. This is done with photo diodes. In order to get a good average measurement of the intensity as many as 16 photo diodes are connected in parallel.

The terminal wires to the photo diodes are laid out in a web that is stretched out between the two moving arms that the lamps are mounted on and in this way the photo diodes stay in the same position and perpendicular relative to the beam of light. To obtain a good spatial average the 16 photo diodes are placed in the centre of a 0.3 × 0.3 m grid, and in this way cover the window opening at perpendicular incidence.

The light intensity is also monitored at one point with a pyranometer that gives the spectrally correct irradiation reading. In spite of the incorrect spectral response of the photo diodes, they are used to compensate for the variation in light intensity because of the good spatial averaging. However, when variations in the power grid result in a shift in the value from the photo diodes, the same pattern is seen on the pyranometer.

3.3.4 Light distribution

Using large reflectors facilitates generation of parallel light. The trade-off is that fewer lamps are used resulting in a more patchy distribution over the test area.

The peaks in light intensity are situated at the central axis of the parabolic reflectors. At this point the whole surface of the reflector including the rim is shining, but in other positions the illumination emanates more or less from the central parts only.

Adding a folded extra reflector surface at the rim could probably substantially reduce this peak at the central axis of the parabolic reflector. The deflected light from the folded reflector addition could at the same time enhance the weak areas. This has however not yet been tested.

The diagram in Figure 3.5 shows the result from a measurement of the irradiation distribution using a pyranometer. The measured area is 1.2 m × 1.2 m, covering the window area at perpendicular incidence. A grid with 0.1 m division was used. The average value for the 1.2 m × 1.2 m area is 952 W/m^2.

Because of the uneven distribution of irradiation, two more temperature measuring points have been added on the sunshade and the window for the tests in the laboratory. In this way a more accurate average value can be obtained. The point on the windows used for the outdoor measurements is placed in the horizontal and vertical centre of the window. For the windows used for the indoor measurements, one point 0.4 m above and another point 0.4 m below are added. For the outdoor measurements, only the inner pane was fitted with temperature sensors at these points.

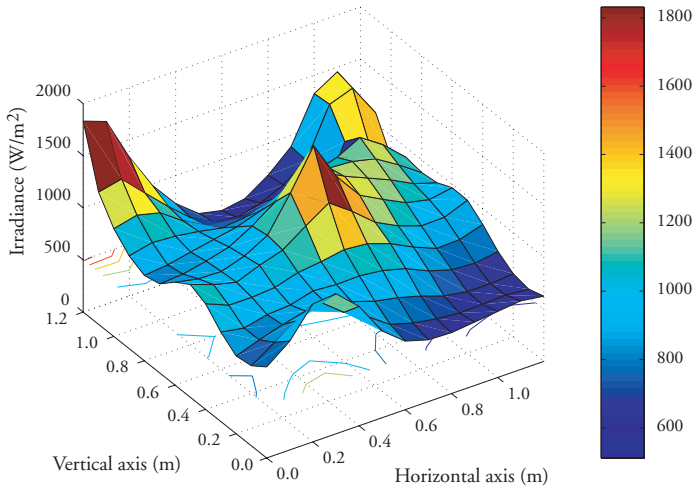

Figure 3.5 *The distribution of irradiation from the simulator on the tested window at perpendicular incidence.*

3.3.5 Light divergence

In order to investigate the divergence from the lamps at the window, the following measurement was made. A moveable screen with a circular hole and a circular shade placed in the centre was mounted on a rod parallel to the beam of light. The intensity of the light was measured with a photo diode placed at the axis perpendicular to the centre of the hole in the screen. In this way a narrow angular interval of incident light passes the screen and falls onto the photo diode. Moving the screen closer or further away can alter the angular interval. The arrangement is shown in the figure below.

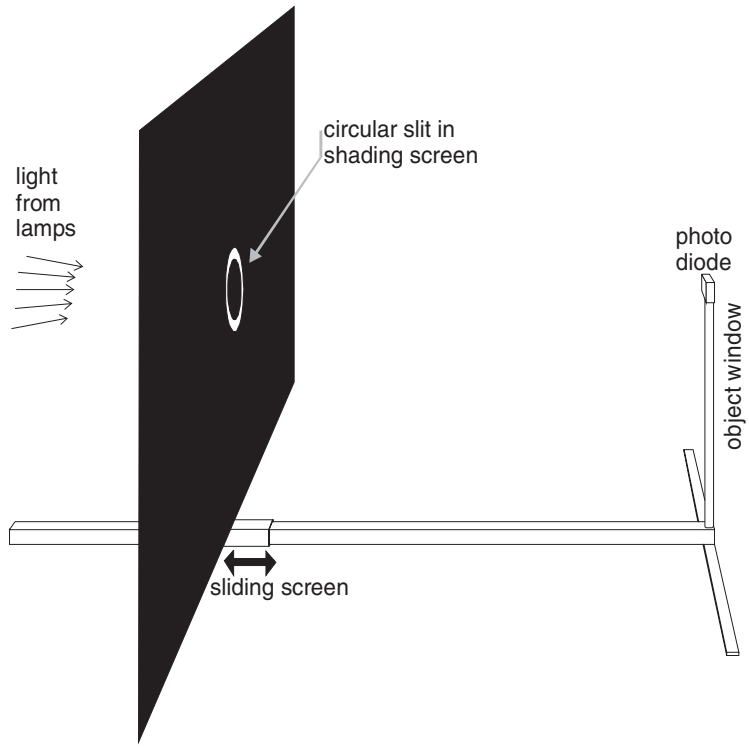

Figure 3.6 Arrangement for measurement of divergence.

The light from a single lamp is unstable and a reasonably constant value is hard to obtain. The result is an average of two measurement occasions. The light levels were measured in angular steps of 0.43°. Including the result from the two adjacent angles to form an average smooths out the curves shown in the diagram in Figure 3.7. The two curves show the angular distribution of the beam at the same distance from the lamps to the object as used in the tests. between the lamps and the object used in the tests. Curve |1| shows the angular distribution at a point placed at the central axis of the parabolic reflector, and for the lamp placed at the centre of the window. Curve |2| shows the distribution at a point perpendicular to the gap between three reflectors. The curves are truncated at very small angles of incidence but both curves are expected to come to near zero. For Curve |1| these small angles are related to the small reflector in the centre that the lamps are fitted with which throws the light back into the focus so it can be utilized by the main reflector. For Curve |2| these small angles of incidence are related to the dark gap between three reflectors. The explanation for the well defined drop in curve |1| at

angles exceeding 4° is that this is the angle corresponding to the border of the Ø 0.8 m reflector at 5.5 m distance and that the surrounding lamps corresponding to higher angles give little stray light

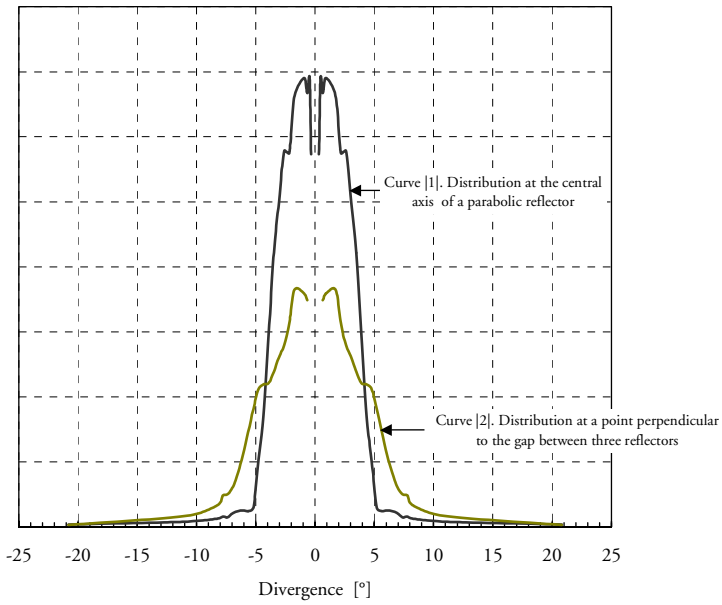

Figure 3.7 *The angular divergence of the light from the simulator at the point in centre of the simulator and at the point between three parabolas.*

A corrugated horizontal black sheet of metal is placed close to the floor in front of the calorimeter box to reduce the reflection from the floor for those high solar altitudes when the beam from the lamps extends to the floor. A large diameter fan cools this plate from below to reduce the effect of radiative heat.

3.3.6 Light level variations in time

The thyristor dimming unit is used to control the voltage to the lamps but it is not averaging over the three phases of power supply. This could be one reason for the resulting variations in intensity.

The light intensity measured by the photodiodes is recorded with a low-pass filter with a time constant of 6 s. A sometimes very noticeable flickering with periods of around a second is not recorded when this filter is used. The standard deviation of the intensities recorded using the low pass filter is 2.3% over the duration of a 2.7 h test based on 17 test

occasions. Most of these variations occur in steps, probably caused by loads on the power grid. The standard deviation of the intensity recorded on different days is higher. The deviation between the 17 tests is 4.4%. The thyristor unit has the option of external control. This provides a means of controlling the light level from the feedback of the photo diodes. This has not yet been done.

3.3.7 Relative measurements, shading coefficient

In the outdoor measurements two identical boxes, twin boxes, are used. The boxes are exposed to the same climatic conditions simultaneously, and owing to this measuring principle the relative difference between a window with and without a sunshade is obtained with a higher degree of accuracy compared with a measurement that is relative to a value of the irradiation falling onto the façade. The first type of measurement gives the shading coefficient, g-value for the sunshade and the second the g-value for the window system.

When the performance of shading devices is tested in the laboratory, the simulated climatic conditions are repeatable and it is possible to make relative comparisons by performing two identical runs with two different set-ups, one run with sunshade and a reference run without sunshade for comparison. On the other hand, a certain degree of non-uniformity of the irradiation distribution is unavoidable when solar radiation is simulated. This gives an angle-dependent error but in the subsequent reference run the same non-uniformity is repeated for the respective angles and a good relative measurement is still achieved.

3.3.8 Measurement of temperature in a solar radiation environment

The different excess temperatures of the components in a window system during irradiation are the direct driving force behind the secondary solar transmittance. It is hence valuable to record these temperatures to be able to analyse these various energy flows in more detail. Using very thin thermocouples facilitates accurate measurements. The thermocouple wires used are Ø 0.08 mm. The copper wire adjacent to the junction that measures the temperature is silver plated.

The thermocouple wires for measurement on glass panes are glued with a UV curing glass adhesive behind a 0.1 mm thick microscope cover slide. In this way very good thermal contact is achieved with the underlying glass, and at the same time the emissivity for long wave radiation on

the surface is still equal to that of glass. The surface of the point of measurement is kept flat and its projection outside the pane of glass is negligible.

A thin wire has better thermal contact with its surroundings compared with the disturbances from radiation (both short wave solar radiation and long wave thermal radiation). When temperatures on a surface are measured, a thin wire can be mounted closer to the surface and will not protrude so much into the air. In our application the thermocouples are well positioned in the inner part of the stagnant air in the boundary layer.

A calculation is made here to estimate the disturbance from solar radiation on a thin thermocouple wire close to a surface. The thin wire is assumed to be in the inner part of the boundary layer of the air, and therefore the temperature gradient in the region of the thickness of the wire is small. A distance of 0.5 wire diameter is assumed between the wire and the surface. It is realistic to assume the distance to be proportional to the diameter since a thinner wire is more pliable and thus can get nearer to the surface.

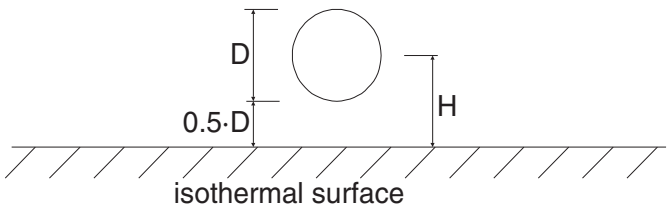

In Heat Transfer (Adrian Bejan, –John Wiley & Sons, Inc. 1993) a conductivity is given for a semi-infinite medium with an isothermal surface to an isothermal cylinder:

K conductivity between wire and surface [W/K]
D diameter of cylinder, $0.08 \cdot 10^{-3}$ [m]
H is assumed $1.0 \cdot D$ [m]
L length of cylinder [m]
λ thermal conductivity for air, 0.025 [W/(m·K)]

$$K = \frac{2 \cdot \pi \cdot \lambda \cdot L}{\cosh^{-1}(2 \cdot H / D)} = \frac{2 \cdot \pi \cdot 0.025 \cdot L}{\cosh^{-1}(2)} = 0.119 \cdot L \quad [\text{W/K}]$$

The absorptivity for sunlight on the thermocouple wire is assumed to be A = 0.2. With an irradiation of 1000 W/m^2 a wire absorbs $1000 \cdot 0.2 \cdot 0.08 \cdot 10^{-3} \cdot L = 0.016 \cdot L$ W. The excess temperature for the wire compared with the surface is :

$$\Delta T = \frac{0.016 \cdot L}{0.119 \cdot L} = 0.13 \quad [°C]$$

Despite the strong irradiation, the excess temperature due to disturbances from the sunlight is very small for such a thin thermocouple under the assumed conditions.

The thin thermocouple wires were usually attached to the fabric of sunshades by binding them with loops of thin copper wires at some distance from the measuring junction to avoid unnecessary disturbances and at the same time close enough to get a tight connection to the fabric at the junction. Proper tension in the thermocouple wires is also essential to get a tight fit.

The same advantages of thin thermocouple wires apply when the temperatures are measured on the slats in a venetian blind. The thermocouple wires are placed on top on the surface but no glue is used in the vicinity of the measuring junction. In this way the absorptivity and emissivity are not altered on the measured point of the surface.

The temperature of the air in the laboratory is measured at the same level as the centre of the window box. The temperature is measured on a Ø 2 mm polished silver rod. Silver has low absorption both for short and long wave radiation and a low radiative disturbance can be expected. The rather high thermal mass gives a stable reading. The rod is soldered to very thin thermocouples to reduce the influence from the terminals.

3.3.9 Influence of wind on the g-value of sunshades

A couple of indoor measurements have been made to give examples of the influence on the g-value due to different simulated wind conditions for a window with external sunshades.

The wind on the exterior is simulated by a row of fans as shown in Figure 3.1. The influence on the convective heat transfer coefficient on a bare window is described in 3.2.7 for different types of regulation of the power to the fans.

The first example of the tests is a dark, fully extended awning. A section of the calorimeter box and the awning is shown in Figure 3.8. On solar exposure the dark fabric becomes very warm, and heat is transferred to the outer pane by long wave radiation due to the large view factor

between the fabric and the window at this position. A pocket of warm air is also formed under the awning. This heat transfer is very wind dependent, since both sides of the awning and the surface of the window are cooled by the air. This is illustrated by the result from two measurements in Figure 3.9. The result is shown as a quotient between the g-values derived from a measurement with the fans simulating the wind at full power (24V) and the g-value from the measurement with no agitation of the air. To be able to illustrate also the relative importance of the result for different horizontal and vertical angles, circles with areas proportional to the total cooling load are plotted in the diagram. For instance, the influence of wind at high vertical angles is quite substantial, but the cooling demand is not so large here.

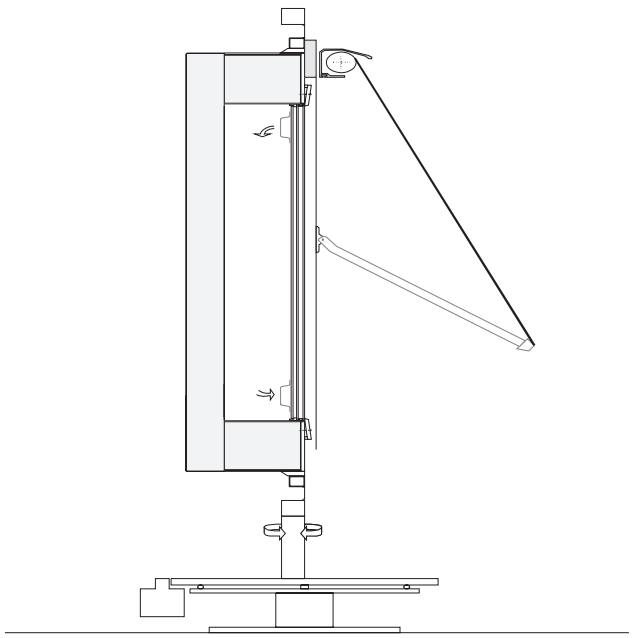

Figure 3.8 *Set-up for indoor measurement of a fully extended awning.*

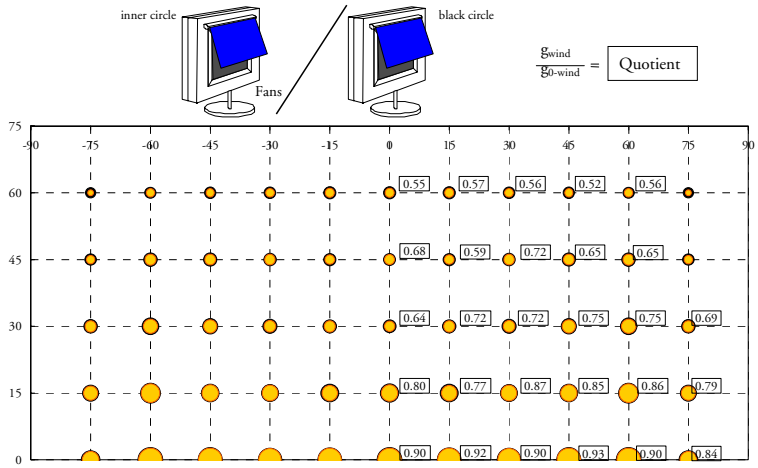

Figure 3.9 *Measured quotients between g-values under simulated wind conditions and no wind for a number of angles. The areas of the circles represent total cooling load for the two cases.*

The position of the sun in Lund at different times of the year is shown in Figure 3.10 and can be compared for a south-facing window in Figure 3.9. The areas of the circles represent the measured total cooling load for a window without sunshades for the measured combination of angles.

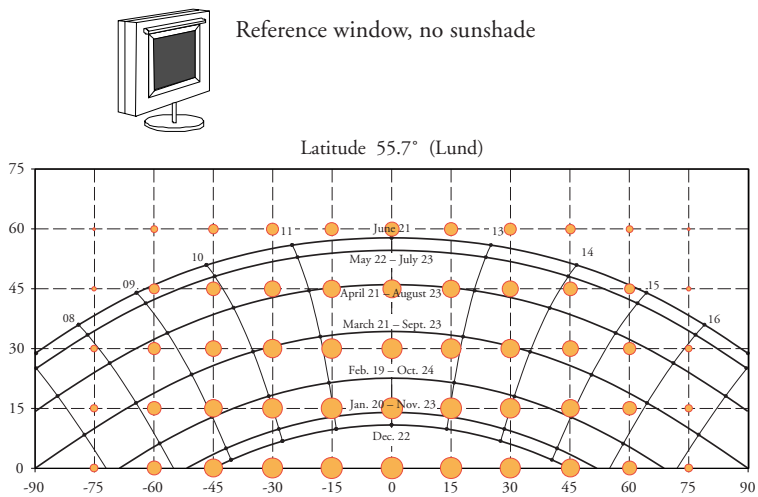

Figure 3.10 *Solar paths for the latitude of Lund (55.7° N).*

Another example of the influence of wind on g-values for shading devices is a number of tests made on an exterior screen. The screen is dark and non-transparent but is perforated in a random pattern. The direct transmittance through this perforation is around 3.2%. It is mounted on a four-sided frame attached to the calorimeter box. The distance between the screen and the window pane is 70 mm. With this arrangement the volume behind the screen is closed except for only small slits around the periphery. To test the effect of opening up the volume behind the screen, the frame was replaced by mounting strips only at the sides. This created 40 mm open slits at the top and bottom. The result from the measurements of g-values at perpendicular incidence is shown in the table below. The g-value for the original mounting and the normal setting of the fans is underlined.

	g-value, closed volume	*g*-value, volume opened up
No fans	0.15	0.15
Fans at 12 V	<u>0.14</u>	0.13
Fans at 24 V	0.11	—

The rather small absolute differences in the *g*-values give a rather high degree of uncertainty for the differences between the cases. For a more accurate relative comparison of the different cases, the temperatures on the screen and outer pane can give additional information. The temperature difference between the outer pane and the calorimeter plate is the driving force for the secondary transmittance. This temperature difference is on average reduced by 9% when the volume between the window and the screen is opened up. As regards the cases with only the original closed volume, the temperature difference between the outer pane and the calorimeter plate is increased by 28% when the fans are shut off and reduced by 25% when the voltage to the fans is altered from 12 V to 24 V.

3.4 Measuring procedure

3.4.1 Angular measuring sequences

For measurements that are meant to test the shading properties for a combination of solar altitude and azimuth angles a scheme of consecutive angles is used. Six horizontal angles are combined with five vertical

angles. The order of measurements between the different positions, as indicated by the arrows in Figure 3.11, is designed in such a way as to minimize steps in angle of incidence and thus the energy flow. This measuring scheme is used for shading devices such as awnings that project from the façade.

In the most frequently used scheme, only the vertical angles are varied and the azimuth angle is kept constant and perpendicular to the window. The measured points start with a solar altitude of 70° with steps of 5°. This scheme is specially suited for investigation of the angle dependence of the g-values of venetian blinds.

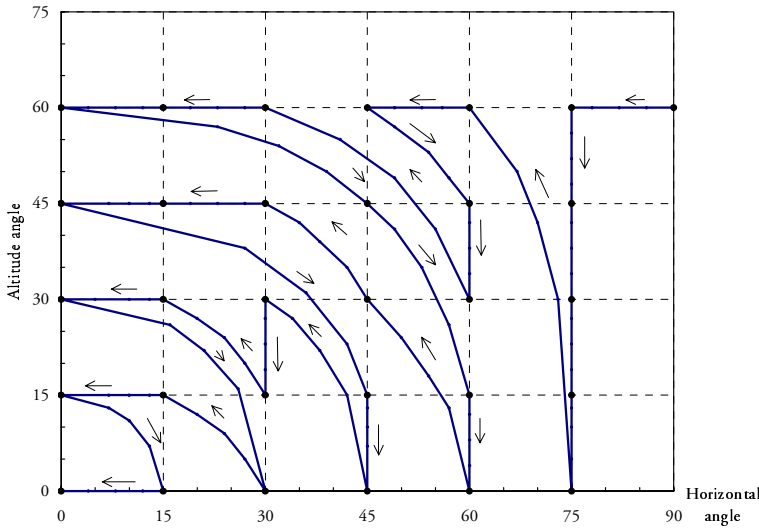

Figure 3.11 *An example of a measurement scheme for a succession of combinations of horizontal and vertical angles in a test run.*

3.4.2 Diffuse light

For calculation of the influence of diffuse light, the half hemisphere representing the sky seen from the window is assumed to be isotropic. For each measuring point as shown in Figure 3.11, a surrounding angle area is allocated to represent that direction. This is illustrated in Figure 3.12. In this area the cosine of the angle of incidence is integrated over the solid angle of the area to give a view factor representing the contribution from the diffused light associated with that measured point.

The g-values of the sunshade for the specific directions and the corresponding view factors can now be multiplied and summarized to give the g-factor for diffuse light from the total half hemisphere.

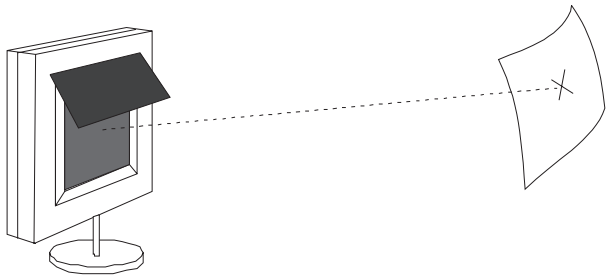

Figure 3.12 A measured direction with adjacent angle area.

3.4.3 Data collection and evaluation

The measured data are sampled and logged every 18 seconds. The period between steps in angles of incidence is normally 9 minutes. In the evaluation, the calorimeter value for each step is averaged over 5.5 minutes allowing 3.5 minutes after a step for stabilisation.

In the most frequently used scheme only the vertical angles are varied and steps of 5° are used. The last step in this scheme is at perpendicular angle of incidence. This 9 minute step is repeated in this scheme. In this way the repeatability for consecutive steps can be obtained. The standard deviation between two consecutive g-values evaluated in this way was 1.3%. This deviation was calculated from a series of measurements on interpane venetian blinds. One source of difference between the two values is oscillations in the controlled temperature of the cooling water discussed in 3.3.1.

3.4.4 Measuring conditions for an external sunshade

The window was of the same double glazed type as for the outdoor measurements (4 mm – 12 mm – 4 mm, clear glass) with a 1.17 m × 1.17 m light opening.

3.4.5 Measuring conditions for an interpane sunshade

The inner pane for the assembly is permanently fixed to a 30 mm × 14 mm wooden frame. To this frame sunshades can be mounted. The front pane is removable and supported at the base by a small protruding ledge

on the wooden frame. The entire window is pressed in position by the outer frame on the calorimeter box. The two glass panes are 1.7 mm thick clear glass. This thin glass absorbs little irradiation and has low thermal capacity. This makes the measurements less complicated and more accurate. A few simulations have been made for interpane sunshades and the difference between the normal 4 mm and 1.7 mm glass was insignificant. In any case, comparisons between different sunshades can still be made.

3.4.6 Measuring conditions for an internal sunshade

In order to test the g-value for internal sunshades, the convective heat transfer around the sunshade and the inner pane needs to be simulated. The conditions should be as close as possible to those for a whole room. When exterior and interpane sunshades were tested, the inner thermal resistance was simulated by an 8 mm air gap between the inner pane and the calorimeter plate. The same method could be applied for internal sunshades by placing the flat calorimeter plate with the same air gap to the sunshade, provided that the sunshade is also flat. But with this method it is only possible to simulate the conditions when airflow between the sunshade and the window is prevented. With airflow, more of the secondary heat is transported to the room. This increases the g-value. The measurements in the calorimeter box had a closed volume between the internal sunshade and the inner pane. Therefore, the resulting g-values should be regarded as the lower limit.

Strips of acrylic sheets were mounted on the sides in the calorimeter box. This made it possible to mount the curtain flatter by stretching it to the sides and at the same time to prevent unwanted air leakage.

The window was of the same double glazed type as for measuring external sunshades (4 mm – 12 mm – 4 mm, clear glass). The width of the closed volume between the sunshade and the inner pane was 48 mm.

3.5 Measurement results

3.5.1 Measurement results for external sunshades

Two fabrics of different colours have been combined with three awning arrangements in the measurements. One fabric was light beige and the other dark blue. The traditional awning was tested partially extended and fully extended. The third arrangement is an Italian awning.

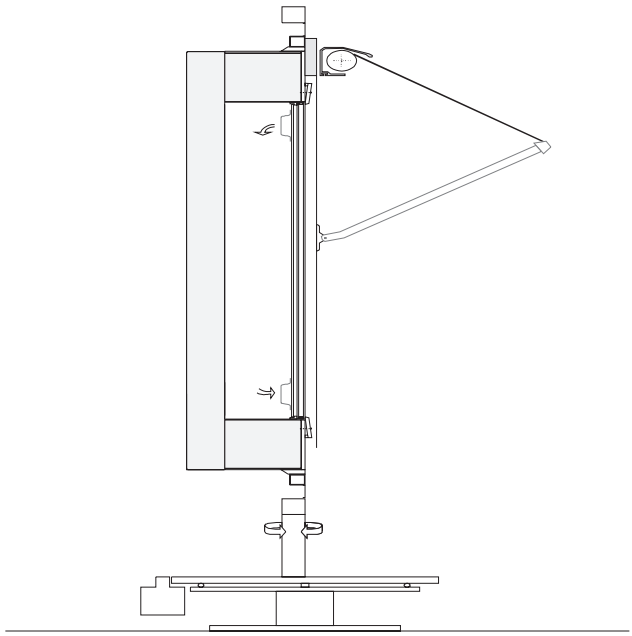

Figure 3.13 Set-up for indoor measurement of a partially extended awning.

The result of the measurement on the partially extended dark blue awning is shown in Figure 3.14. As in the illustration in 3.3.9 the areas of the circles are proportional to a total cooling load. To illustrate g-values, the black circles represent the cooling load for the window without the sunshade and the inner circles represent the cooling load with the sunshade.

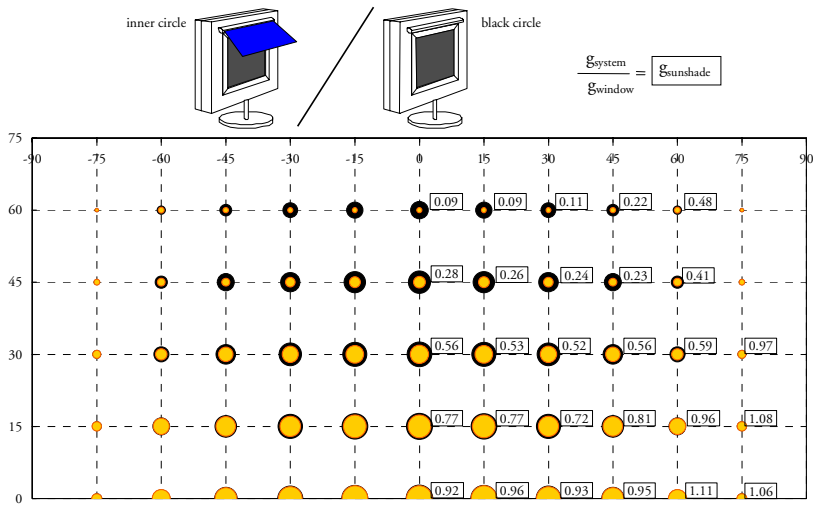

Figure 3.14 *Measured g-values on a dark, partially extended awning for a number of angles. The areas of the circles represent total cooling load. The inner circle /black circle corresponds to the cooling loads for sunshade /no sunshade.*

With the method devised in 3.4.2 a single g-value can be calculated for the isotropic diffuse light from half a hemisphere of sky. The value is 0.58 for the partially extended, dark blue awning.

The window is also affected by light reflected from the ground. The solar simulator cannot produce light coming from below, but by mounting the sunshade upside down the whole arrangement is inverted and this light can also be simulated.

Figure 3.15 shows such a measurement on a partially extended awning. With the same method as for the diffuse sky, a single g-value can be calculated for the isotropic diffuse light from the ground. The value is 0.98 for the partially extended, dark blue awning.

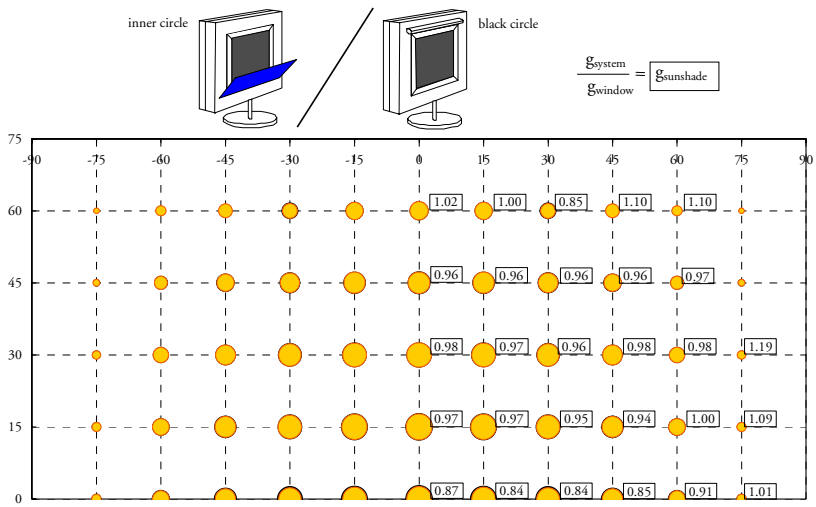

Figure 3.15 *The same type of measurement as the previous figure. The awning is mounted upside down to measure the influence of the reflection from the ground.*

The result of the measurement on the light beige, partially extended awning is shown in Figure 3.16. Only the vertical angle is varied and the horizontal angle is constantly perpendicular. The corresponding g-values for the dark blue awning previously shown in Figure 3.14 are also included in the diagram for comparison.

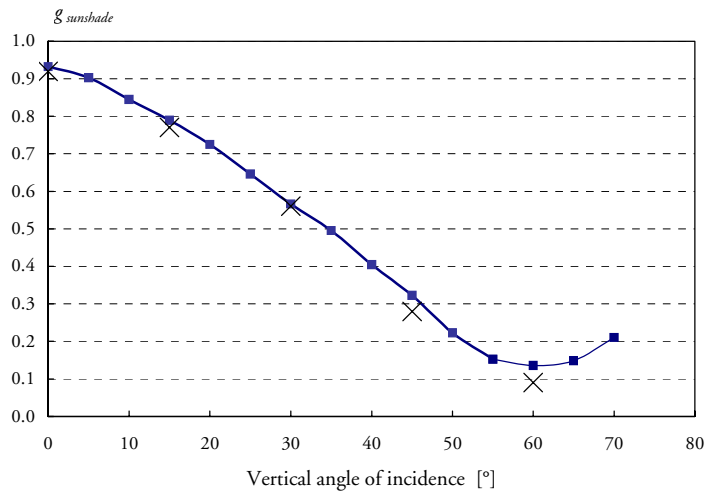

Figure 3.16 *g-values for a light beige, partially extended awning. The crosses denote the corresponding points for a dark blue awning.*

A section of the calorimeter box and a fully extended awning is shown in Figure 3.8. The measured g-values for the fully extended dark blue awning are shown in Figure 3.17. With the method of calculating the single g-value for the diffuse sky, a value of 0.22 was obtained.

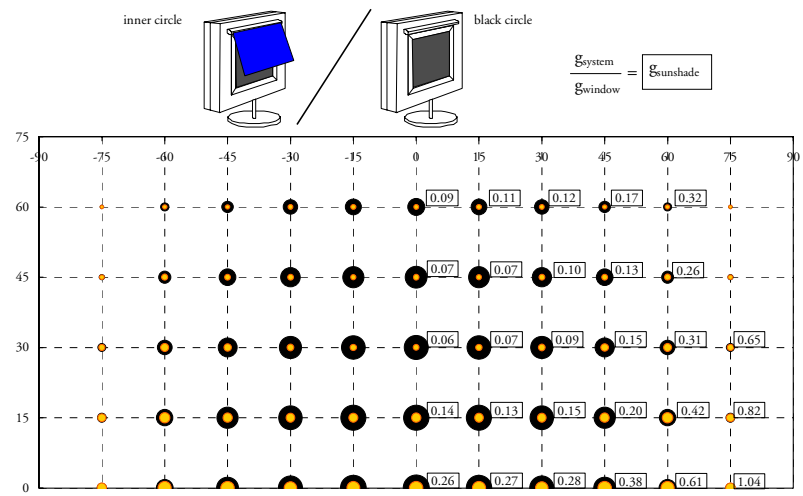

Figure 3.17 *Measured g-values on a dark, fully extended awning for a number of angles. The areas of the circles represent total cooling load. The inner circle /black circle corresponds to the cooling loads for sunshade /no sunshade.*

To measure the influence from the ground, the same type of measurement with inverted mounting as for a partially extended awning was performed . The resulting g-values are shown in Figure 3.18. The single g-value for isotropic diffuse light from the ground was 0.78 for this dark blue, fully extended awning.

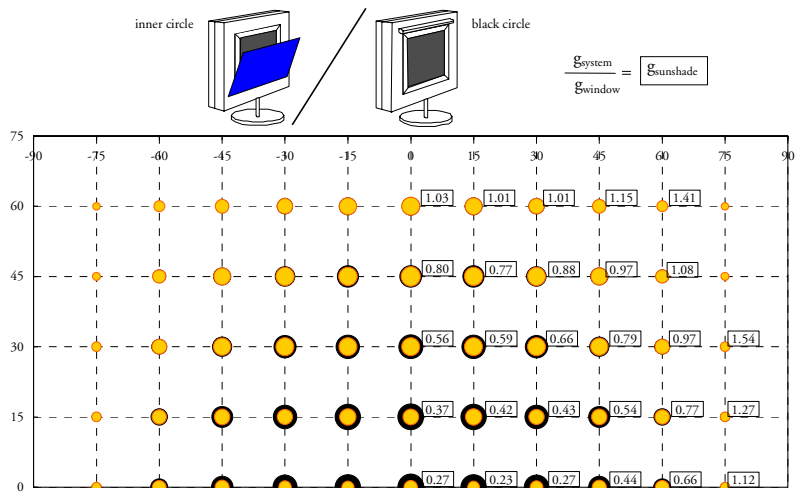

Figure 3.18 *The same type of measurement as in the previous figure. The awning is mounted upside down to measure the influence of the reflection from the ground.*

The result of the measurement on a light beige, fully extended awning is shown in Figure 3.19. The corresponding g-values for the dark blue awning previously shown in Figure 3.17 are also included in the diagram for comparison. These g-values can be compared with those for a partially extended awning in Figure 3.16. The large difference between the two fabrics, especially pronounced at high vertical angles, can be explained by light passing through the light beige awning in diffused form, in combination with the large view factor for the fully extended position. The dark blue fabric is almost completely non transparent.

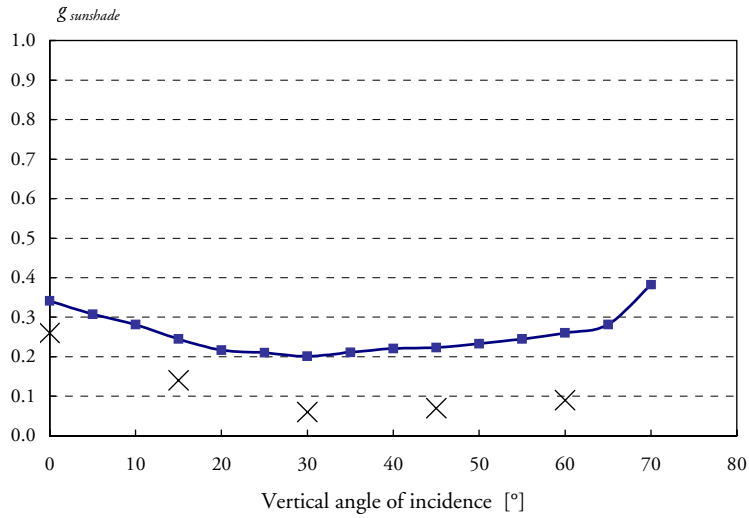

Figure 3.19 *g-values for a light beige, fully extended awning. The crosses denote the corresponding points for a dark blue awning.*

The two fabrics have also been measured as an Italian awning. A section of the arrangement is shown in Figure 3.20. The measured g-values for a dark blue awning are shown in Figure 3.21. A prerequisite for such low g-values as those obtained at vertical angles above 25° is not only that the light is shielded off, but also that there is little thermal contact between the outer pane and the sun heated dark fabric. The result can be compared with the result for an exterior dark screen in 3.3.9. The g-value for this screen is as high as 0.14 in spite of the fact that the screen has a transmittance as low as 3.2%. Between the screen and the outer pane there is however a rather closed volume, whereas in the Italian awning arrangement, air movements are much less restricted.

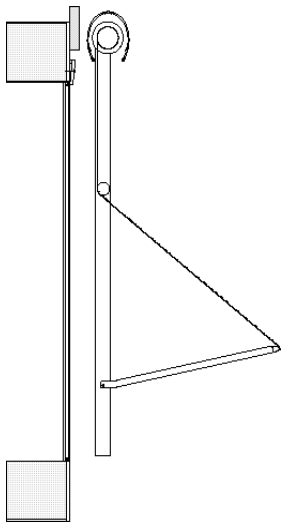

Figure 3.20 Set-up for indoor measurement on an Italian awning.

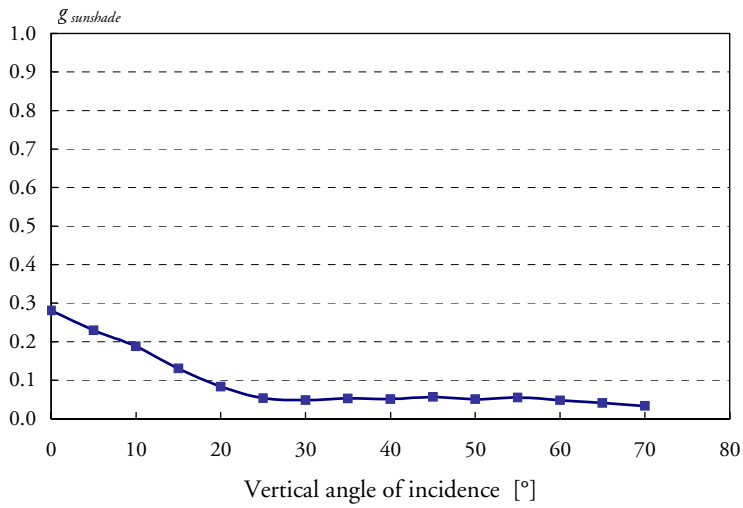

Figure 3.21 g-values for a dark blue Italian awning.

In Figure 3.22 the measured g-values for the same Italian awning arrangement are shown for the light beige fabric.

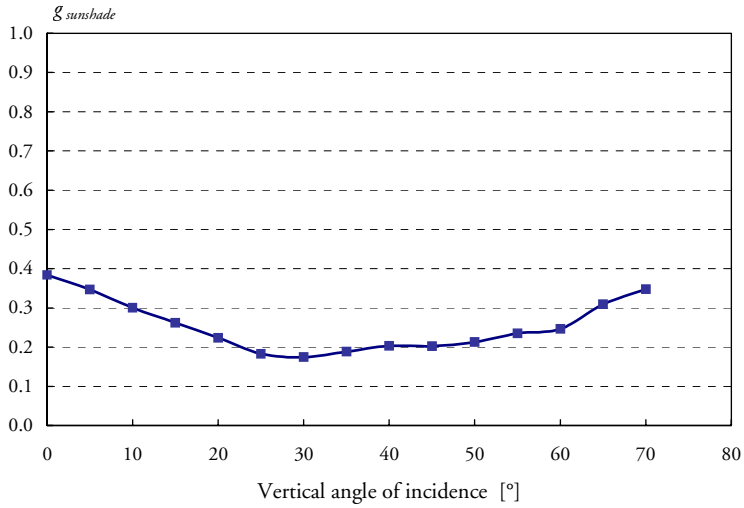

Figure 3.22 *g-values for a light beige Italian awning.*

3.5.2 Measurement results for interpane sunshades

Venetian blinds of three colours have been tested in the interpane position. A fully closed venetian blind is defined as 80° and horizontal slats are 0°. A slat angle sloping downwards seen from the inside is defined as positive.

Figure 3.23 shows the measured g-values for venetian blinds with metallic finish for five different angular positions of the slats.

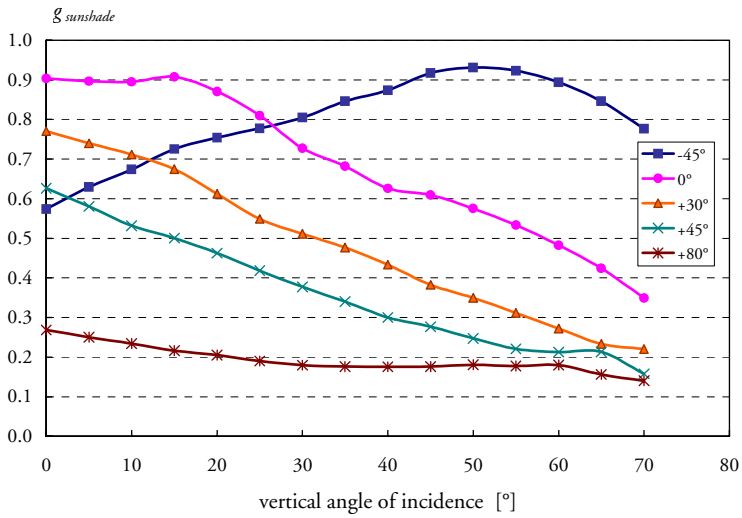

Figure 3.23 *g-values for an interpane venetian blind, metallic, for a number of slat angles.*

In Figures 3.24 to 3.27 the measured g-values for the three colours are compared, one diagram for each slat angle position. In Chapter 6.3 the simulated g-values are compared with those measured for white and dark blue venetian blinds.

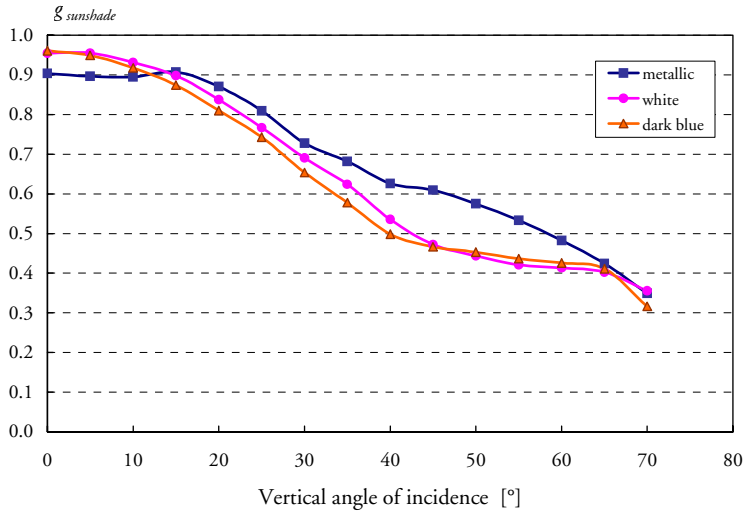

Figure 3.24 *g-values for an interpane venetian blind, horizontal slat angle, for a number of colours.*

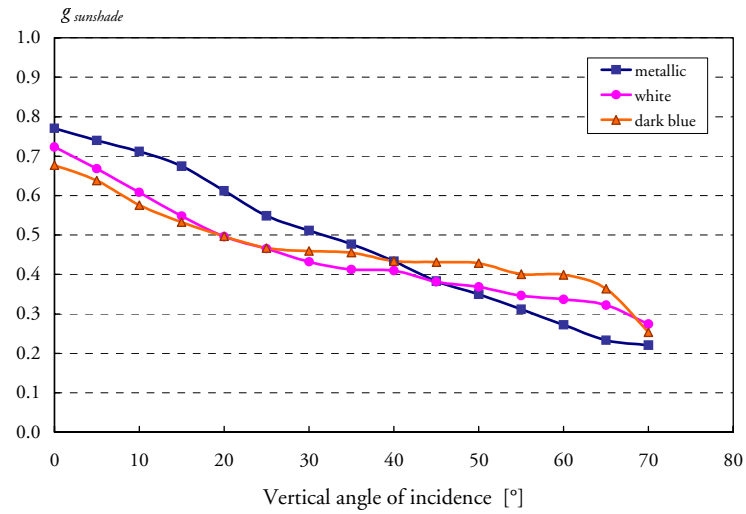

Figure 3.25 *g-values for an interpane venetian blind, 30° slat angle, for a number of colours.*

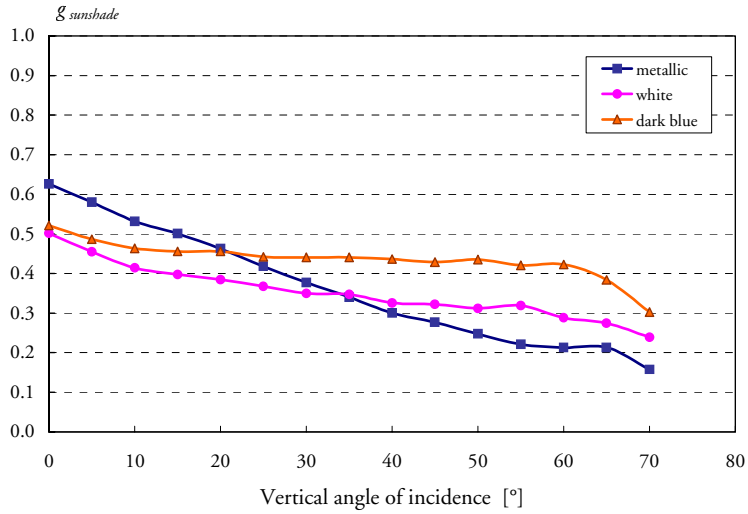

Figure 3.26 *g-values for an interpane venetian blind, 45° slat angle, for a number of colours.*

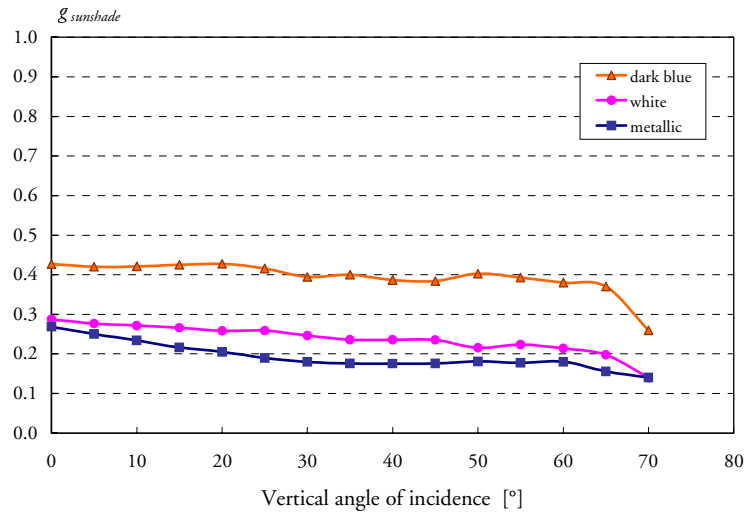

Figure 3.27 *g-values for an interpane venetian blind, closed slats, for a number of colours.*

Figure 3.28 shows a photo of a pleated curtain mounted in the calorimeter box in the interpane position. The fabric of the curtain in the picture has a metallic coating. There is a tendency for the pleats to get narrower at the lower parts of the curtain due to less stretching from its own weight there. This alters the optical properties over the height of the window somewhat and makes the testing conditions less well defined.

Figure 3.28 A picture of a pleated curtain with metallic coating.

Figures 3.29 and 3.30 show the measured g-values for two interpane pleated curtains of different fabrics. In Figure 3.31 the measured result for a non-transparent, white curtain is shown.

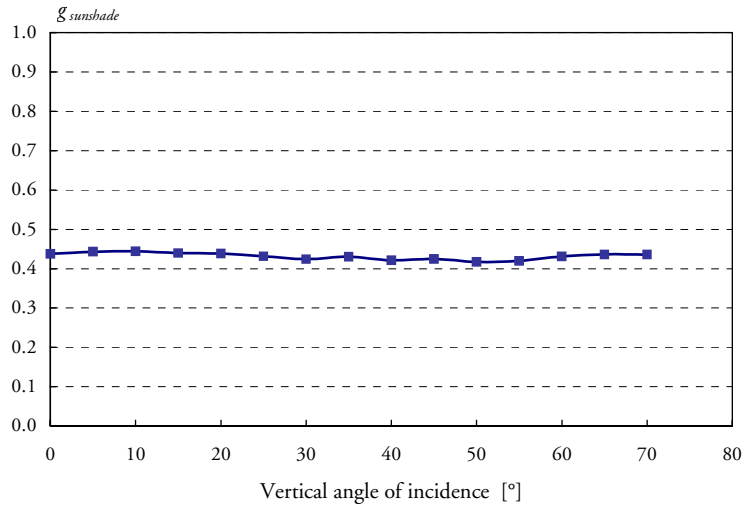

Figure 3.29 g-values for an interpane pleated curtain, light beige.

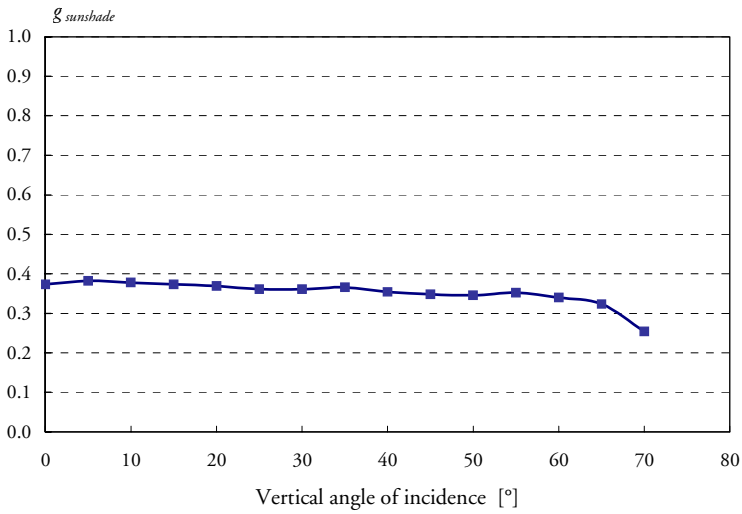

Figure 3.30 g-values for an interpane pleated curtain, silver-grey.

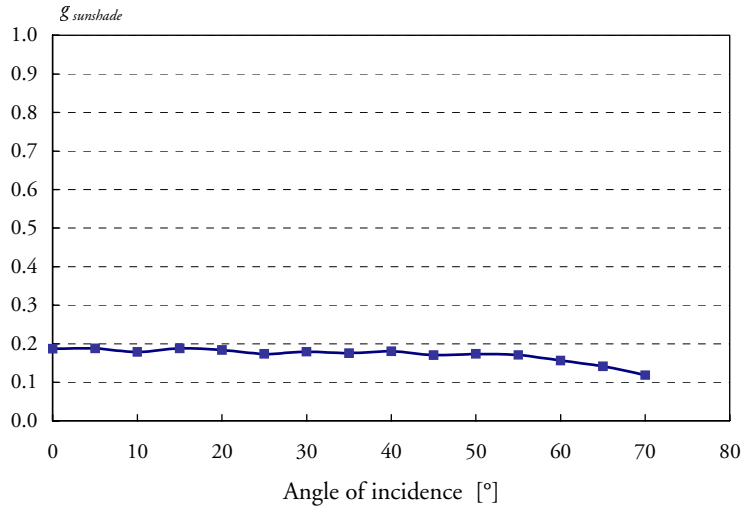

Figure 3.31 g-values for an interpane non-transparent white curtain.

3.5.3 Measurement results for internal sunshades

In Chapter 4 measured results for internal sunshades are shown together with simulated values.

3.5.4 Measurement results for films attached to window panes

Tests were made on a double glazed unit (4 mm – 12 mm – 4 mm) with films attached. Figure 3.32 illustrates the difference between the *g*-values for two films obtained when they are applied to the inside of the inner or the outside of the outer pane. As seen in the figure, the difference between the two positions is substantial.

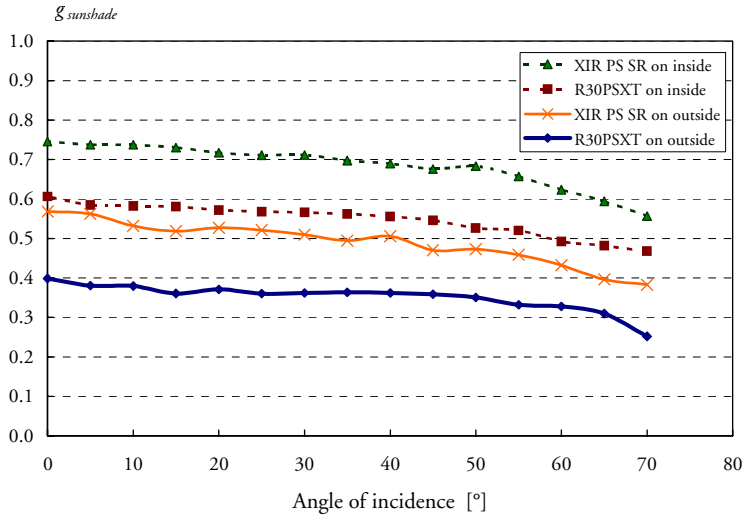

Figure 3.32 *g-values for films attached to the inner pane and to the outer pane respectively.*

3.6 Discussion and conclusions

One of the obvious advantages of a solar simulator with a movable light source is that it can produce the desired solar altitudes on a window kept in the normal vertical position and at any time of the year. This is especially valuable for angle e -dependent sunshades e.g. venetian blinds. For such a sunshade a complete set of tests for different angles can be performed on one occasion. For those distinctly angle- dependent measurements a parallel light source is vital. Our solar simulator has very good qualities in this respect.

Another valuable advantage of a solar simulator is that the convective conditions for the exterior can be repeatedly produced and also altered. This is especially important for several types of exterior sunshades, for instance those that are dark and absorbent and have a tendency to build up a hot air pocket.

A set-up for testing a sunshade with a solar simulator can be made simpler and more convenient than the outdoor set-up . The window has no need to be rain resistant and there is no demand on the sunshade to endure gusts of strong wind.

Fans with adjustable speed simulate the convective conditions in front of the window caused by wind. Tests to investigate the convective heat transfer on the front pane for different fan settings have been performed. The sensitivity to wind of the g-values was investigated by using different settings on the fans for measurements on two types of exterior sunshades.

The solar simulator produces only direct light, but methods have been devised to obtain measured g-values for the diffuse light both from the sky and the ground.

Awnings have been tested as partially extended, fully extended and as Italian awning. For these geometries two fabrics have been used; a dark almost non-transparent fabric and a light coloured rather transparent and diffusing fabric. An exterior screen was also tested.

Venetian blinds, pleated curtains and one flat curtain have been tested in the interpane position. Venetian blinds of three colours were tested in combination with five slat angles. The solar altitude was altered in steps of 5° in these tests.

A few measurements were made on internal sunshades. These measurements were limited to shading devices without an open air gap and thus without natural convection between the shading and indoors.

Along with all the different measurements, the test methods were evaluated and improvements made, or they will be further tested within future research work. One conclusion was that the lamps in the light source show some instability, also during periods long enough to affect the calorimeter measurements. In an effort to reduce the influence of this instability, the light intensity is measured on a grid of photodiodes in front of the window so that compensation can be made.

The high thermal capacity of water makes it important to have good temperature control over the water used for calorimetric measurements. The experience gained in the solar laboratory using several types of calorimeter plates stresses the importance of keeping the water volume inside the calorimeter box down to an absolute minimum. A small water volume benefits the control and hence the precision and also the reduces the need for long delay times after a step to reach equilibrium and the need for time to get a good average value of the measured cooling demand.

The calorimeter measurements are made with an inductive flow meter and thermocouples arranged as a thermopile for the temperature difference. The thermopile with as many as 10 pairs of thermocouples has a high precision and since it is based on a passive measuring principle, it produces a zero signal when the temperature difference is zero.

The reflector arrangement used for the lamps gives good divergence quality with very little stray light. The distribution over the measured object area is however rather uneven. A modification to improve the light distribution is suggested with probably only a moderate degradation of the divergence.

Also for the calorimeter plate improvements are recommended. It is suggested that the front sheet should be made of metal to achieve good heat transfer to the water. The current calorimeter plate is made of glass for its non-corrosive and stability properties.

Only internal sunshades with flat inner surface have been measured. The radiative and convective heat transfers between the sunshade and the room have been simulated by an air gap. It is a simple and well-defined method. Measurements on other internal sunshades, and especially for the situation with natural convection which occurs when the volume between the inner pane and the sunshade is not closed, are more complex. In that case the calorimeter box must be designed with a substantial volume behind the window to reasonably reproduce the conditions for the natural convection of a whole room. The calorimeter box must then meet a number of demanding requirements to be able to provide accurate measurements. Firstly, almost all internal surfaces that are struck by irradiation have to be cooled so that the energy can be collected immediately to avoid excess temperatures. To simulate a room, the air temperature also has to be close to those of the surfaces. The necessary cooling load from the air can become very large for a dark internal sunshade and an effective heat exchanger is required for the air.

An alternative or complement to measuring g-values could be to measure surface temperatures on the components of a sunlit window with sunshade in an ordinary room. A simulation program could then be used to fit a g-value. The temperature measurement methods on surfaces using very thin thermocouples have worked very well also in a sunlit environment. Such measurements can also verify components and systems in a simulation program.

4 Modelling internal and interpane sunshades in ParaSol

Bengt Hellström

Internal and interpane sunshades are new options in ParaSol, version 2.0.

From yearly simulations, max. cooling and heating loads as well as yearly energy demands for a room with a window, with and without sunshades, can be obtained. Monthly average values of T (primary solar transmittance) and g (total solar transmittance) for the window, the sunshade(s) and the system can also be obtained from yearly simulations. In the ParaSol simulations it is possible to have two sunshades if one internal or interpane sunshade is combined with an external one.

A new feature of ParaSol version 2.0 is that U, T and g-values for standardized conditions and normal incidence of the solar radiation are calculated when a window or a system of a window and an internal or interpane sunshade is chosen. However, if an external sunshade is also included in the system, the system values will be calculated without it.

The U, T and g-values are calculated for the glazed part of the window. Vented air gaps are not yet an option in ParaSol. All air gaps are treated as closed, even for internal sunshades, which are often mounted with an open air gap.

4.1 Implementing models into the simulation engine of ParaSol

ParaSol is built on the building energy simulation program DEROB-LTH, so these programs use the same simulation engine. For practical and time limit reasons, the old structure of the program code has been kept as far as possible.

The program was not originally built to treat IR (long-wave) transparent layers (wavelength range 2.5-50 μm), so special solutions had to be made for the cases with an IR-transparent layer between two glass panes (interpane sunshades) or with an IR-transparent layer inside the inner glass pane (internal sunshades). The case with an IR-transparent layer outside the outer pane was not treated, since the programming for the external sunshades from the old version was kept unchanged.

The IR exchange factor is defined as F_1 in the equation:

$$q = F_1 \cdot \sigma \cdot (T_1^4 - T_2^4), \text{ where}$$

q = the net heat radiation from layer 1 to layer 2 (W/m^2)
σ = the Stefan-Boltzmann constant = $5.67 \cdot 10^{-8}$ (W/m^{2}K^4)
T_1 = the temperature of layer 1 (K)
T_2 = the temperature of layer 2 (K)

For the case of one IR-transparent layer between two (IR opaque) glass panes, the IR exchange factors between the three layers are calculated from the IR properties of the layers. For an internal IR-transparent layer, the IR exchange factors are calculated between the two inner layers and the room. The IR exchange factors between the different layers are used in the heat balance equation system for calculating the temperatures of all the layers. When the IR exchange factors are calculated, no edge effects are considered, which means that all layers are approximated as infinitely large compared with the gap size.

4.2 Plane structures

Plane solar shading devices (screens, roller blinds etc.) are treated as plane layers, parallel with the glass panes. Although some plane structures are in actual fact air permeable, all internal and interpane plane sunshades in ParaSol are calculated as non permeable. All air layers are also treated as closed (non-vented). This is important, especially for internal sunshades, which are often mounted with an open air gap. The results from the program must in such a case be used with caution, since the *g*-value for a window with an internal sunshade and an open air gap is higher than for a closed one. This is because, if the air gap is open, part of the solar energy absorbed by the internal sunshade and the inner pane will be transferred to the room by an air flow through the gap. The results will show a lower limit of the *g*-value.

Convective heat transfer in the air layer between a plane sunshade and a glass pane is calculated in the same way as between two glass panes, which means using a correlation of ElSherbiny et al (1982) for 90° declination (since only vertical windows are used in ParaSol). The convection between an internal sunshade and the room air is calculated in the same way as for an inner glass pane of a window, which means using a correlation by Min et al (1956). The convective heat transfer coefficient between the outside pane and the ambient air is in ParaSol simulations set to 15 W/m^2K.

The program uses the following angle of incidence and side dependent (front and back) solar (short-wave) properties of the shading device:

- Direct – direct transmittance (direct transmittance)
- Direct – diffuse transmittance (diffuse transmittance)
- Direct – direct reflectance (specular reflectance)
- Direct – diffuse reflectance (diffuse reflectance)
- Absorptance of direct solar radiation (absorptance)

The program also uses the following side dependent IR (long-wave) properties of the solar shading device:

- Diffuse – diffuse transmittance (transmittance)
- Diffuse – diffuse reflectance (reflectance)
- Absorptance/emittance of diffuse IR radiation (emittance)

"Diffuse" here means isotropically diffuse. Direct – diffuse means that the incoming radiation is direct and the outgoing radiation (after interaction with the layer) is diffuse. The notation used in the program is given within brackets.

The optical data for the glass panes are calculated (using Fresnel's formulas and Snell's law of refraction) for different angles of incidence (every 5:th degree) and the program calculates the optical properties of the window for the direct solar radiation using these data. The optical properties of the window for diffuse insolation are calculated by integrating the properties for direct insolation over the different angles of incidence of the hemisphere.

When an internal or interpane solar shading device is used together with the window, the same properties are calculated in the same way as for the window alone. However, due to lack of angle resolved optical data for plane solar shading materials, the ParaSol program reads optical data for only the normal incidence and then uses it for all incidence angles.

4.3 Venetian blinds

The input data for the venetian blinds are the side dependent *slat* properties (at normal incidence) in the solar (short-wave) range (0.3-2.5 µm):

- Direct – direct transmittance (direct transmittance)
- Direct – diffuse transmittance (diffuse transmittance)
- Direct – direct reflectance (specular reflectance)
- Direct – diffuse reflectance (diffuse reflectance)
- Absorptance of direct radiation (absorptance)

These properties are approximated to be the same for all angles of incidence. The program also uses the following side dependent IR properties of the slats:

- Diffuse – diffuse transmittance (transmittance)
- Diffuse – diffuse reflectance (reflectance)
- Absorptance/emittance of diffuse radiation (absorptance)

Three geometrical properties are also given (see Figure 4.1.a):

- The slat angle (φ)
- The slat width (w)
- The (vertical) distance between two slats (d)

The venetian blind is treated as a layer. The optical properties of the *layer*, solar or IR, which are the same categories as for the plane sunshades (see Chapter 4.2), are calculated from the slat optical and geometrical properties. This calculation is performed using a procedure which will be described below.

A cell consisting of two plane slat walls (one upper and one lower) and two fictitious side walls (the outside and the inside), see Figure 4.1.b, is what is used for calculating the optical properties of the layer. The coordinates of the boundaries of the area where the beam strikes the slat or its extension are calculated. The part of the beam that does not strike the slat adds to the direct transmittance of the layer. As indicated by the optical properties of the slat (see above), the insolation which impinges on the slat is divided into 5 categories, namely directly and diffusely transmitted, specularly and diffusely reflected, and absorbed.

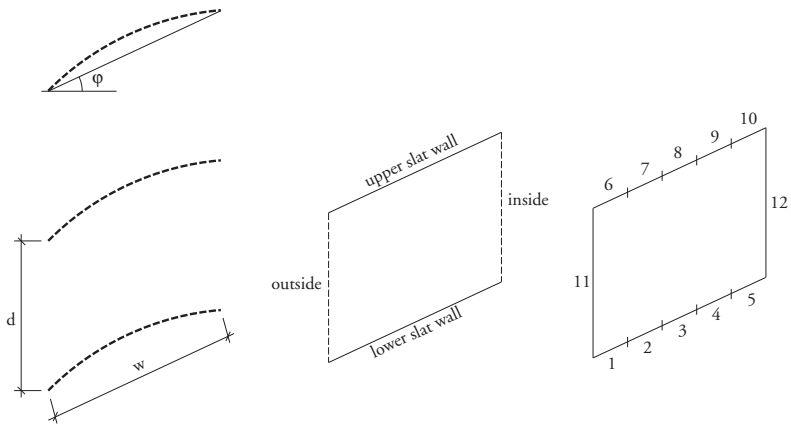

Figure 4.1
a. Width (w), angle (φ), slat spacing (d). *b. Model for calculation of layer properties.* *c. Division of the slat into parts for view angle calculations.*

The way the *diffusely transmitted* and *diffusely reflected* parts of the beam contribute to the optical properties of the layer is calculated. The technique for this is described below. The *absorbed* part, of course, adds to the absorptance of the layer. The *directly transmitted* and *specularly reflected* parts, however, give rise to two new beams, the transmitted one having an unchanged angle of incidence and the reflected one a new angle of incidence towards the slat on the opposite side (unless the slat angle is 0°). The new beam from the transmitted part is treated as originating from the slat wall opposite to the one which was struck by the beam. The two new beams are calculated in the same way as the original beam, which means that after the next step, 4 new beams may result, after that 8 and so on.

One difference from the original beam, however, is that the new beams may also strike the outside, which adds to the diffuse reflectance of the layer. All of the layer reflectance is treated as diffuse, because, depending on the slat angle, the angle of reflection for some radiation will differ strongly from the angle of incidence. The transmittance is also, for the same reason, regarded as diffuse, except for the beams that have never been reflected, which add to the direct transmittance of the layer.

The original beam is in this way traced until it has almost vanished (less than 0.1% left). The rest is added to the absorptance. In order to limit the number of beams generated for strongly low-absorbing and low-

scattering materials at some slat and angle of incidence combinations, the process stops after 9 steps (2^9 beams) and the rest is added to the layer absorptance. The sum of all the layer properties is then 1.

When each beam strikes a slat, part of the beam will be diffusely transmitted or reflected. Those parts are calculated in the following way:

The slat is divided into 5 parts, see Figure 4.1.c. View factors between the 5 parts on the slat, the 5 parts on the opposite slat, the outside and the inside are calculated. They are then, together with the optical properties of the slat, used for calculating the amount of the diffuse radiation from the different slat parts which will be absorbed by the inside and the outside, considering all multiple reflections/transmissions. This is done by solving a radiation balance equation system for the cell, described, for instance, by Siegel and Howell (2002).

It is calculated which slat parts are illuminated by the beam. If one part of the slat is only partly illuminated, this part of the beam is then distributed over the whole slat . For the *diffusely reflected* radiation we now know how much will go to the inside, which adds to the diffuse transmittance of the layer. The part that goes to the outside adds to the diffuse reflectance, while the rest, absorbed by the slats, adds to the absorptance of the layer. For the *diffusely transmitted* radiation the same thing is done, except that the radiation leaving the slat after the transmission is calculated as originating from the slat on the opposite side to the one which was struck by the beam.

IR properties are calculated in a similar way. From the IR properties of the slat and the view factors between the outside, the inside and the slat surfaces, the IR properties of the layer are calculated.

Convection in the gap between two glass panes with a venetian blind is a very complex phenomenon, depending among other things on the slat angle. In the absence of validated correlations, a simple correlation based partly on reasoning was made. Because of this, *U*-values calculated for glazings with venetian blinds must be used with caution in view of the uncertainties. The correlation is regarded as a provisional arrangement. It is based on two extreme cases:

1. The slat angle is 90° or –90°: In this case the slats are closed and we have two air gaps, one on each side of the venetian blind layer. Convective heat transfer in each gap is calculated as between two plane layers.

2. The slat angle is 0°: In this case the slats are open and air can freely circulate between the two surrounding glass panes. Convective heat transfer for this case is assumed to take place only between the two

surrounding glass panes and is assumed to be of the same magnitude as if the venetian blind did not exist. It is therefore also calculated in that way.

For all slat angles in between these extremes, convection is assumed to be a mixture between the two, following the rule that the type 2 convection heat transfer coefficient is multiplied by cos(φ), while type 1 is multiplied by 1-cos(φ), where *j* is the slat angle. For example, at 60° slat angle, both types of heat transfer coefficients are multiplied by 0.5.

All slats are approximated as plane, although in reality they are usually slightly curved. An improvement of the model could be to consider the curvature of the slat also. This work has partly been carried out, but some programming remains and it was not implemented in the model. The results should also be compared with measurements to show that this really improves the model.

The diffuse model used in ParaSol is similar to the one developed in the ALTSET project, where the concept of dividing the slat into 5 parts was suggested, (see for instance Rosenfeld et al., 2000). This model was also used in the WIS program.

International standards for calculation of venetian blind layers are being developed (ISO, 2000), but are yet not approved. However, it appears from the drafts that the models of these standards will consider only diffusely reflected and transmitted radiation. In ParaSol, this can be achieved by setting the direct properties to zero and regarding the total reflectance/transmittance as diffuse. The reflectance of real slats is mostly diffuse and the transmittance is in general zero.

4.4 Input data for the sunshades

In Sections 4.2 and 4.3 it has been shown what input data is needed for plane sunshades and venetian blinds. One way to get accurate data, at least for materials without too large heterogeneous structures, is to use spectral measurements from a spectrophotometer instrument and to integrate them into the desired properties. For normal incidence in the solar wavelength range this can be done for most materials.

With a spectrophotometer, the IR properties will be measured at angles of incidence close to normal, instead of with diffuse irradiation. This approximation could however be acceptable, since the difference between normal and diffuse IR properties is usually small and the IR properties

are usually not very crucial for the results. For many materials, like most non-transparent fabrics, the emittance could, without measurement, be set to 0.9 and the IR-reflectance to 0.1.

The problem of obtaining angle of incidence-dependent measured data for plane sunshades to use in the model is not yet solved. Therefore, in version 2.0 of ParaSol, only data for the normal incidence of the plane sunshades are used for all angles of incidence. This problem does not occur for venetian blinds, since the angle dependent data for the layer are calculated from the slat data.

4.5 Direct calculation of properties

As mentioned above, U, T and g-values for irradiation at normal incidence are calculated when a window or a system of a window and an internal or interpane sunshade is chosen. The calculations are made with the following boundary conditions:

Winter case:	Summer case:
t_i = 20°C	t_i = 25°C
t_o = 0°C	t_o = 30°C
$h_{c,i}$ = 3.6 W/m^{2}K	$h_{c,i}$ = 2.5 W/m^{2}K
$h_{c,o}$ = 20 W/m^{2}K	$h_{c,o}$ = 8 W/m^{2}K
G_b = 300 W/m^2	G_b = 500 W/m^2

where

t_i = inside air/radiant temperature
t_o = outside air/radiant temperature
$h_{c,i}$ = convective heat transfer coefficient between the inner pane/sunshade and the inside air
$h_{c,o}$ = convective heat transfer coefficient between the outer pane and the outside air
G_b = irradiation at normal incidence

Since the U-value is most important for heating loads, it is calculated according to the winter case. In the same way, the g-value is most important for cooling loads, so therefore it is calculated according to the summer case.

For calculating the convective heat transfer in the gap(s) between the layers, the correlation of ElSherbiny et al (1982) for 90° declination was used. This correlation is also used for the Parasol simulations.

The conditions agree with what was suggested in a draft for a new international standard, ISO/DIS 15099. If needed, they will be updated when the standard is approved. Window manufacturers often show *U* and *g*-values according to the standard EN673, which gives *U*-values slightly lower than the ones calculated in ParaSol. This is mostly because a different correlation is used for calculating the gap convection. However, EN673 could not be used in ParaSol, partly because it does not include solar shadings and partly because it sets the outer and the inner panes at fixed temperatures, which is not consistent with how ParaSol is programmed.

4.6 Calculation of properties from yearly simulations

The monthly mean values of *T* and *g* are calculated for the window, the system of window and sunshade(s), and finally for the sunshade(s). The sunshade *g*-value is here defined as the quotient of the system *g*-value and the window *g*-value:

$$g_{sunshade} = g_{system} / g_{window}$$

The *T* and *g*-values are calculated for the glazed part of the window. They are only marginally influenced by the window frame data and the window size. This influence exists because the frame will cut off irradiation from high angles of incidence, resulting in slightly higher *T* and *g*-values.

The monthly mean *g*-values are calculated from the difference between the cooling and the heating loads with insolation, minus the same without insolation, divided by the irradiation through the window (Wall and Bülow-Hübe, 2001):

$$g = ((E_{c,s} - E_{h,s}) - (E_{c,n} - E_{h,n})) / G = (E_{c,s} - E_{c,n} - E_{h,s} + E_{h,n}) / G$$

$E_{c,s}$ = cooling load for the month with insolation through the window glass area
$E_{c,n}$ = cooling load for the month without insolation
$E_{h,s}$ = heating load for the month with insolation through the window glass area

$E_{h,n}$ = heating load for the month without insolation
G = insolation on the window glass area

The way the monthly mean *g*-values are calculated has been changed in version 2.0. In the earlier version, the secondary heat from the irradiation of the wall and the window frame was included in the *g*-value of the window. Also, only daytime hours were counted. This means that heat from the irradiation, which was stored in the walls in the daytime and transferred to the air at night, was not included in the calculation of the *g*-value. This is inconsistent with the usual definition of a *g*-value, and has therefore been changed.

For the same reason, the calculation of the design values (index dim) of *g* (and *T*) has been removed. The calculation was made by weighting the hours with high insolation. In this way the night hours, when the energy stored in the walls was transferred to the room air, were not counted, which is not consistent with the common definition of *g*.

4.7 Conclusions

Models of internal and interpane sunshades, including both fabrics and venetian blinds, have been integrated into the ParaSol program. The models use, as input to the program, optical data at normal incidence for the materials of the different sunshade products. The model for the fabrics assumes that the air gap between the sunshade and any glass pane is closed.

The ParaSol program, apart from annual cooling and heating loads for a room with or without sunshades, also gives monthly average values of *T* and *g* for the window, the sunshade(s) and the system. It is possible to have two sunshades if one internal or interpane sunshade is combined with an external one.

A new feature is introduced in ParaSol, where *U*, *T* and *g*-values are calculated for standardized conditions and normal incidence of the solar radiation for a window or for a system of a window and an internal/interpane sunshade. External sunshades are not part of this feature.

5 ParaSol v2.0

Hasse Kvist

A design tool with the name ParaSol v2.0 has been completed during this phase of the project. The main purpose of the design tool is to be a simple but still accurate design aid for architects, building services consultants and other engineers. It can be used to study the potential of solar protection for different types of sunshades and also their influence on the building energy performance at an early design phase. Since this target group has a very varied technical background, the intention is to make a tool that is sufficiently advanced to produce relevant data, but not so complicated that the user introduces unnecessary errors in the input data or quite simply will not use the tool at all. This tool is mainly intended for simulations of buildings like offices, schools and hospitals.

The graphical user interface of ParaSol is based on a dynamic energy simulation engine named DEROB-LTH. The simulation engine is a monolithic, detailed hour by hour energy simulation program.

Physical solar radiation models for the combination of sunshades and window are developed in this project and implemented in the DEROB-LTH simulation engine. ParaSol can simulate different types of sunshades positioned either externally, interpane or internally.

Different strategies for controlling sunshades as well as an air conditioning unit to heat or cool the inlet air have been added to this version of ParaSol.

Input data to ParaSol is given via a number of forms or windows. On each form there is a glossary and help function. The output from a simulation is in the form of both diagrams to display the effectiveness of solar protection for sunshades and the combination of sunshades and windows, and diagrams to show different characteristics of the building energy performance. Thermal comfort can also be studied.

ParaSol can be run in Swedish or English mode.

ParaSol is developed for the operating systems MS Windows 95/98/NT/2000/XP. Because the simulations are based on relatively heavy calculations it is recommended to run ParaSol on a powerful PC.

5.1 Start form

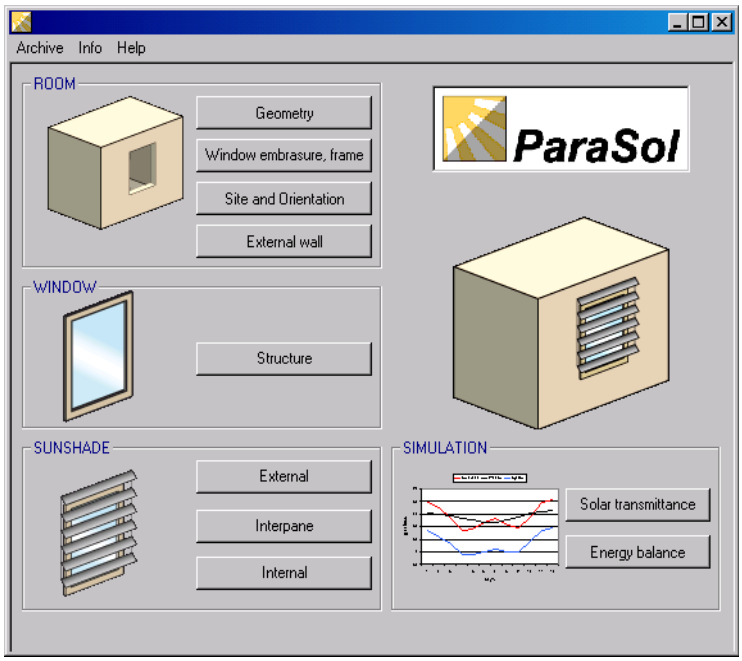

Fig. 5.1 *Start form.*

The main functions of ParaSol are related to the room of a building, its window structure, the external, interpane and internal sunshades and two types of simulations. A standard calculation of the direct (T) and total (g) solar transmittance for the window structure and a combination of windows and sunshades is performed and displayed in related forms. Simulation models can be saved and retrieved via the entry *Archive/Model* in the main bar. In the entry *Info/Contacts* there is a link to an internet connection to the home page of the Division of Energy and Building Design.

The *Help* button gives overall information about this form.

5.2 Geometry

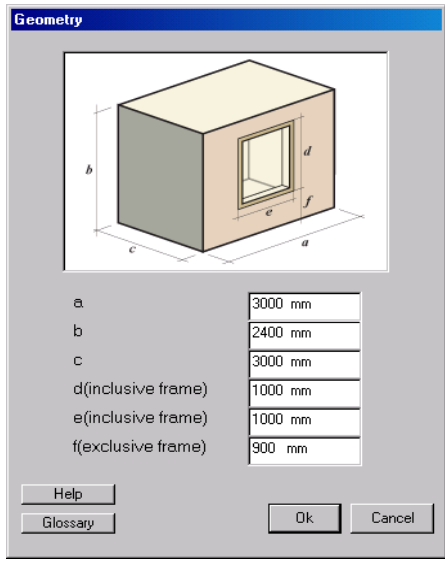

Fig. 5.2 *Geometry form.*

One geometry for the room is available: a rectangular office module with *one* external wall with *one* window. In future versions of ParaSol it may be possible to define several other geometries. All geometrical dimensions can be changed and the chosen sunshades are adapted to the changes.

The *Help* button gives overall information about this form.

5.3 Window embrasure and frame width

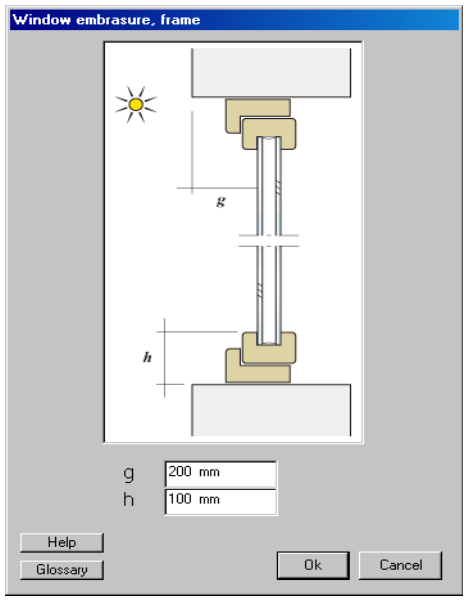

Fig. 5.3 *Window embrasure and frame width.*

Window embrasure and frame width are needed to describe how the window is mounted in the wall. These are parameters whose importance is often underestimated. In the present version of ParaSol, a wooden frame is assumed.

The *Help* button gives overall information about this form.

5.4 Site and orientation

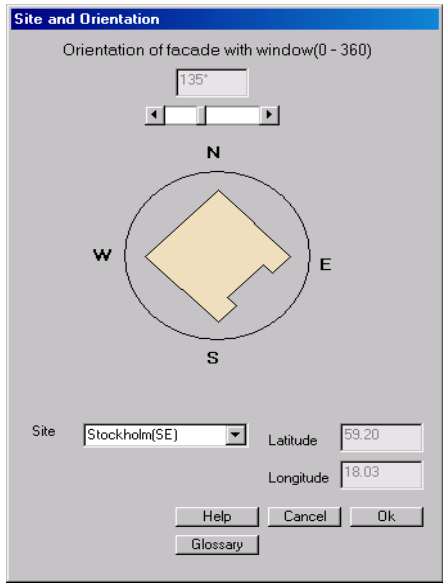

Fig. 5.4 *Locality and orientation.*

The orientation of the building is important for the simulation of transmission properties. For the simulation of the direct transmission T and the total transmission g both latitude and climate are needed. ParaSol has a climatic library for a number of sites in Europe. Climatic data for almost any site can be produced by using the software METEONORM from the company METEOTEST in Bern, Switzerland.

By dragging the horizontal scroll bar the orientation changes and the illustrated room rotates according to the input of the orientation.

The *Help* button gives overall information about this form.

5.5 Walls

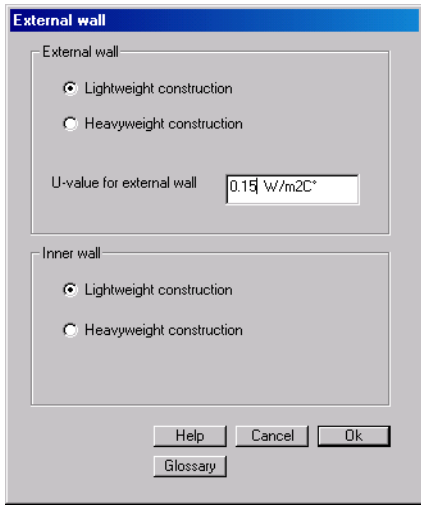

Fig. 5.5 *Walls.*

Description of the walls is made as simple as possible. Since it is only the external wall that abuts on a different climate, the *U*-value is only needed for this wall. All other surfaces are adiabatic. This means that the temperature in the studied room is assumed the same as the temperature in adjacent rooms and corridors. No energy transfer will therefore occur to connecting rooms. The subdivision into lightweight and heavyweight construction for heat storage is perhaps too simple. In coming versions of ParaSol it is however easy to make a more detailed subdivision, perhaps with different construction types.

The *Help* button gives overall information about this form.

5.6 Window structure

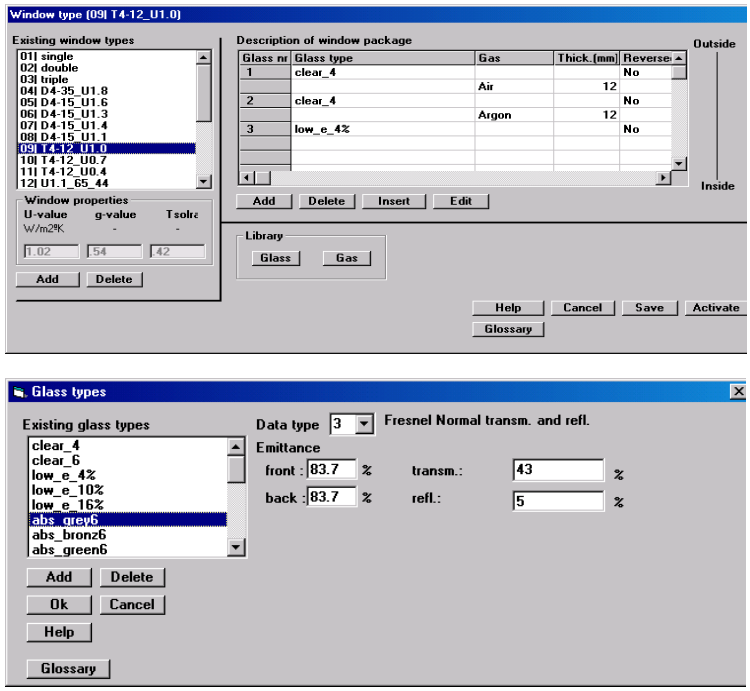

Fig. 5.6 Window structure.

These forms are used to activate a window type or to add new glass and window types to the library. The glass type form is accessed from the window type form. There is a library of ready made examples of window and glass types. When a window type is selected from the list the window properties *U-value*, *g-value* and T_{sol} are calculated with a steady state procedure according to a draft international standard (ISO/DIS 15099). Note that during the simulation, ParaSol calculates the actual heat transfer coefficients for the window construction excluding the frame.

The *Help* button gives overall information about this form.

5.7 Description of sunshades

All types of sunshades have their own form for input data. The structure of the active system (i.e. the selected window type and shading device) is shown in all forms. The system properties *U-value, g-value* and T_{sol} are calculated for the combination of interpane or internal sunshades and the window. The system properties are calculated with a steady state procedure according to a draft international standard (ISO/DIS 15099). External sunshades have been excluded in these calculations. The main reason is that the model of external sunshades is based on a different data structure. A revision of the data structures and inclusion of the external sunshades in the calculations is planned in coming releases of the program.

All forms have an update function to add or delete sunshades to the library.

An external sunshade can be active at the same time as an interpane or an internal sunshade. However, interpane and internal sunshades can not be active simultaneously.

All forms have the buttons *Sunshade off* and *Sunshade on* to manage the system sunshade-window. A sunshade is activated, (i.e. added to the system) by clicking the button *Sunshade on.* The button *Sunshade off* removes a sunshade from the active system. A selected sunshade is removed from the library by clicking the button *Delete type*. All modifications to the library are made permanent by clicking either *Sunshade off* or *Sunshade on.*

The *Help* button gives overall information about the form.

5.7.1 External sunshades

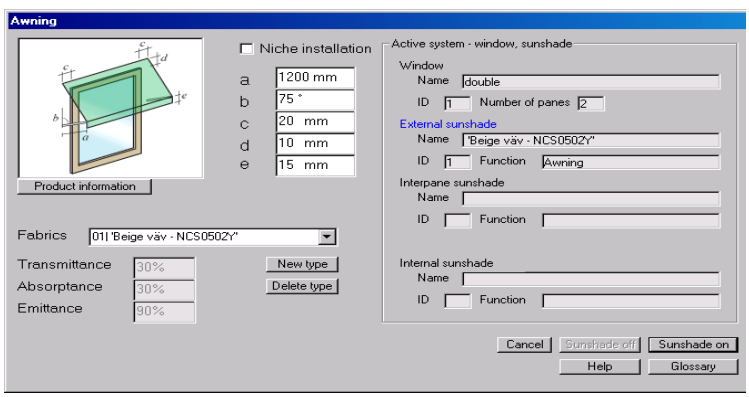

Fig. 5.7 Awning.

Input data needed is:
- Geometry of the sunshade
- Type of fabric

Other types of external sunshades included in ParaSol are:
- Italian awning
- Venetian blind
- Horizontal slatted baffle
- Plane sunshades such as screens

Forms for these sunshades are designed in a similar way as for the awning.

5.7.2 Interpane sunshades

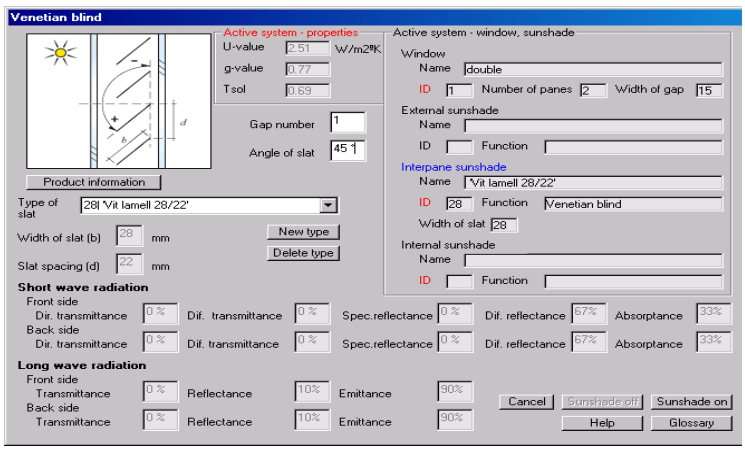

Fig. 5.8 Venetian blind.

The active system of sunshades combined with a window is shown.

The system properties *U-value*, *g-value* and T_{sol} are calculated and displayed in the form each time a sunshade is selected or its position or properties are changed. The system properties are calculated with a steady state procedure according to a draft international standard (ISO/DIS 15099). Note that external active sunshades are not included in the calculated properties for the system. Only components marked in red are included in the standardized calculation.

Input data needed is:

Gap number in a window where the shading device is placed. If the window has more than two panes then the gap number is the number of one of the spaces enclosed by the panes. The spaces are numbered from the outside to the inside.

Angle of slat. The angle is 0 degrees for a horizontal slat. A negative angle indicates an upward rotation from a horizontal position (view of the sky) of the slat while a positive angle is a rotation downwards (view towards the ground).

Type of slat with its properties shown in the form. The front side of a sunshade is facing the outside while the back side is facing the room.

Width of slat (only if a new type is defined).

Slat spacing (only if a new type is defined).

Other types of interpane sunshades included in ParaSol are:

Plane sunshades like screens, roller blinds, unattached films (i.e. freely hanging solar control films) and pleated curtains.

Forms for these sunshades are designed in a similar way as for the venetian blind.

5.7.3 Internal sunshades

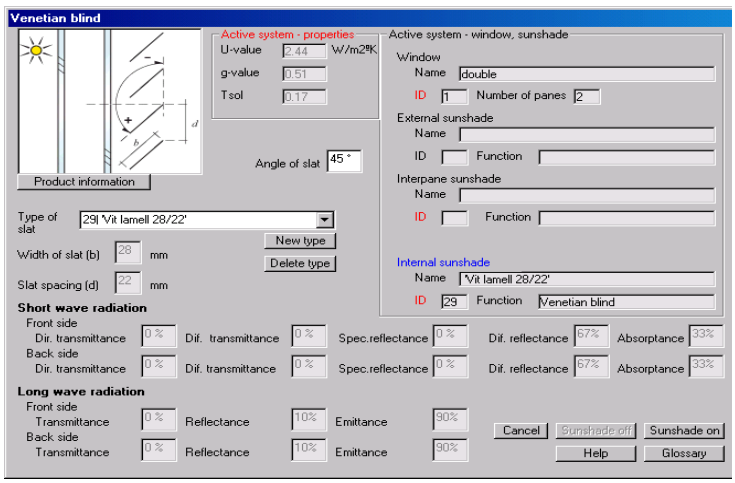

Fig. 5.9 Venetian blind.

The active system of sunshades combined with a window is shown.

The system properties *U-value*, *g-value* and T_{sol} are calculated and displayed in the form each time a sunshade is selected or its position or properties are changed. The system properties are calculated with a steady state procedure according to a draft international standard (ISO/DIS 15099). Note that external active sunshades are not included in the calculated properties for the system.

Input data needed is:

Angle of slat. The angle is 0 degrees for a horizontal slat. A negative angle indicates an upward rotation from a horizontal position (view of the sky) of the slat while a positive angle is a rotation downwards (view towards the ground).

Type of slat with its properties shown in the form. The front side of a sunshade is facing the outside while the back side is facing the room.

Width of slat (only if a new type is defined).

Slat spacing (only if a new type is defined).

Other types of internal sunshades included in ParaSol are:

Plane sunshades like screens, roller blinds, unattached films (i.e. freely hanging solar control films) and pleated curtains.

Forms for these sunshades are designed in a similar way as for the internal venetian blind.

5.8 Simulation

Two different types of simulations can be run in ParaSol, *Solar transmittance* or *Energy balance.* The solar transmittance simulation calculates the *g* and the *T-values* (i.e. total and primary solar energy transmittance) for the active sunshade-window system in a room at a specified site while the energy balance simulation calculates insolation, peak heating and cooling loads, daily annual heating and cooling demands for the room and specified site. Both simulations are dynamic and hourly for a period of one year.

The *Help* button gives overall information about the form.

5.9 Solar transmittance

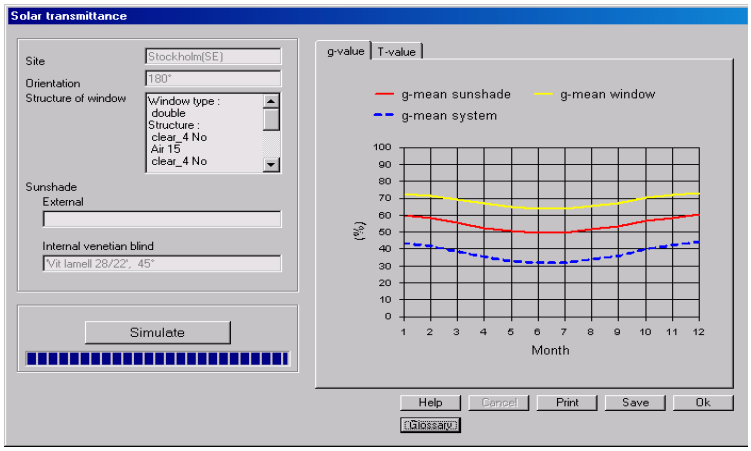

Fig. 5.10 Solar transmittance.

Input data is based on default values for HVAC parameters like thermostat setpoints, internal loads, infiltration rates, temperatures and flow rates for inlet air.

Monthly mean values for g and T are calculated for the system sunshade-window. The values displayed can be saved in a file for later use in other programs. A screen dump of the form can be printed.

5.10 Energy balance

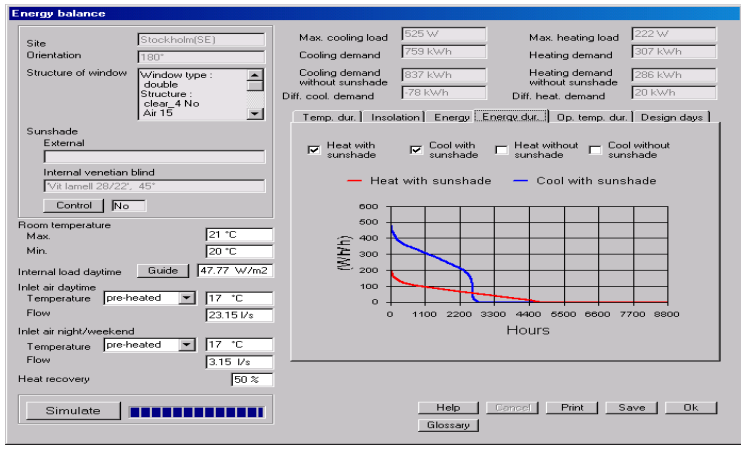

Fig. 5.11 Energy balance.

The energy balance simulation needs more detailed input data compared with a solar transmittance simulation. The types of input data needed for the room are :

- Max. and/or min. temperatures for heating and/or cooling the room (°C). The temperatures are valid for the whole period of simulation.
- Internal loads (W/m^2). Default values are calculated in accordance with the Swedish Building Regulations BBR. The internal loads are valid for daytime (08.00-17.00 Mon. - Fri.) only. There are no internal loads during night/weekend (00.00-08.00 and 17.00-24.00 Mon. - Fri. ; 00.00-24.00 Sat. - Sun.).
- HVAC functions for ventilation and recovery of energy for heating and cooling the room.

The HVAC functions can be illustrated as follows:

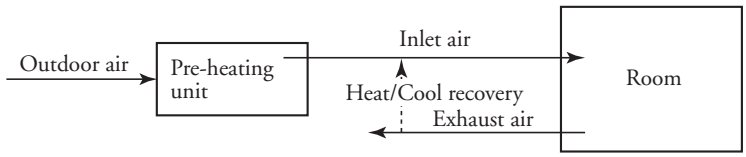

- Temperatures and flows of the inlet air for the room. The temperature and flow are given in two separate entries for daytime (08.00-17.00 Mon. - Fri.) and night/weekend (00.00-08.00 and 17.00-24.00 Mon. - Fri.; 00.00-24.00 Sat. - Sun.). The inlet temperature can either be given a constant value (for example 17°C) or set equal to the outdoor temperature. The flow of the inlet air is equal to the flow of the exhaust air. Default flow rates from the preheating unit to the room are calculated in accordance with the Swedish Building Regulations BBR94 but can be changed as needed.
- Heat recovery. Energy for both heating and cooling the inlet air is recovered to the room (%). The given value is valid for the whole period of simulation. However, it only affects the energy balance, the inlet air temperature is defined by the settings for the inlet air.

- Control of sunshades

  Two different strategies have been implemented:
  - No control, active sunshades are on at all times.
  - Control based on direct solar radiation intensity incident on the window without external sunshades. A limit value is given in kLux (1000 Lux). During hours when the direct solar radiation intensity incident on the window exceeds this limit, all active sunshades are on, otherwise off. Both external and interpane /internal sunshades are controlled simultaneously.

The following results are displayed:
Single values for the simulated period:

- Max cooling load with sunshades (W)
- Max heating load with sunshades (W)
- Max cooling load without sunshades (W)
- Cooling demand with sunshades (kWh)
- Heating demand with sunshades (kWh)
- Cooling demand without sunshades (kWh)
- Heating demand without sunshades (kWh)

- Difference in cooling demand with and without sunshades (kWh)
- Difference in heating demand with and without sunshades (kWh)

Diagrams:

- Indoor air temperatures – duration diagram (°C)
- Energy loads for heating and cooling – duration diagram (Wh/h)
- Global operative temperatures – duration diagram (°C)
- Daily sums of energy demands for heating and cooling with and without sunshades (Wh/day)
- Daily sum of primary transmitted solar radiation incident into the room (Wh/day)
- Design days for heating and cooling loads (the maximum values for the simulation period) with sunshades.

The values displayed can be saved to a text file for further analysis or later use in other programs e.g. a spreadsheet program. A screen dump of the form can be printed.

5.11 Product information

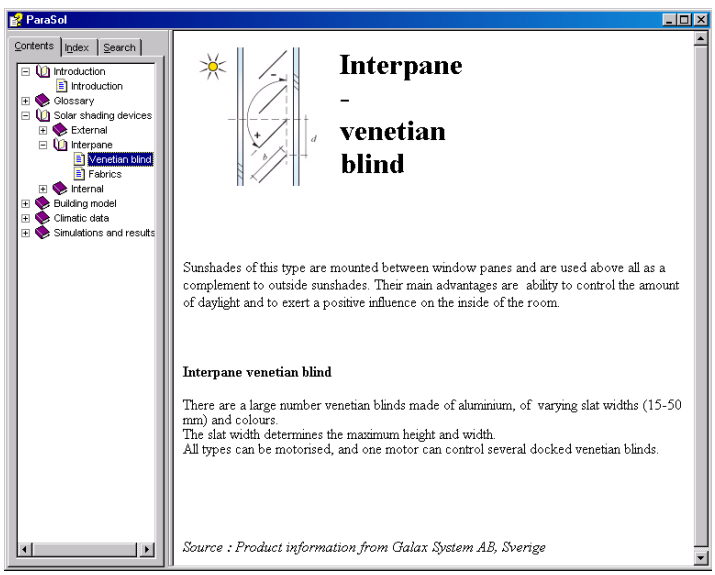

Fig. 5.12 Product information – main form.

In each form there is an entry for product information about the sunshade. The same information is also accessible from the main form.

5.12 Future work

Version 2.0 of this program has been completed in a Swedish and English version. Physical solar radiation models for the combination of external and interpane or internal sunshades and a window have been developed and implemented in the user interface and the DEROB-LTH simulation engine. Control of sunshades and scheduled inlet air temperatures and flows have been implemented as well.

There are still a number of improvements to be discussed and implemented in coming releases of ParaSol:

- Additional strategies for controlling sunshades should be added.
- A new structure and interface for the window, glass, and gas libraries is desirable.
- Capability to change the boundary (e.g. environmental) conditions for the calculations of the U, g and T_{sol} values for the system sunshades-window. External sunshades will be included in the calculation. The current calculations are based on a draft international standard (ISO/DIS 15099) and will be upgraded as soon as a final standard is available.
- A more detailed description of the types of wall and frame constructions available is desired.
- Simulation models for sunshades in ventilated cavities need to be developed.
- A more homogeneous documentation of input data and results for a simulation is needed, to save or print out as a product information sheet.
- Functions for comparisons between different simulations need to be implemented.
- Presentation of statistics for the energy demand of the air conditioning unit needs to be added to the energy simulation.
- It should be possible to combine external, interpane and internal sunshades in a system.

6 Comparison of ParaSol results with measurements

Bengt Hellström

Different sunshade products have been measured both outdoors in the twin-boxes and indoors with the solar simulator device. Others have only been measured outdoors. Comparisons between the measurements and the ParaSol results have been made for products for which we have obtained optical properties from spectral measurements at the Ångström Laboratory in Uppsala.

In all measurements, two pane windows have been used. For the measurements with interpane sunshades, the air gap between the panes was 30 mm. For the internal sunshades, it was 12 mm. For the interpane measurements indoors, the thickness of the two glass panes was 1.7 mm, while in all other cases, 4 mm clear glass panes were used.

Results from measurements and simulations/calculations are in most cases given as percentages. Differences between the results are likewise mostly given as percentages, and in all cases they are absolute, not relative percentages.

For the venetian blinds, a 80° slat angle corresponds to closed slats and 0° to horizontal slats.

A negative slat angle means that, seen from the inside, the slats are turned upwards, providing a view of the sky.

6.1 Results for fabrics with interpane mounting

"**White Texienne**" (H 925-90, double coating), a white and almost opaque fabric, was measured both outdoors in the twin-boxes and indoors with the solar simulator device. The product was also measured optically (in the solar wavelength range, 0.3-2.5 μm) with the following results: R = 0.82, T = 0.06, A = 0.12. The diffuse parts were not meas-

ured, but all of the reflectance (R) and transmittance (T) were assumed to be diffuse. The emittance (E) was not measured either, but was assumed to be 0.9. The results for the interpane application are as follows:

For normal incidence of the solar radiation and standardized conditions, the ParaSol calculations give: g_{system}: 13.2% and g_{window}: 76.9%, which by division gives $g_{sunshade}$: **17.2**%.

In Figure 6.1.a, indoor measurement results of $g_{sunshade}$, using the solar simulator, are shown. The values are at normal incidence **18.7**%, on average 18.5% for 0-20° and 17.0% for 40-60° angle of incidence.

In Figure 6.1.b, outdoor measurements of the twin boxes are shown. The energy weighted average values for 990507, 8:00-16:00 were: g_{system}: 9.3%, g_{window}: 64.5%, $g_{sunshade}$: **14.4**%.

In Figure 6.1.c, the results of the ParaSol simulations are shown. Energy weighted average values for May are: g_{system}: 10.2%, g_{window}: 61.6%, $g_{sunshade}$: **16.6**%. The $g_{sunshade}$ values are almost independent of the season (indicating that they are also almost independent of the angle of incidence).

The indoor measurements for normal incidence gave a $g_{sunshade}$ value 1.5% higher than the ParaSol calculated result.

At higher angles of incidence the $g_{sunshade}$ value of the indoor measurements drops. For the outdoor measurements this would correspond to lower values in the morning and the late afternoon, since the angle of incidence then is larger than at noon. This is however not found, the tendency is rather the opposite. Also in the ParaSol simulation results, the mean $g_{sunshade}$ values are slightly higher for the summer months, when the average angle of incidence is higher, than for the winter months.

The outdoor measurements gave an average $g_{sunshade}$ value for 990507, 8:00-16:00 which was 2.2% lower than the ParaSol simulation value for May, but the value is drifting during the day.

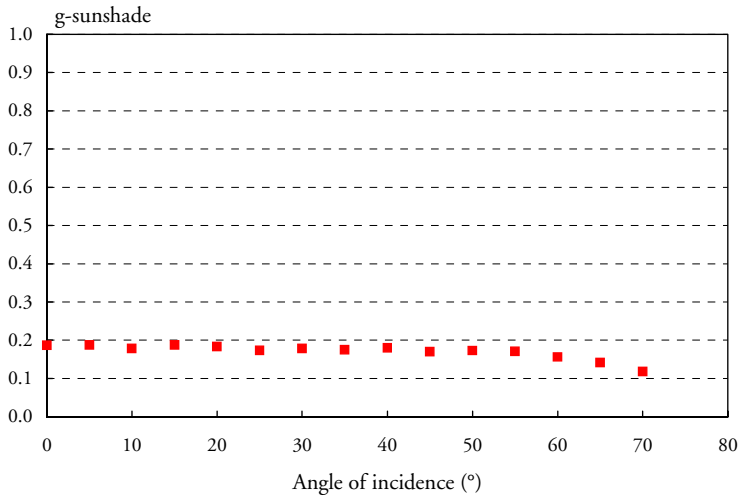

Figure 6.1.a $g_{sunshade}$ *for "White Texienne", interpane mounted, measured with the solar simulator.*

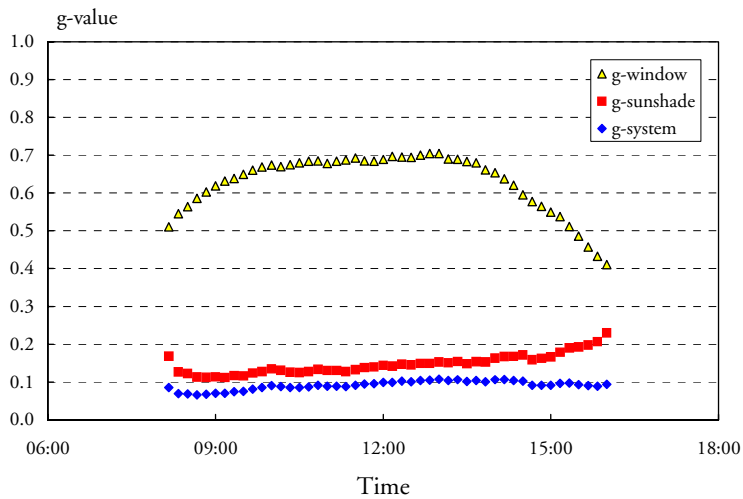

Figure 6.1.b *g-values for "White Texienne", interpane mounted, measured in the twin boxes, 990507, 8:00-16:00.*

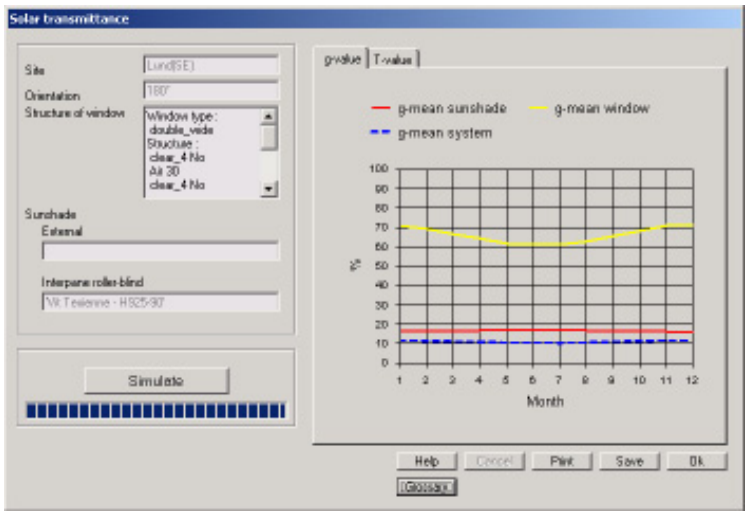

Figure 6.1.c *Monthly mean g-values for "White Texienne", interpane mounted, from ParaSol simulations.*

6.2 Results for fabrics with internal mounting

"White Texienne" (H 925-90) was measured also when mounted on the inside of the window. Here are the results:

For normal incidence of the solar radiation and standardized conditions, the ParaSol calculations give: g_{system}: 22.9% and g_{window}: 76.8%, which gives $g_{sunshade}$: **29.8**%.

In Figure 6.2.a, results of $g_{sunshade}$ for one indoor measurement occasion are shown. The values are on average **26**% for 0-20° and 19% for 40-60° angle of incidence .

In Figure 6.2.b, outdoor measurements of the twin boxes are shown. The energy weighted average values for 990521, 8:00-16:00 are: g_{system}: 20.2%, g_{window}: 65.3%, $g_{sunshade}$: **30.8**%.

In Figure 6.2.c, the results of the ParaSol simulations are shown. The energy weighted average values for May are: g_{system}: 18.3%, g_{window}: 61.5%, $g_{sunshade}$: **29.7**%.

The ParaSol results in this case agree well with the outdoor measurements, while the indoor measurement gave results around 4% lower at normal incidence. However, this sample was measured indoors at several times and the results varied between 24% and 30%. The variation was partly due to attempts to prevent possible intergap convection and edge

effects by sealing the sunshade and placing aluminium foil on the inner edges, but partly also due to poor repeatability. This shows that some work still remains to improve and validate the measurements of the solar simulator instrument. The outdoor measurements were also performed several times. For this product the results were rather consistent, giving a $g_{sunshade}$ value around 30%.

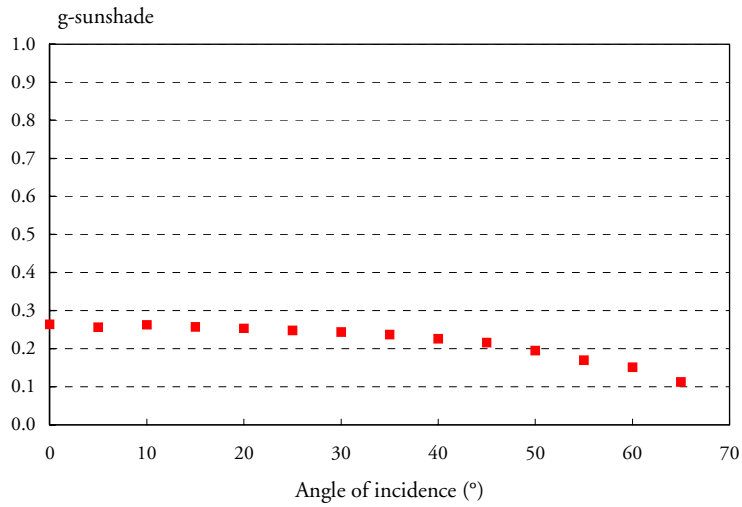

Figure 6.2.a *$g_{sunshade}$ for "White Texienne", internally mounted, measured with the solar simulator.*

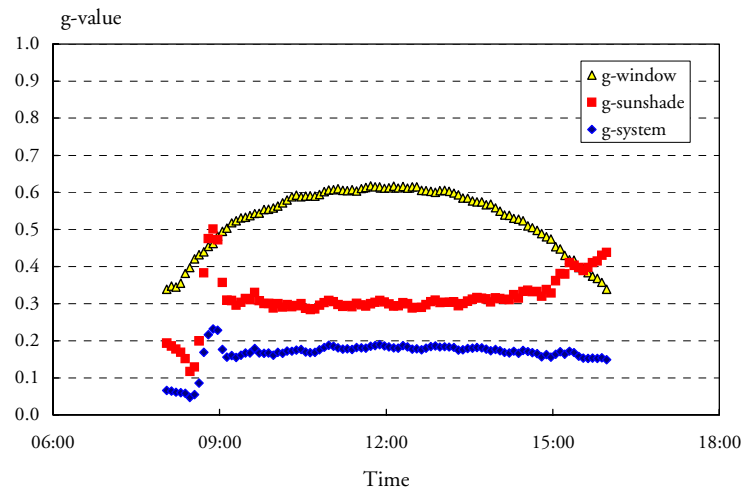

Figure 6.2.b *g-values for "White Texienne", internally mounted, measured in the twin boxes, 990521, 8:00-16:00.*

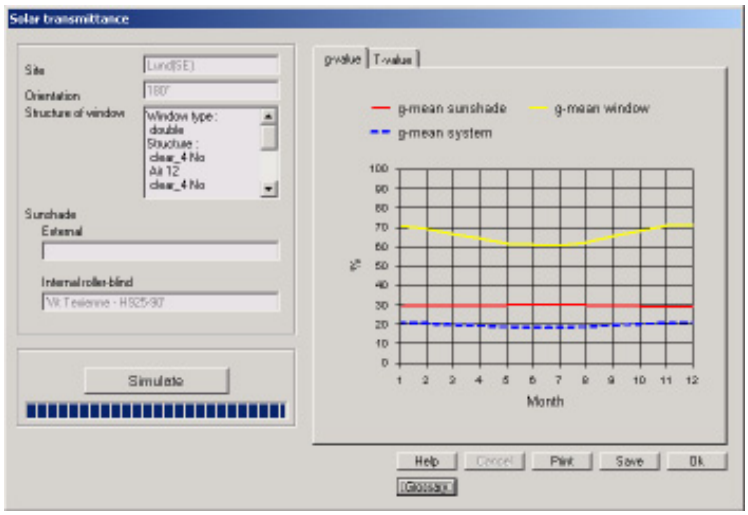

Figure 6.2.c *Monthly mean g-values for "White Texienne" internally mounted, from ParaSol simulations.*

The product "**Ombra, white thread**" is a fabric with aluminium strips covering about half the surface, with air in between, woven with a white thread. The solar optical properties for the front side have been measured to R_{spec} = 0.14, R_{diff} = 0.34, T_{dir} = 0.21, T_{diff} = 0.20, A = 0.11, while the IR properties were measured to T = 0.37, E_{front} = 0.32, E_{back} = 0.38. Here are the results for the internal mounting:

For normal incidence of the solar radiation and standardized conditions, the ParaSol calculations give: g_{system}: 46.2% and g_{window}: 76.8%. Dividing the two gives $g_{sunshade}$: **60.2**%.

In Figure 6.3.a, results of $g_{sunshade}$ for one indoor measurement occasion, using the solar simulator, are shown. The values are rather independent of angle of incidence and are on average **58.1**% for 0-60°.

In Figure 6.3.b, outdoor measurements of the twin boxes are shown. The energy weighted average values for 010522, 8:00-16:00 are: g_{system}: 41.9%, g_{window}: 64.2%, $g_{sunshade}$: **65.3**%.

In Figure 6.3.c, the results of the ParaSol simulations are shown. The energy weighted average values for May are: g_{system}: 37.6%, g_{window}: 61.5%, $g_{sunshade}$: **61.2**%.

The outdoor measured $g_{sunshade}$ value is around 4% higher than the ParaSol simulation result. The indoor measurements were performed several times and the results varied between 58% and 66%.

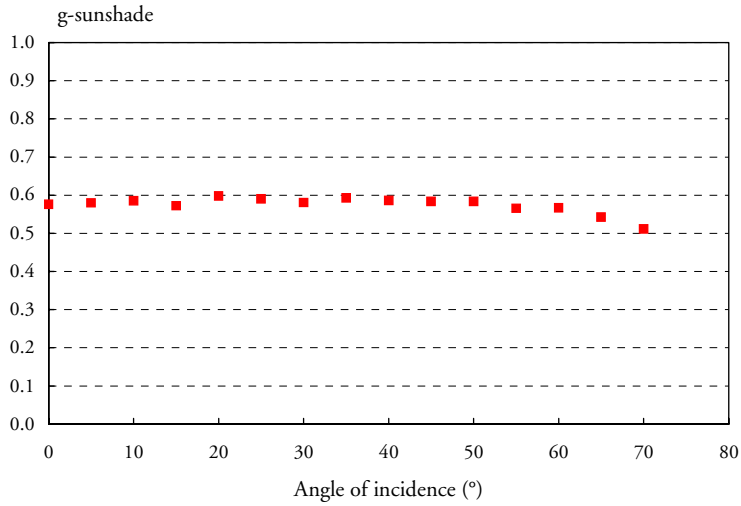

Figure 6.3.a *$g_{sunshade}$ for "Ombra, white thread", internally mounted, measured with the solar simulator.*

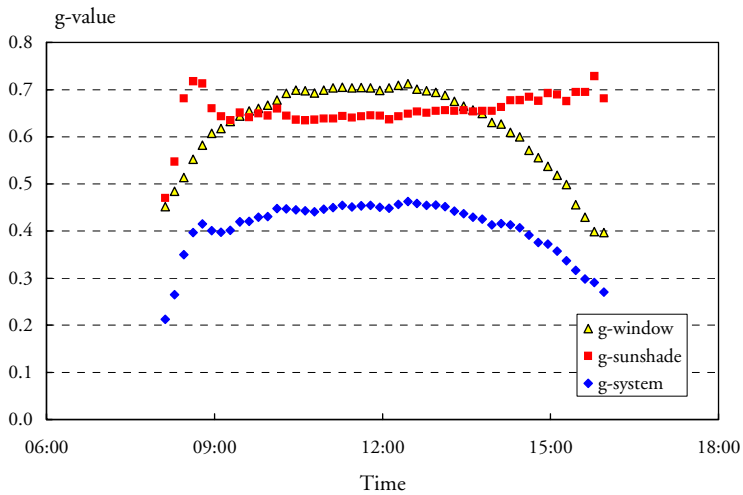

Figure 6.3.b *g-values for "Ombra, white thread", internally mounted, measured in the twin boxes, 010522, 8:00-16:00.*

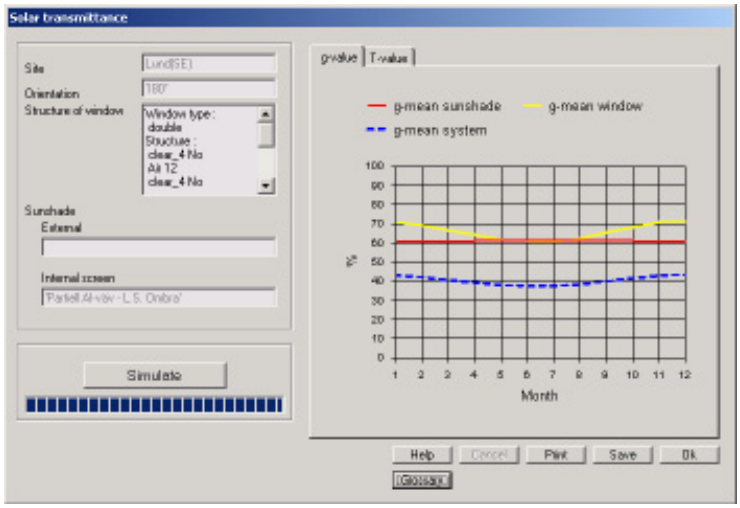

Figure 6.3.c *Monthly mean g-values from ParaSol simulations for the internal mounting of "Ombra, white thread".*

The product "**Optic**" is a fabric with aluminium strips, covering almost all the surface, which are woven with a white thread. The solar optical properties for the front (out-) side have been measured to R_{spec} = 0.28, R_{diff} = 0.54, T_{dir} = 0.01, T_{diff} = 0.03, A = 0.14, while the IR-properties were measured (at normal incidence) to T = 0.03, E_{front} = 0.24, E_{back} = 0.39. Here are the results for the inside application:

For normal incidence of the solar radiation and standardized conditions, the ParaSol calculations give: g_{system}: 18.8% and g_{window}: 76.8%, which by dividing the two gives $g_{sunshade}$: 25%.

In Figure 6.4.a, results of $g_{sunshade}$ for one indoor measurement occasion with the solar simulator are shown. The values are on average 25% for 0-20° and 26% for 40-60° angle of incidence.

In Figure 6.4.b, results are shown for one occasion of outdoor measurements in the twin boxes. The energy weighted average values for 020904, 8:00-16:00 are: g_{system}: 17.8%, g_{window}: 59.9%, $g_{sunshade}$: 29.8%.

In Figure 6.4.c, the results of the ParaSol simulations are shown. The energy weighted average values for September are: g_{system}: 18.4%, g_{window}: 65.1%, $g_{sunshade}$: 28.2%.

The simulation result agrees well with the outdoor measurement result given above. However, this was the measurement out of several with the lowest $g_{sunshade}$. The value varied between 30 and 40%. In general, higher values were obtained during summer than in spring and autumn.

If these measurements are correct, one possible explanation is that the solar absorptance of the sunshade increases with higher angle of incidence, since the angle of incidence for the direct radiation is higher in summer than in spring or autumn. Another contributing effect could be that the edge effects of the window are stronger for a specular than for a diffusely reflecting sunshade.

The calculated result at normal incidence also agrees well with the indoor measurement result, but the indoor measurements were also performed several times. The $g_{sunshade}$ values varied between 23 and 29%. This is similar to the indoor measurement results of "White Texienne" and the comments made for that product are valid also here.

The indoor measurements of the sunshade "Optic" have a tendency towards increasing values of $g_{sunshade}$ for increasing angles of incidence, as opposed to most other sunshades which have the opposite tendency. This agrees with the results from the outdoor measurements. It is however not seen in the ParaSol simulations, the reason for which could be that the program does not consider edge effects and does not (yet) handle angle dependent optical properties of the sunshades, although the simulation engine calculates angle resolved.

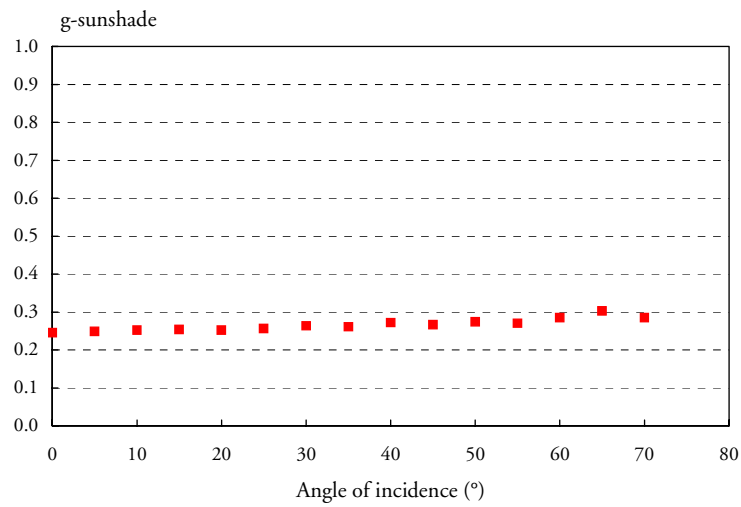

Figure 6.4.a $g_{sunshade}$ *for "Optic", internally mounted, measured with the solar simulator.*

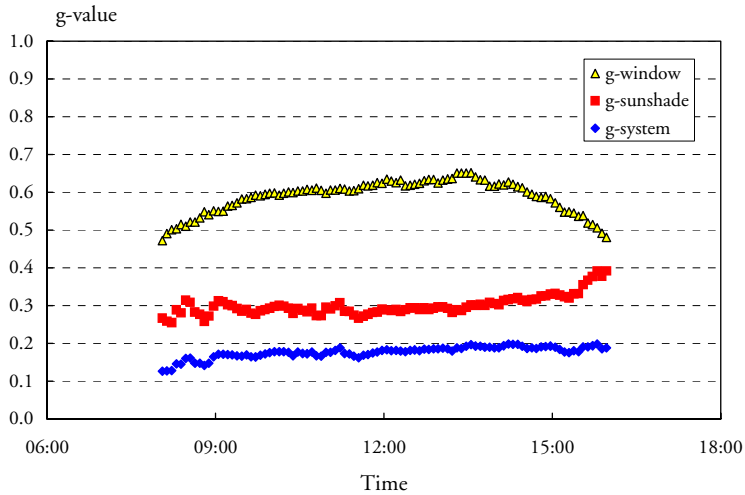

Figure 6.4.b *g-values for "Optic", internally mounted, measured in the twin boxes, 020904, 8:00-16:00.*

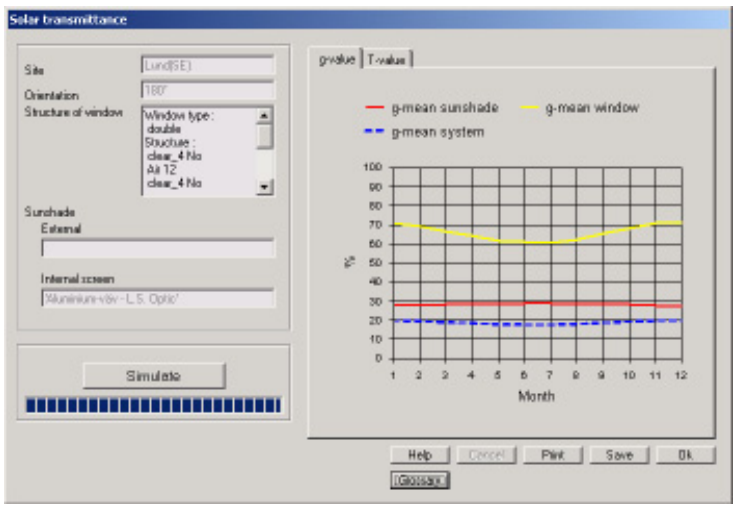

Figure 6.4.c *Monthly mean g-values for "Optic", internally mounted, from ParaSol simulations.*

Some of the products were measured outdoors, but not indoors. The results for these measurements and ParaSol simulations are shown in Figures 6.5 - 6.10, a-b.

The product "**Blue roller blind**" (H 500-54) has the solar optical properties: R_{diff} = 0.15, T_{diff} = 0.04, A = 0.81, while the emittance is assumed to be 0.9. Here are the results for the inside application:

For normal incidence and standardized conditions, the ParaSol calculations give: g_{system}: 52.5% and g_{window}: 76.8%, which by dividing the two gives $g_{sunshade}$: 68.4%.

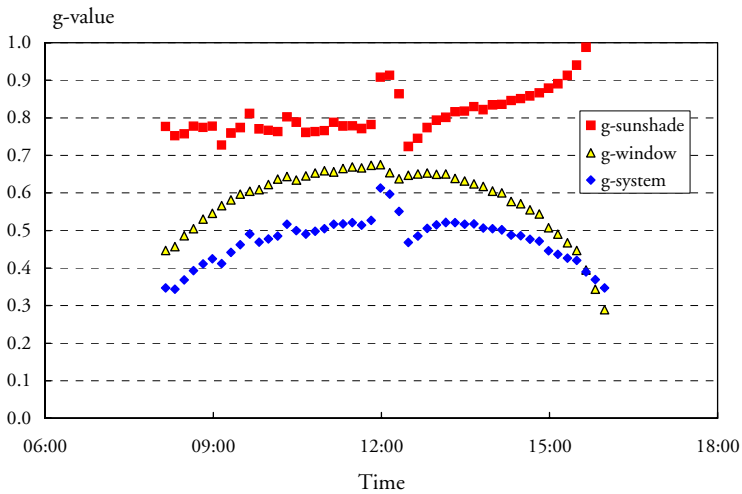

Figure 6.5.a *g-values for "Blue roller-blind", internally mounted, measured in the twin boxes, 010725, 8:00-16:00.*

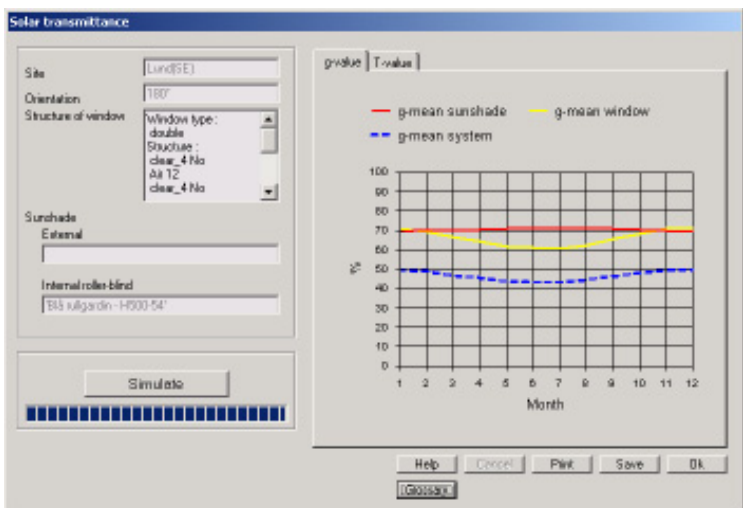

Figure 6.5.b *Monthly mean g-values for "Blue roller-blind", internally mounted, from ParaSol simulations.*

In Figure 6.5.a, outdoor measurement results are shown. The energy weighted average values for 010725, 8:00-16:00 are: g_{system}: 48.5%, g_{window}: 60.0%, $g_{sunshade}$: **80.9**%. Some disturbance obviously occurs at noon. For the first half day, $g_{sunshade}$ is on average 77.4%.

In Figure 6.5.b, the results of the ParaSol simulations are shown. The energy weighted average values for July are: g_{system}: 42.9%, g_{window}: 60.6%, $g_{sunshade}$: **70.8**%.

The product "**White roller blind**" (H 500-90) has the solar optical properties: R_{diff} = 0.58, T_{diff} = 0.37, A = 0.05, while the emittance is assumed to be 0.9. Here are the results for the inside application:

For normal incidence and standardized conditions, the ParaSol calculations give: g_{system}: 40.9% and g_{window}: 76.8%, which by dividing the two gives $g_{sunshade}$: **53.3**%.

In Figure 6.6.a, outdoor measurement results are shown. The energy weighted average values for 010719, 8:00-16:00 are: g_{system}: 32.7%, g_{window}: 60.3%, $g_{sunshade}$: **54.2**%.

In Figure 6.6.b, the results of the ParaSol simulations are shown. The energy weighted average values for July are: g_{system}: 32.1%, g_{window}: 60.6%, $g_{sunshade}$: **52.8**%.

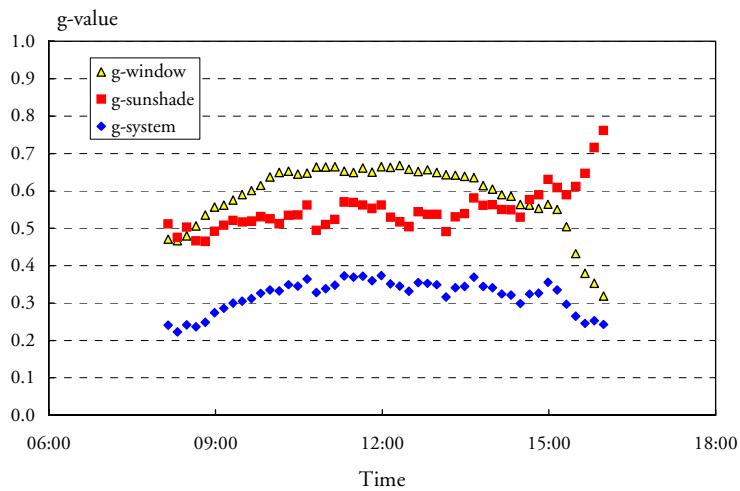

Figure 6.6.a *g-value for "White roller-blind", internally mounted, measured in the twin boxes, 010719, 8:00-16:00.*

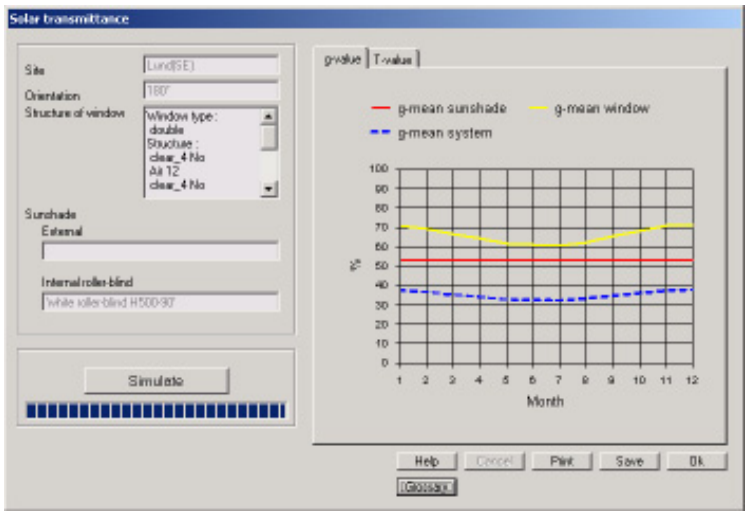

Figure 6.6.b *Monthly mean g-values for "White roller-blind", internally mounted, from ParaSol simulations.*

The product "**Silver-grey blind**" (H 981-95) has the solar optical properties: R_{spec} = 0.30, R_{diff} = 0.29, T_{diff} = 0.05, A = 0.36, while the emittance is assumed to be 0.9. The diffuse parts were not measured, but the reflectance was assumed to be around 50% specular. Applied on the inside, the results were:

For normal incidence and standardized conditions, the ParaSol calculations give: g_{system}: 33.1% and g_{window}: 76.8%, which by dividing the two gives $g_{sunshade}$: **43.1**%.

In Figure 6.7.a, outdoor measurement results are shown. The energy weighted average values for 010608, 8:00-16:00 are: g_{system}: 32.1%, g_{window}: 61.9%, $g_{sunshade}$: **51.8**%.

In Figure 6.7.b, the results of the ParaSol simulations are shown. The energy weighted average values for June are: g_{system}: 27.0%, g_{window}: 60.9%, $g_{sunshade}$: **44.3**%.

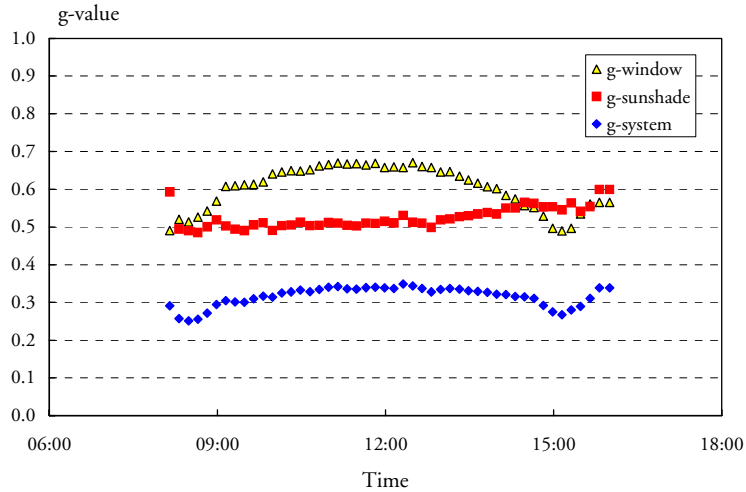

Figure 6.7.a *g-values for "Silver-grey blind", internally mounted, measured in the twin boxes, 010608, 8:00-16:00.*

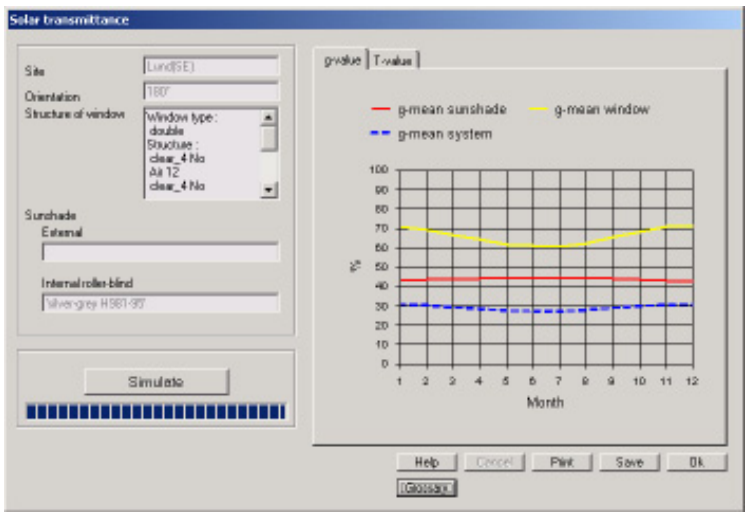

Figure 6.7.b *Monthly mean g-values for "Silver-grey blind" internally mounted, from ParaSol simulations.*

The product "**White-grey Texienne**" (H 927-95) has the solar optical properties: R_{diff} = 0.78, T_{diff} = 0.05, A = 0.17, while the emittance is assumed to be 0.9. Applied on the inside, the results were:

For normal incidence and standardized conditions, the ParaSol calculations give: g_{system}: 24.8% and g_{window}: 76.8%, which by dividing the two gives $g_{sunshade}$: **32.3**%.

In Figure 6.8.a, outdoor measurement results are shown. The energy weighted average values for 010704, 8:00-16:00 are: g_{system}: 21.2%, g_{window}: 58.3%, $g_{sunshade}$: **36.3**%. For the first half day, $g_{sunshade}$ is on average 34.9%.

In Figure 6.8.b, the results of the ParaSol simulations are shown. The energy weighted average values for July are: g_{system}: 19.6%, g_{window}: 60.6%, $g_{sunshade}$: **32.4**%.

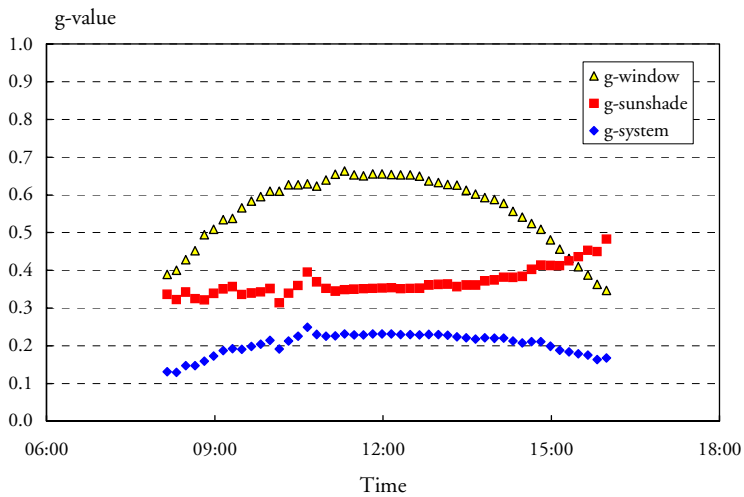

Figure 6.8.a *g-values for "White-grey Texienne", internally mounted, measured in the twin boxes, 010704, 8:00-16:00.*

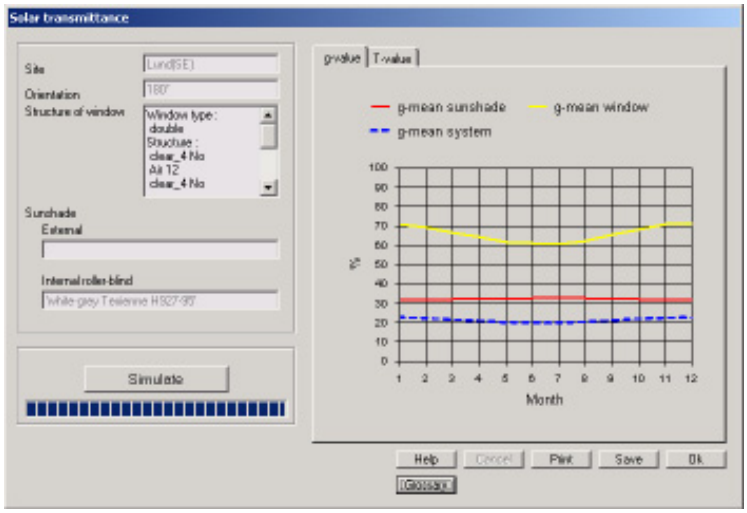

Figure 6.8.b *Monthly mean g-values for "White-grey Texienne", internally mounted, from ParaSol simulations.*

The product "**Ombra, black thread**" (H 542-98) has the solar optical properties for the front side: R_{spec} = 0.16, R_{diff} = 0.16, T_{dir} = 0.19, A = 0.49. The diffuse parts of the optical properties were not measured, but the reflectance was assumed to be around 50 % specular and the transmittance was assumed to be 100% direct. The IR properties were not measured either, but were set to the same values as the corresponding solar properties, which means emittance = 0.49 and IR-transmittance = 0.19. The assumed properties are not critical for the results. With the product applied on the inside, the results were:

For normal incidence and standardized conditions, the ParaSol calculations give: g_{system}: 49.4% and g_{window}: 76.8%, which by dividing the two gives $g_{sunshade}$: **64.3**%.

In Figure 6.9.a, outdoor measurement results are shown. The energy weighted average values for 010625, 8:00-16:00 are: g_{system}: 48.4%, g_{window}: 63.0%, $g_{sunshade}$: **76.9**%. For the first half day, $g_{sunshade}$ is on average 73.8%.

In Figure 6.9.b, the results of the ParaSol simulations are shown. The energy weighted average values for June are: g_{system}: 39.5%, g_{window}: 60.9%, $g_{sunshade}$: **64.9**%.

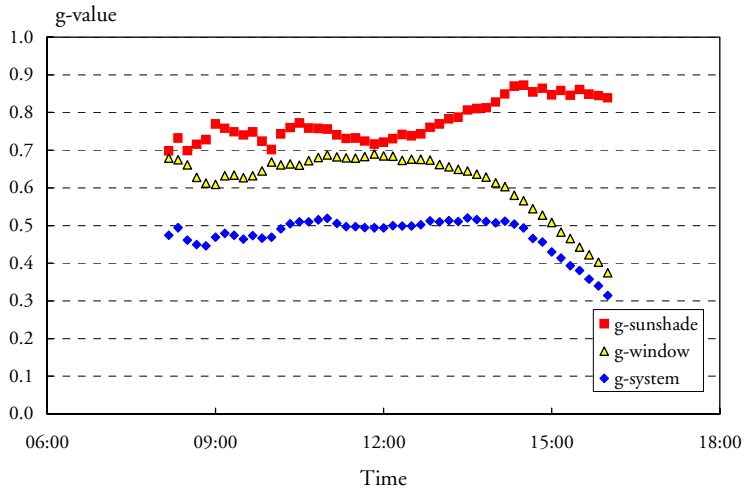

Figure 6.9.a *g-values for "Ombra, black thread", internally mounted, measured in the twin boxes, 010625, 8:00-16:00.*

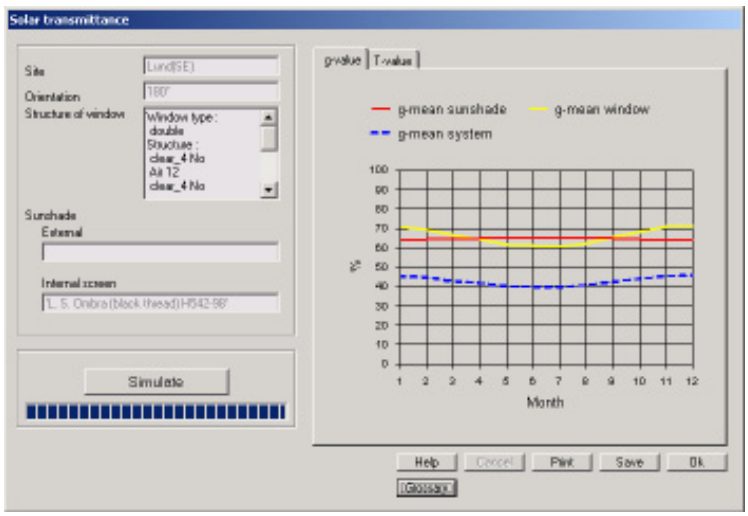

Figure 6.9.b *Monthly mean g-values for "Ombra, black thread", internally mounted, from ParaSol simulations.*

For the above five products, the results of the outdoor measurements are 1.4 – 12% higher than for the ParaSol simulations. However, there is a strong correlation between the difference and the absorptance of the material. The largest differences are obtained for the darkest sunshades. For the two products with the lowest absorptance, the difference is on average less than 3%.

The reason for this is probably that for absorbing solar shading materials, placed on the inside of the window, the *g*-value is very sensitive to the heat transfer coefficient between the solar shading and the room. If the heat transfer coefficient is large, the *g*-value also becomes high. In the twin boxes , the convective part of heat transfer coefficient might be higher than what is assumed in the simulations, due to a fan which blows the air along the absorber in the box. An air change due to convection between the air gaps on both sides of the sunshade could also give a larger *g*-value.

6.3 Results for venetian blinds with interpane mounting

The product "**White slat 28/22**", a white venetian blind with slat spacing of 22 mm and width of 28 mm has the measured solar optical properties: R = 0.67, A = 0.33. The diffuse part of the reflectance was not measured, but is here assumed to be 100%. The emittance was not measured either and is assumed to be 0.9. The outdoor measurements will be compared first and thereafter also the indoor measurements.

The results for **80°** slat angle and interpane position were:

In Figure 6.10.a, the outdoor measurements are shown. The energy weighted average values for the measured day 020314, 9:30-16:00 are: g_{system}: 17.4%, g_{window}: 71.2%, $g_{sunshade}$: **24.4**%.

In Figure 6.10.b, the results of the ParaSol simulations are shown. The energy weighted average values for March are: g_{system}: 14.0%, g_{window}: 66.5%, $g_{sunshade}$: **21.1**%.

The results for **45°** slat angle and interpane position were:

In Figure 6.11.a, outdoor measurements are shown. The energy weighted average values for the measured day 020309, 9:00-16:00 are: g_{system}: 27.0%, g_{window}: 72.3%, $g_{sunshade}$: **37.3**%. For the first half day, $g_{sunshade}$ is on average 33.8%.

In Figure 6.11.b, the results of the ParaSol simulations are shown. The energy weighted average values for March are: g_{system}: 21.9%, g_{window}: 66.5%, $g_{sunshade}$: **32.9**%.

The results for **0°** slat angle and interpane position were:

In Figure 6.12.a, outdoor measurements are shown. The energy weighted average values for the measured day 020324, 8:00-16:00 are: g_{system}: 45.9%, g_{window}: 70.0%, $g_{sunshade}$: 65.6%.

In Figure 6.12.b, the results of the ParaSol simulations are shown. The energy weighted average values for March are: g_{system}: 40.5%, g_{window}: 66.5%, $g_{sunshade}$: 60.9%. For April they are: g_{system}: 33.3%, g_{window}: 64.3%, $g_{sunshade}$: 51.8%. Interpolation to an average for 020324 gives: g_{system}: 38.5%, g_{window}: 65.9%, $g_{sunshade}$: 58.4%.

The outdoor measurements for 80° slat angle are around 3% higher than the simulated result, around 4-5% higher for 45° and around 7% higher for 0°. The higher difference for the smaller slat angles can maybe partly be explained by a higher sensitivity to the vertical angle of incidence (which corresponds to the solar altitude angle, projected in the south-vertical plane). The outdoor measurements are performed during a sunny day, while the simulations are made for a whole month, including cloudy days. In March, the south-vertical projected solar altitude in Lund is around 30° - 40° all day, which is lower than the average for a cloudy day. A lower angle corresponds to a larger $g_{sunshade}$ (and a larger g_{window}, see the results above).

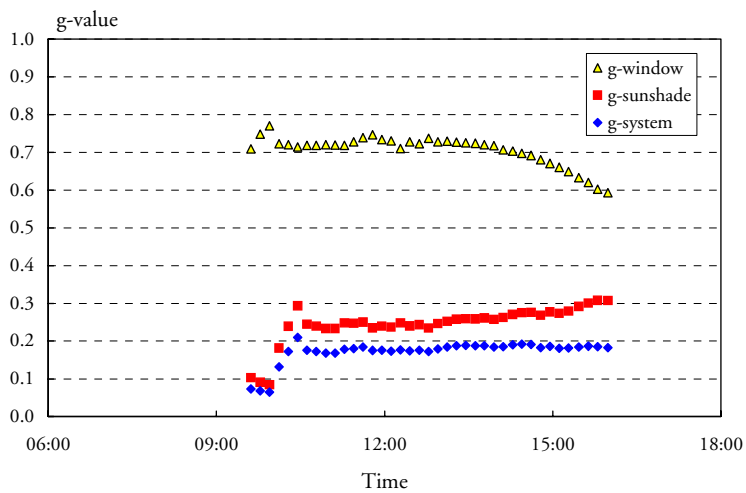

Figure 6.10.a *g-values of "White slat 28/22", interpane mounted, 80° slat angle, measured in the twin boxes, 020314, 9:30-16:00.*

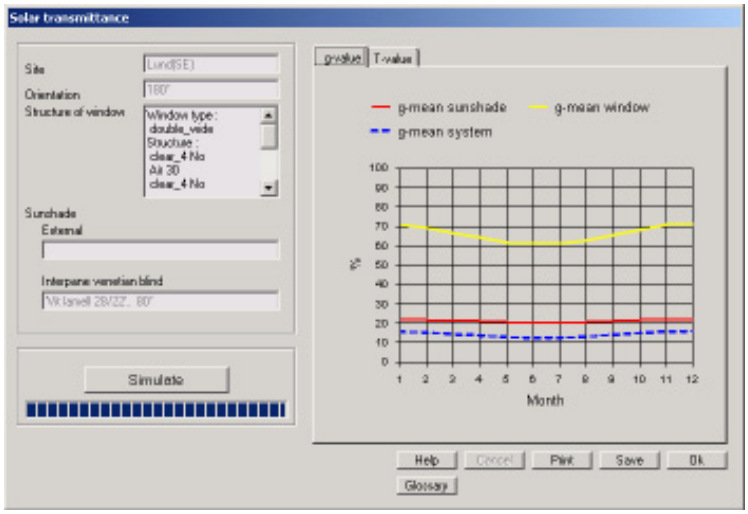

Figure 6.10.b Monthly mean g-values of "White slat 28/22", interpane mounted, 80° slat angle, from ParaSol simulations.

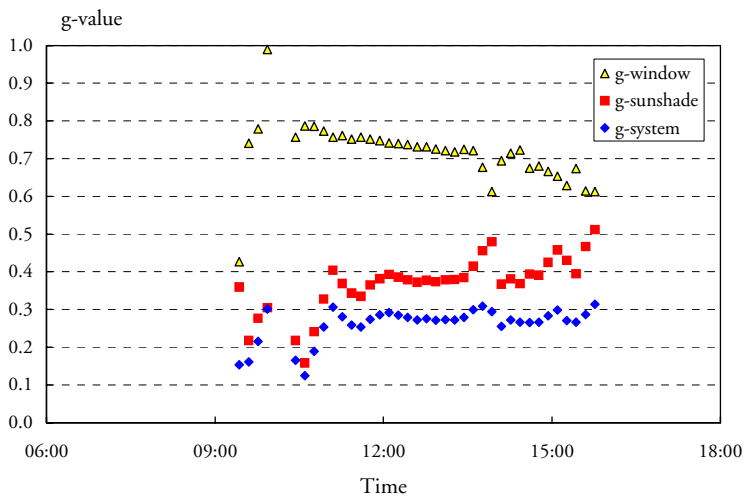

Figure 6.11.a g-values of the interpane sunshade: "White slat 28/22", 45° slat angle, measured in the twin boxes, 020309, 9:00-16:00.

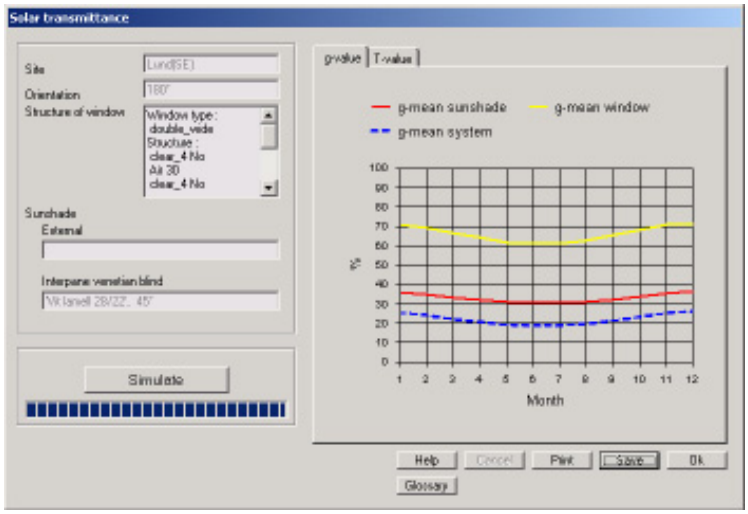

Figure 6.11.b Monthly mean g-values of the inside sunshade "White slat 28/22", 45° slat angle, from ParaSol simulations.

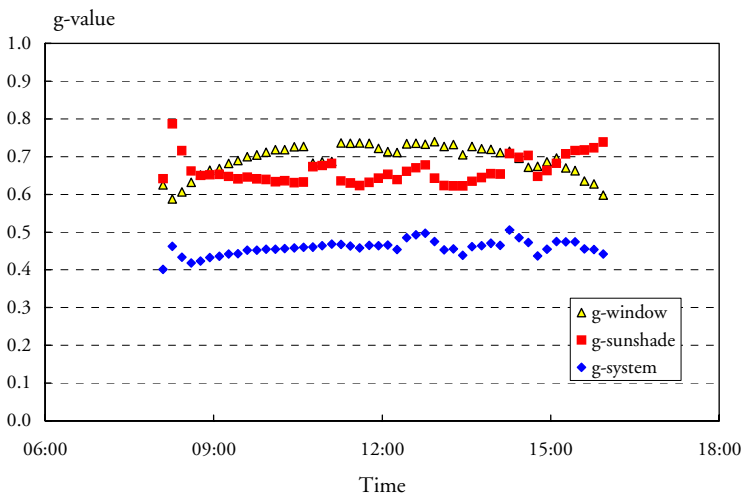

Figure 6.12.a g-values of the interpane sunshade: "White slat 28/22", 0° slat angle, measured in the twin boxes, 020324, 8:00-16:00.

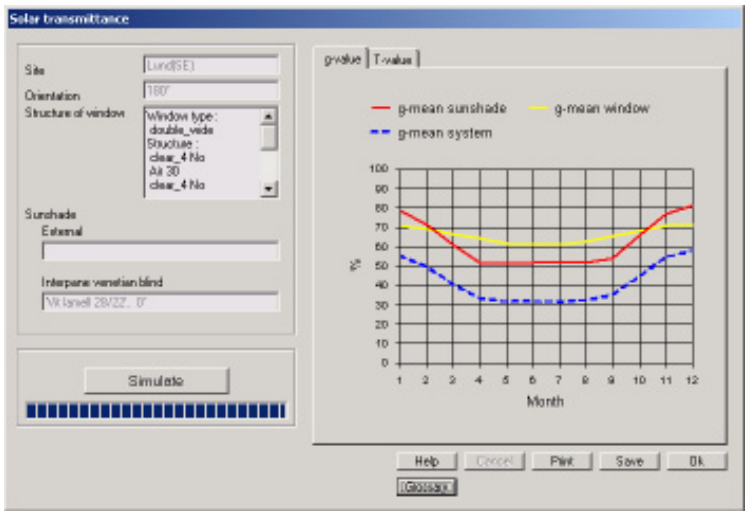

Figure 6.12.b Monthly mean g-values of the interpane sunshade "White slat 28/22", 0° slat angle, from ParaSol simulations.

The indoor measurements for "**White slat 28/22**" should be compared with the ParaSol calculated result at normal incidence.

The results for **80°** slat angle and interpane position were:

For normal incidence and standardized conditions, the ParaSol calculations give: g_{system}: 19.2% and g_{window}: 76.9%, which by dividing the two gives $g_{sunshade}$: **25.0%**.

In Figure 6.13, indoor measurement results of $g_{sunshade}$, using the solar simulator, are shown. At normal incidence, the measured value is **28.7%**.

The results for **45°** slat angle and interpane position were:

For normal incidence and standardized conditions, the ParaSol calculations give: g_{system}: 36.4% and g_{window}: 76.9%, which by dividing the two gives $g_{sunshade}$: **47.3%**.

In Figure 6.13, indoor measurement results of $g_{sunshade}$, using the solar simulator, are shown. At normal incidence, the measured value is **50.2%**.

The results for **0°** slat angle and interpane position were:

For normal incidence and standardized conditions, the ParaSol calculations give: $g_{system} = g_{window}$ = 76.9%, which gives $g_{sunshade}$: **100%**.

In Figure 6.13, indoor measurement results of $g_{sunshade}$, using the solar simulator, are shown. At normal incidence, the measured value is **95.5%**.

The results for **-45°** slat angle and interpane position were:

For normal incidence and standardized conditions, the ParaSol calculations give: g_{system}: 36.4% and g_{window}: 76.9%, which by dividing the two gives $g_{sunshade}$: **47.3%**.

In Figure 6.13, indoor measurement results of $g_{sunshade}$, using the solar simulator, are shown. At normal incidence, the measured value is **47.5%**.

Except for 0° slat angle, the solar simulator measured results for the white venetian blind at normal incidence are 0-4% higher, on average 2% higher than the ParaSol calculated results.

To reach the theoretical $g_{sunshade}$ value 100% for 0° slat angle, perfectly parallel light and non-curved slats are required. Since none of these requirements are fulfilled, this could partly explain the 4.5% lower measured value.

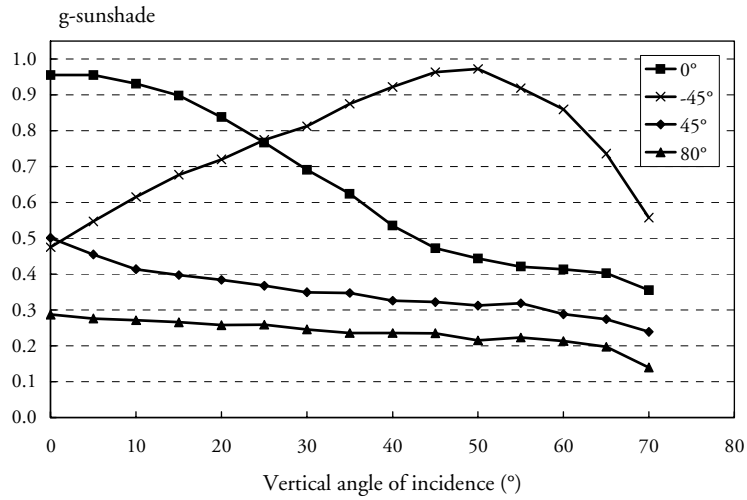

Figure 6.13 *$g_{sunshade}$ measured with the solar simulator for the interpane mounting of "White slat 28/22" with the slat angles 0, 45, 80 and -45°.*

The product "**Blue slat 28/22**", a blue venetian blind with slat spacing of 22 mm and width of 28 mm has the measured optical properties: R = 0.19, A = 0.81. The diffuse part of the reflectance was not measured, but is here assumed to be 100%. Neither was the emittance measured, but was set to 0.9. The outdoor measurements will be compared first and thereafter also the indoor measurements.

The results for **80°** slat angle and interpane position were:

In Figure 6.14.a, the outdoor measurement results are shown. The energy weighted average values for 020217, 8:30-16:00 are: g_{system}: 30.1%, g_{window}: 71.0%, $g_{sunshade}$: 42.5%. For the first half day, $g_{sunshade}$ is on average 37.2%.

In Figure 6.14.b, the results of the ParaSol simulations are shown. The energy weighted average values for February are: g_{system}: 26.7%, g_{window}: 69.3%, $g_{sunshade}$: 38.5%.

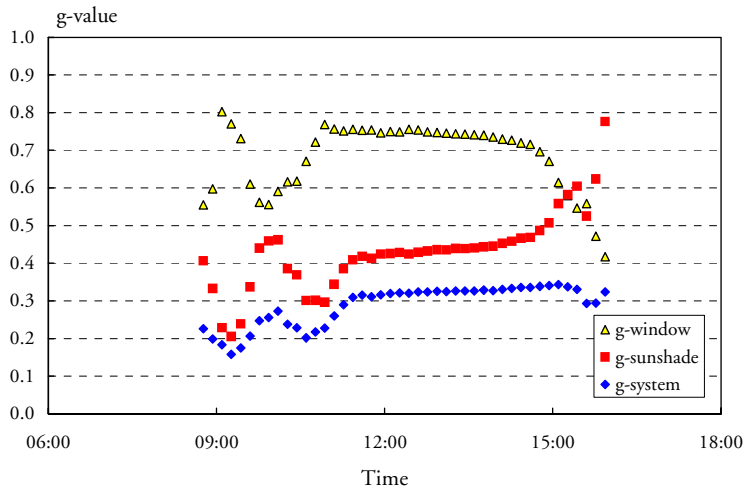

Figure 6.14.a *g-values of the interpane sunshade: "Blue slat 28/22", 80° slat angle, measured in the twin boxes, 020217, 8:30-16:00.*

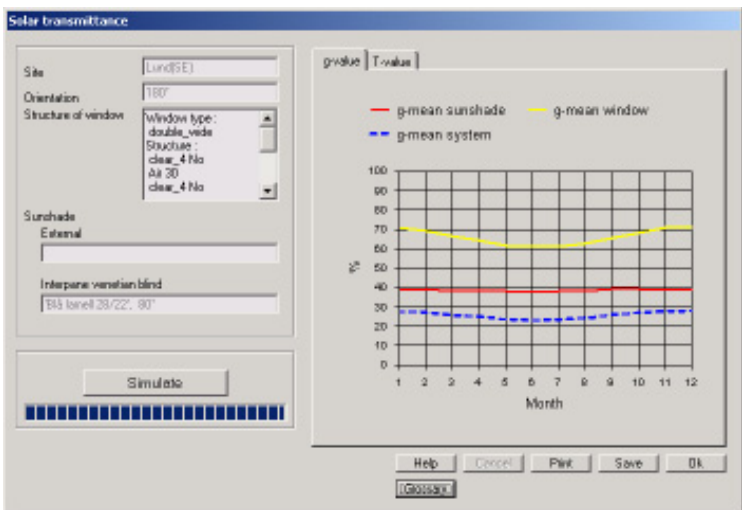

Figure 6.14.b *Monthly mean g-values of the interpane sunshade "Blue slat 28/22", 80° slat angle, from ParaSol simulations.*

The results for 45° slat angle and interpane position were:

In Figure 6.15.a, the outdoor measurement results are shown. The energy weighted average values for 020214, 8:00-16:00 are: g_{system}: 35.0%, g_{window}: 71.4%, $g_{sunshade}$: 49.0%.

In Figure 6.15.b, the results of the ParaSol simulations are shown. The energy weighted average values for Februry are: g_{system}: 28.8%, g_{window}: 69.3%, $g_{sunshade}$: 41.6%.

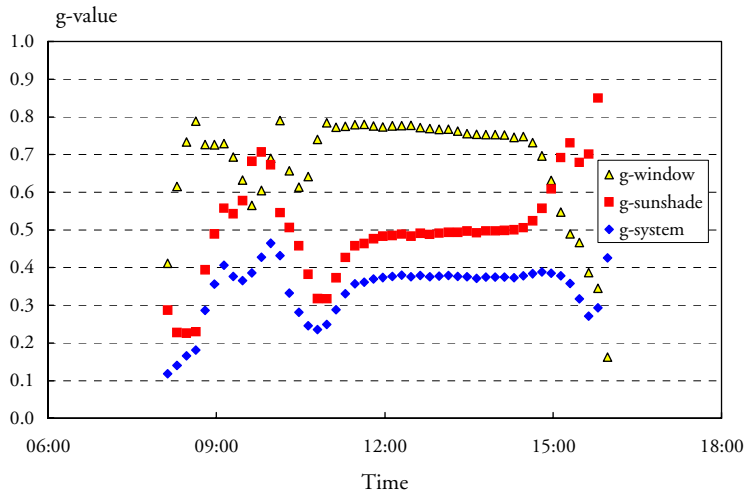

Figure 6.15.a g-values of the interpane sunshade: "Blue slat 28/22", 45° slat angle, measured in the twin boxes, 020214, 8:00-16:00.

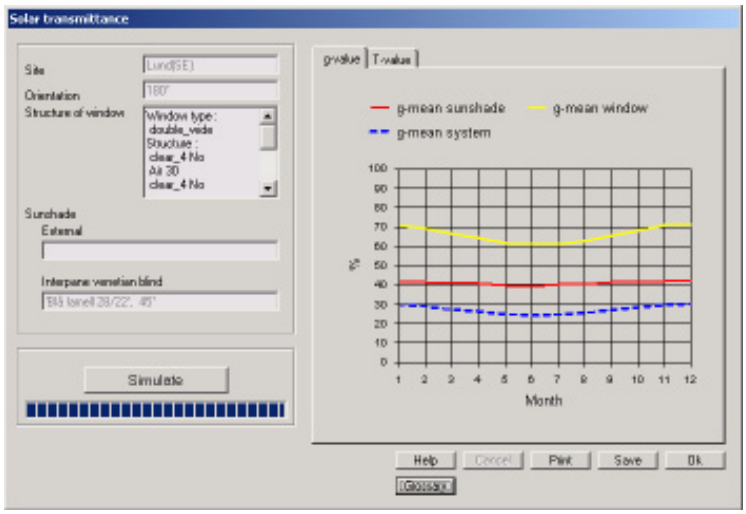

Figure 6.15.b Monthly mean g-values of the interpane sunshade "Blue slat 28/22", 45° slat angle, from ParaSol simulations.

The results for **0°** slat angle and interpane position were:

In Figure 6.16.a, the outdoor measurement results are shown. The energy weighted average values for 020305, 10:00-16:00 are: g_{system}: 51.0%, g_{window}: 72.5%, $g_{sunshade}$: **70.3**%.

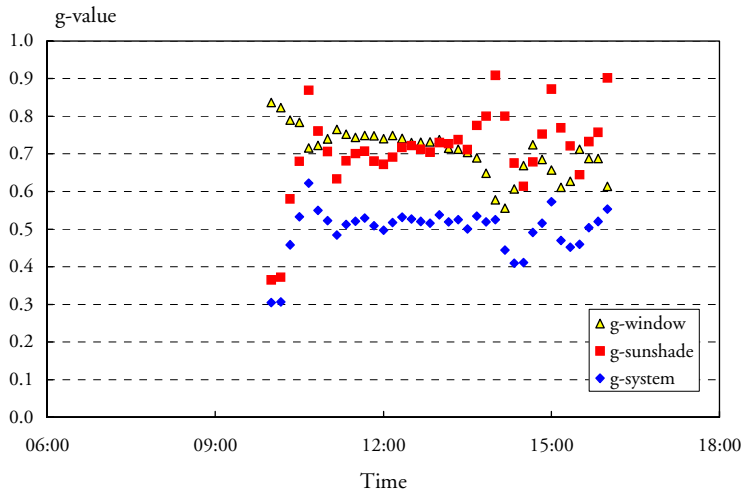

Figure 6.16.a g-values of the interpane sunshade: "Blue slat 28/22", 0° slat angle, measured in the twin boxes, 020305, 10:00-16:00.

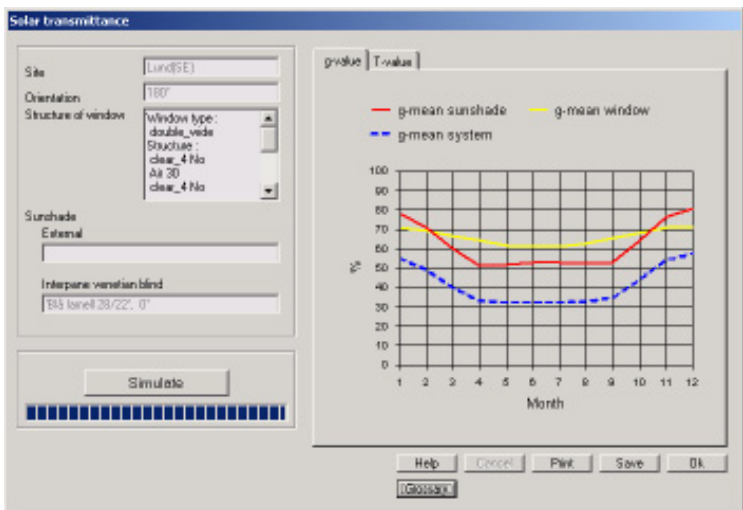

Figure 6.16.b Monthly mean g-values of the interpane sunshade "Blue slat 28/22", 0° slat angle, from ParaSol simulations.

In Figure 6.16.b, the results of the ParaSol simulations are shown. The energy weighted average values for March are: g_{system}: 39.7%, g_{window}: 66.5%, $g_{sunshade}$: 59.7%. For February they are: g_{system}: 49.0%, g_{window}: 69.3%, $g_{sunshade}$: 70.6%. Interpolation to an average for 020305 gives: g_{system}: 43.0%, g_{window}: 67.5%, $g_{sunshade}$: **63.7%**.

The outdoor measurements for 80° slat angle are around 4% higher than the simulated result and for 45° and 0° slat angle around 7% higher. As for the white venetian blind, the higher difference at the lower slat angles could partly be explained by a higher sensitivity to the vertical angle of incidence, corresponding to the solar altitude angle projected on the south-vertical plane. The outdoor measurements are performed during a sunny day, while the simulations are made for a whole month, including cloudy days. In the beginning of March, the south-vertical projected solar altitude in Lund is around 30°, which is lower than the average for a cloudy day. A lower angle corresponds to a higher $g_{sunshade}$ (and a higher g_{window}, see the results above).

The indoor measurements for "**Blue slat 28/22**" should be compared with the ParaSol calculated result at normal incidence.

The results for **80°** slat angle and interpane position were:

For normal incidence and standardized conditions, the ParaSol calculations give: g_{system}: 33.5% and g_{window}: 76.9%, which by dividing the two gives $g_{sunshade}$: **43.6%**.

In Figure 6.17, indoor measurement results of $g_{sunshade}$, using the solar simulator, are shown. At normal incidence, the measured value is **42.7%**.

The results for **45°** slat angle and interpane position were:

For normal incidence and standardized conditions, the ParaSol calculations give: g_{system}: 40.5% and g_{window}: 76.9%, which by dividing the two gives $g_{sunshade}$: **52.7%**.

In Figure 6.17, indoor measurement results of $g_{sunshade}$, using the solar simulator, are shown. At normal incidence, the measured value is **52.1%**.

The results for **0°** slat angle and interpane position were:

For normal incidence and standardized conditions, the ParaSol calculations give: $g_{system} = g_{window}$ = 76.9%, which gives $g_{sunshade}$: **100%**.

In Figure 6.17, indoor measurement results of $g_{sunshade}$, using the solar simulator, are shown. At normal incidence, the measured value is **96.1%**.

The results for **-45°** slat angle and interpane position were:

For normal incidence and standardized conditions, the ParaSol calculations give: g_{system}: 40.5% and g_{window}: 76.9%, which by dividing the two gives $g_{sunshade}$: **52.7%**.

In Figure 6.17, indoor measurement results of $g_{sunshade}$, using the solar simulator, are shown. At normal incidence, the measured value is **54.2%**.

Except for 0° slat angle the agreement between measurements and calculations at 0° angle of incidence is good, on average less than 1% difference.

To reach the theoretical $g_{sunshade}$ value 100% for 0° slat angle, perfectly parallel light and non-curved slats are required. Since none of these requirements are fulfilled, this could partly explain the 3.9 % lower measured value.

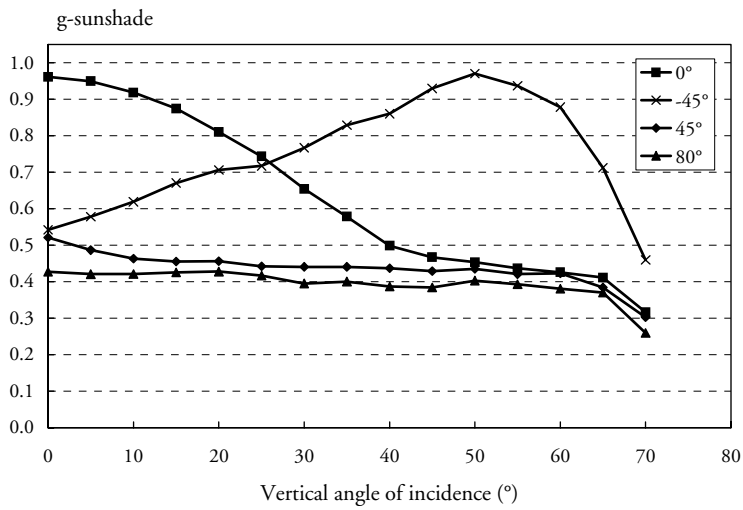

Figure 6.17 *$g_{sunshade}$ measured with the solar simulator for the interpane mounting of "Blue slat 28/22" with the slat angles 0, 45, 80 and -45°.*

6.4 Results for venetian blinds with internal mounting

The venetian blinds were also measured in the twin-boxes when mounted on the inside. The results for the "**White slat 28/22**" (R = 0.67, A = 0.33) for the slat angles 80°, 45° and 0° are shown in Figures 6.18 - 6.20.

The results for **80°** slat angle and internal position were:

In Figure 6.18.a, the outdoor measurement results are shown. The energy weighted average values for 011006, 9:00-16:00 are: g_{system}: 35.5%, g_{window}: 70.2%, $g_{sunshade}$: **50.5**%.

In Figure 6.18.b, the results of the ParaSol simulations are shown. The energy weighted average values for October are: g_{system}: 27.4%, g_{window}: 68.0%, $g_{sunshade}$: **40.3**%.

The results for 45° slat angle and internal position were:

In Figure 6.19.a, the outdoor measurement results are shown. The energy weighted average values for 010727, 8:00-16:00 are: g_{system}: 41.5%, g_{window}: 61.0%, $g_{sunshade}$: 68.1%.

In Figure 6.19.b, the results of the ParaSol simulations are shown. The energy weighted average values for July are: g_{system}: 30.6%, g_{window}: 60.8%, $g_{sunshade}$: 50.3%.

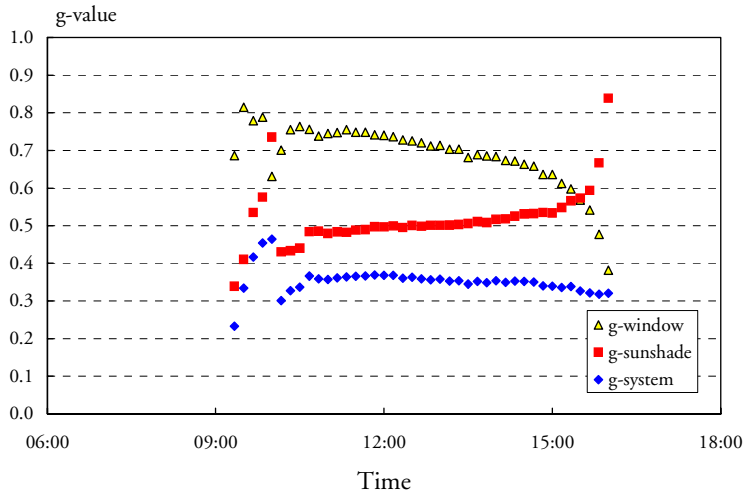

Figure 6.18.a *g-values of "White slat 28/22", internally mounted, 80° slat angle, measured in the twin boxes, 011006, 9:00-16:00.*

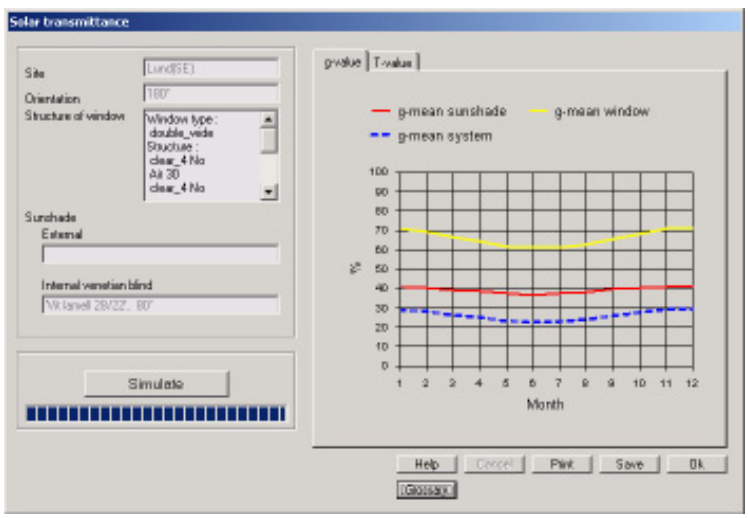

Figure 6.18.b *Monthly mean g-values of "White slat 28/22", internally mounted, 80° slat angle, from ParaSol simulations.*

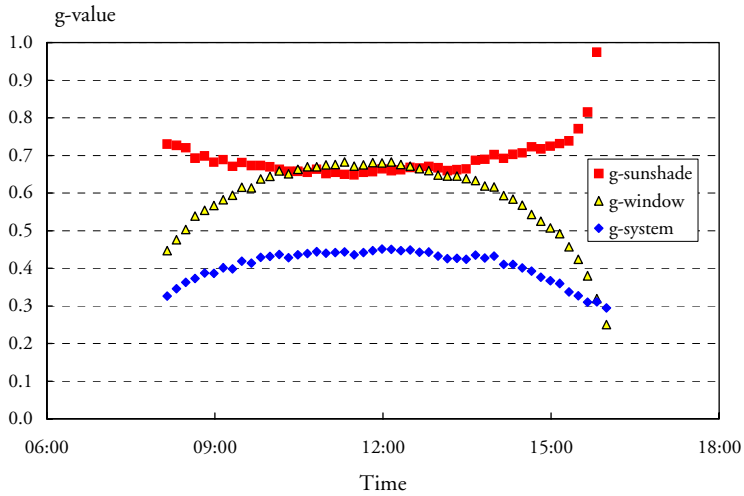

Figure 6.19.a g-values of "White slat 28/22", internally mounted, 45° slat angle, measured in the twin boxes, 010727, 8:00-16:00.

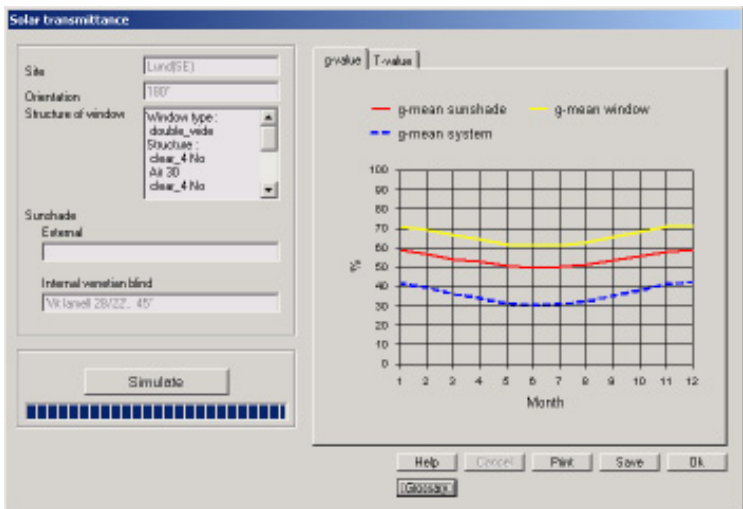

Figure 6.19.b Monthly mean g-values of "White slat 28/22", internally mounted, 45° slat angle, from ParaSol simulations.

The results for **0°** slat angle and internal position were:

In Figure 6.20.a, the outdoor measurements are shown. The energy weighted average values for the measured day 010726, 8:00-16:00 are: g_{system}: 52.1%, g_{window}: 61.8 %, $g_{sunshade}$: **84.3**%.

In Figure 6.20.b, the results of the ParaSol simulations are shown. The energy weighted average values for July are: g_{system}: 40.3%, g_{window}: 60.8%, $g_{sunshade}$: **66.2**%.

The outdoor measurements for 80° are around 10% higher than the simulated result, for 45° and 0° around 18% higher. The high differences can at least partly be explained by the fact that the simulation presumes the air to be undisturbed by external forces, while in the measurements a fan blows air along the absorber and thereby causes disturbances in the air between the absorber and the venetian blind. Since the blind is air permeable, partly also in the 80° slat angle position, the convection from the inner glass pane can also increase due to this.

It is also possible that the convective part of the venetian blind model underestimates the heat transfer to the room. More accurate measurements have to be carried out to see if this is so.

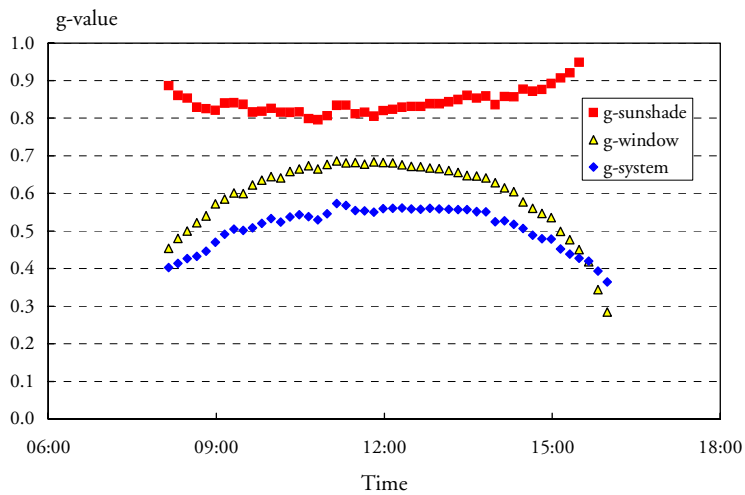

Figure 6.20.a g-values of "White slat 28/22", internally mounted, 0° slat angle, measured in the twin boxes, 010726, 8:00-16:00.

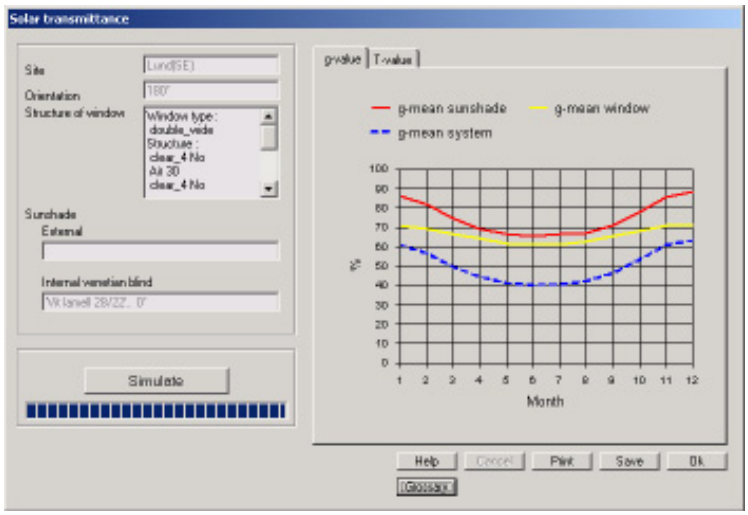

Figure 6.20.b Monthly mean g-values of "White slat 28/22", internally mounted, 0° slat angle, from ParaSol simulations.

The results for the "**Blue slat 28/22**" (R = 0.81, A = 0.19) for the slat angles 45° and 0° are shown in Figure 6.21 - 6.22.

The results for **45°** slat angle and internal position were:

In Figure 6.21.a, outdoor measurements are shown. The energy weighted average values for the measured day 990623, 8:00-16:00 are: g_{system}: 50.2%, g_{window}: 61.1%, $g_{sunshade}$: **82.2%**.

In Figure 6.21.b, the results of the ParaSol simulations are shown. The energy weighted average values for June are: g_{system}: 39.6%, g_{window}: 61.1%, $g_{sunshade}$: **64.7%**.

The results for **0°** slat angle and internal position were:

In Figure 6.22.a, outdoor measurements are shown. The energy weighted average values for the measured day 011017, 9:00-16:00 are: g_{system}: 69.8%, g_{window}: 73.1%, $g_{sunshade}$: **95.5%**.

In Figure 6.22.b, the results of the ParaSol simulations are shown. The energy weighted average values for October are: g_{system}: 56.1%, g_{window}: 68.0%, $g_{sunshade}$: **82.5%**.

Also for the blue venetian blind, the outdoor measurements are significantly higher than the simulated result, for 45° around 17.5% and for 0° around 13% higher. The comments made for the white venetian blind with internal mounting are also valid here.

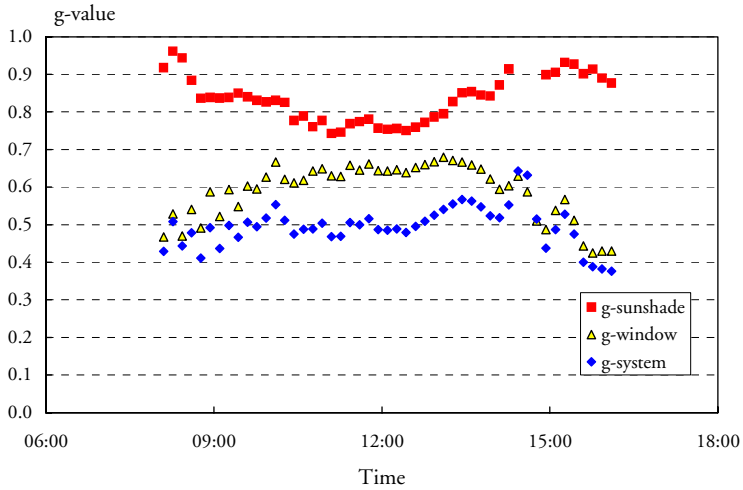

Figure 6.21.a g-values of "Blue slat 28/22", internally mounted, 45° slat angle, measured in the twin boxes, 990623, 8:00-16:00.

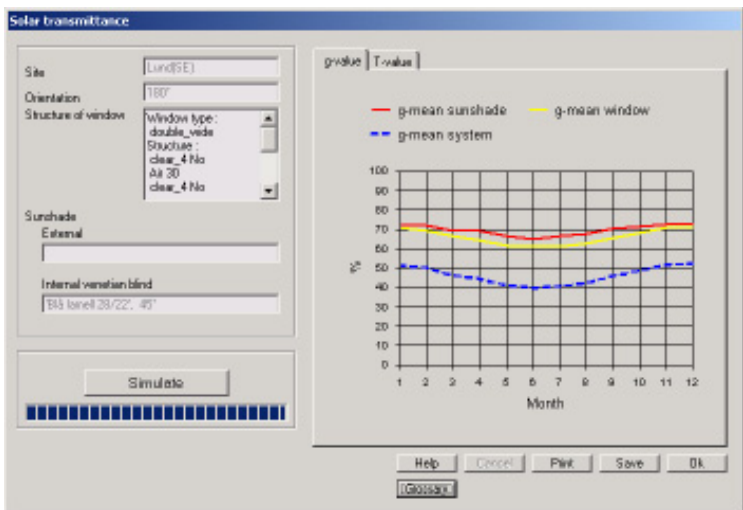

Figure 6.21.b Monthly mean g-values of "Blue slat 28/22", internally mounted, 45° slat angle, from ParaSol simulations.

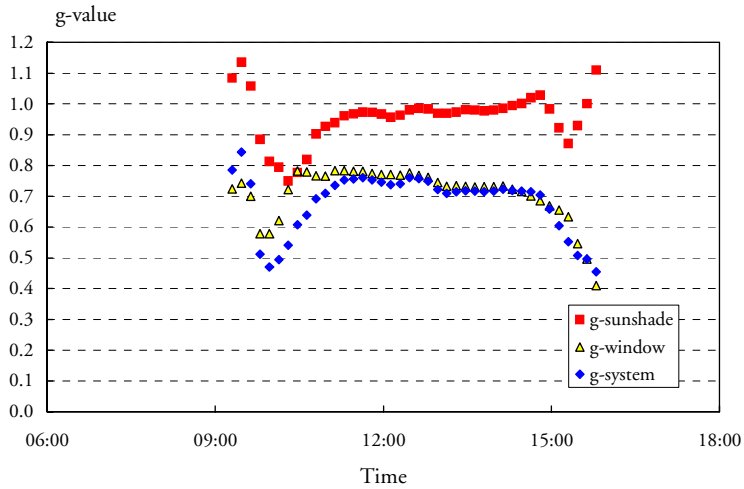

Figure 6.22.a g-values of "Blue slat 28/22", internally mounted, 0° slat angle, measured in the twin boxes, 011017, 9:00-16:00.

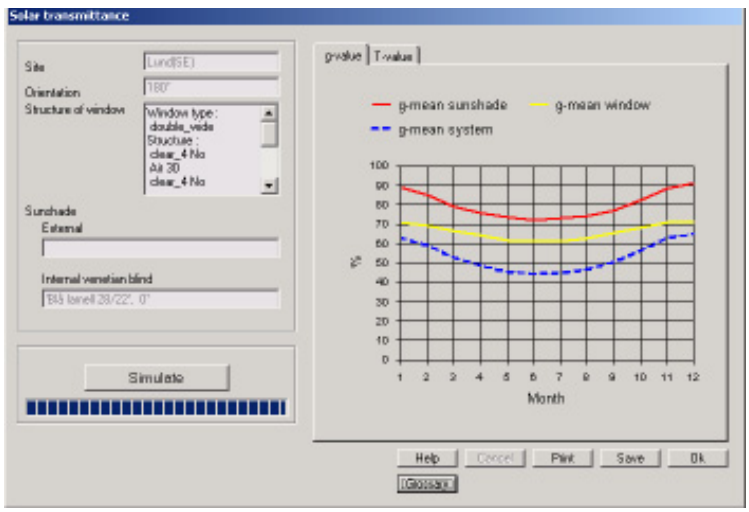

Figure 6.22.b Monthly mean g-values of "Blue slat 28/22", internally mounted, 0° slat angle, from ParaSol simulations.

6.5 Results for other products

A fabric used mainly as an external screen, "Hexcel Satine Sable" was tested also in the interpane and internal positions. The measured solar optical properties are for the front side: R_{diff} = 0.52, T_{dir} = 0.04, T_{diff} = 0.08, A = 0.36. The emittance was assumed to be 0.9.

The results for the interpane position were:

For normal incidence and standardized conditions, the ParaSol calculations give: g_{system}: 26.7% and g_{window}: 76.9%, which by dividing the two gives $g_{sunshade}$: **34.7%**.

In Figure 6.23.a, outdoor measurements are shown. The energy weighted average values for the measured day 020315, 8:00-16:00 are: g_{system}: 19.0%, g_{window}: 69.5%, $g_{sunshade}$: **27.4%**.

In Figure 6.23.b, the results of the ParaSol simulations are shown. The energy weighted average values for March are: g_{system}: 22.5%, g_{window}: 66.5%, $g_{sunshade}$: **33.9%**.

The results for the internal position were:

For normal incidence and standardized conditions, the ParaSol calculations give: g_{system}: 38.7% and g_{window}: 76.8%, which by dividing the two gives $g_{sunshade}$: **50.4%**.

In Figure 6.24.a, outdoor measurements are shown. The energy weighted average values for the measured day 020102, 9:00-15:00 are: g_{system}: 33.9%, g_{window}: 64.1%, $g_{sunshade}$: **52.8%**.

In Figure 6.24.b, the results of the ParaSol simulations are shown. The energy weighted average values for January are: g_{system}: 35.6%, g_{window}: 70.6%, $g_{sunshade}$: **50.4%**.

The results of the measurements for the interpane position are 6.5% lower than the simulated result, while for the internal position they are 2.4% higher. The last value is uncertain due to unstable measurements. One circumstance which may have contributed to the lower result for the interpane measurement is that the sunshade, for mounting reasons, was placed closer to the outer than to the inner glass pane.

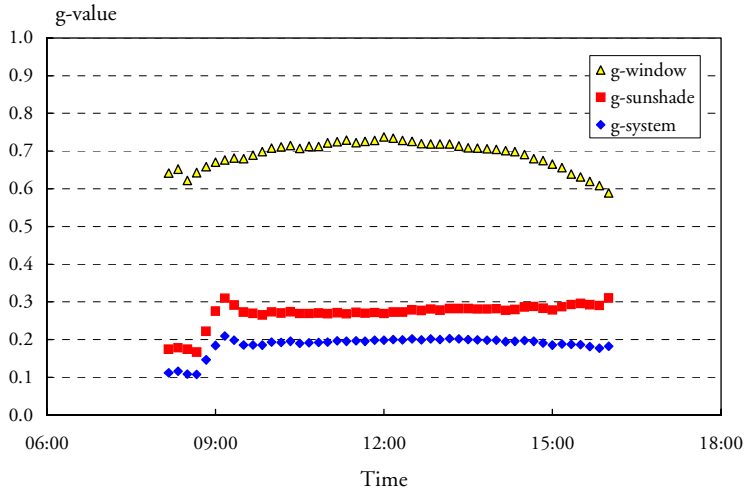

Figure 6.23.a g-values of "Hexcel Satine Sable", interpane mounted, measured in the twin boxes, 020315, 8:00-16:00.

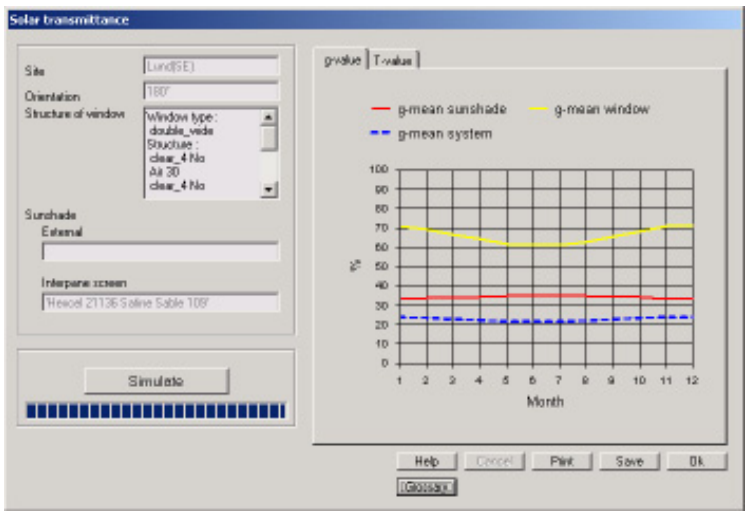

Figure 6.23.b Monthly mean g-values of "Hexcel Satine Sable", interpane mounted, from ParaSol simulations.

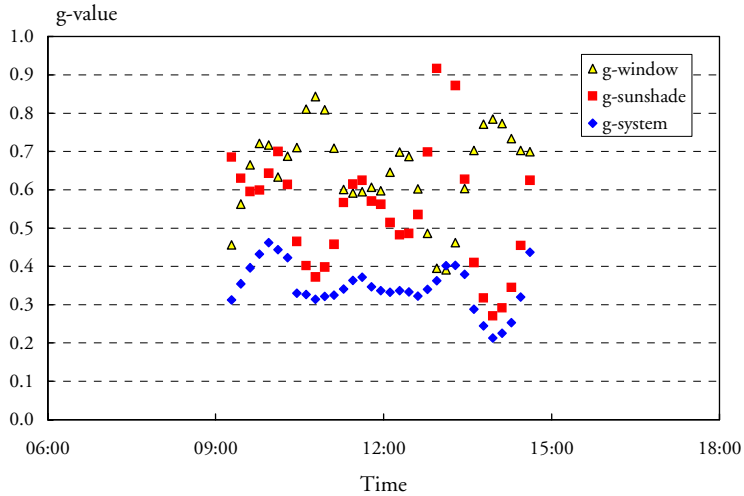

Figure 6.24.a *g-values of "Hexcel Satine Sable", internally mounted, measured in the twin boxes, 020102, 9:00-15:00.*

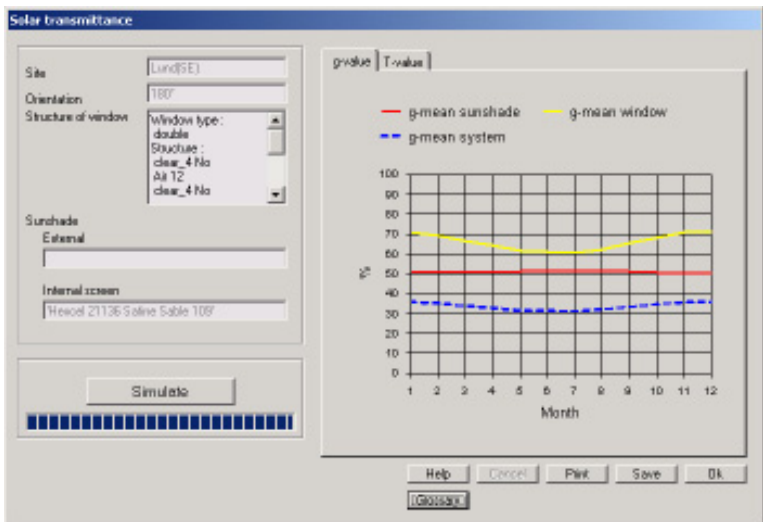

Figure 6.24.b *Monthly mean g-values of "Hexcel Satine Sable", internally mounted, from ParaSol simulations.*

Two non-attached films, mounted internally as roller blinds, were measured outdoors in the twin-boxes.

"**Sun Stop Gold**" had the measured optical properties for the front side: R_{dir} = 0.45, R_{diff} = 0.04, T_{dir} = 0.09, T_{diff} = 0.01, A = 0.41 and for the back side: R_{dir} = 0.41, R_{diff} = 0.03, T_{dir} = 0.09, T_{diff} = 0.01, A = 0.46. The emittance (not measured) was assumed to be 0.8 on both sides.

For normal incidence and standardized conditions, the ParaSol calculations give: g_{system}: 37.8% and g_{window}: 76.8%, which by dividing the two gives $g_{sunshade}$: **49.2%**.

In Figure 6.25.a, outdoor measurements are shown. The energy weighted average values for the measured day 000324, 8:00-16:00 are: g_{system}: 38.6%, g_{window}: 66.9%, $g_{sunshade}$: **57.6%**.

In Figure 6.25.b, the results of the ParaSol simulations are shown. The energy weighted average values for March are: g_{system}: 33.3%, g_{window}: 66.5%, $g_{sunshade}$: **50.1%**.

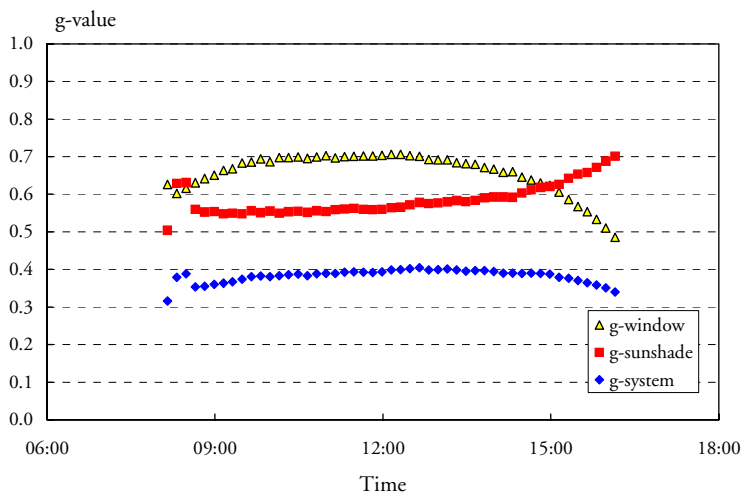

Figure 6.25.a g-values of "Sun Stop Gold", internally mounted, measured in the twin boxes, 000324, 8:00-16:00.

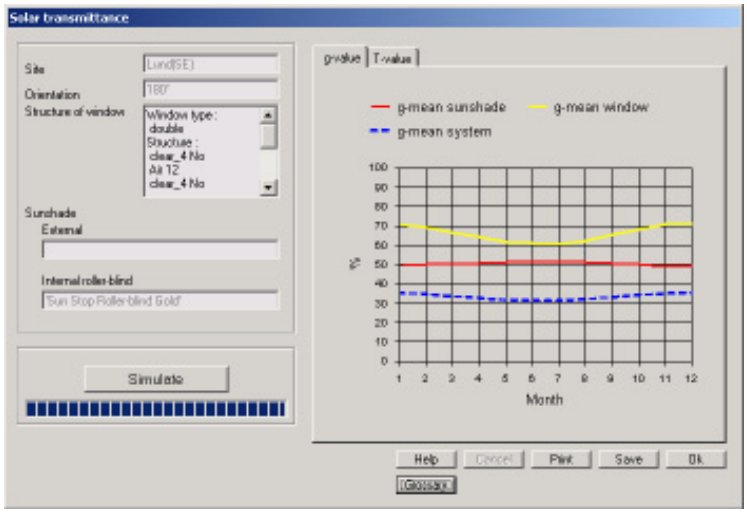

Figure 6.25.b Monthly mean g-values of "Sun Stop Gold", internally mounted, from ParaSol simulations.

"**Sun Stop Bronze**" had the measured optical properties for the front side: R_{dir} = 0.28, R_{diff} = 0.03, T_{dir} = 0.15, T_{diff} = 0.01, A = 0.53 and for the back side: R_{dir} = 0.32, R_{diff} = 0.03, T_{dir} = 0.15, T_{diff} = 0.01, A = 0.49. The emittance (not measured) was assumed to be 0.8 on both sides.

For normal incidence and standardized conditions, the ParaSol calculations give: g_{system}: 47.4% and g_{window}: 76.8%, which by dividing the two gives $g_{sunshade}$: **61.7%**.

In Figure 6.26.a, outdoor measurements are shown. The energy weighted average values for the measured day 010328, 8:00-16:00 are: g_{system}: 46.5%, g_{window}: 65.7%, $g_{sunshade}$: **70.8%**.

In Figure 6.26.b, the results of the ParaSol simulations are shown. The energy weighted average values for March are: g_{system}: 41.3%, g_{window}: 66.5%, $g_{sunshade}$: **62.3%**.

The results show that the measurements give $g_{sunshade}$ values 7.5-8.5% higher than the simulations. This agrees with what were obtained for the internally mounted fabrics and the comments made for these are valid also here.

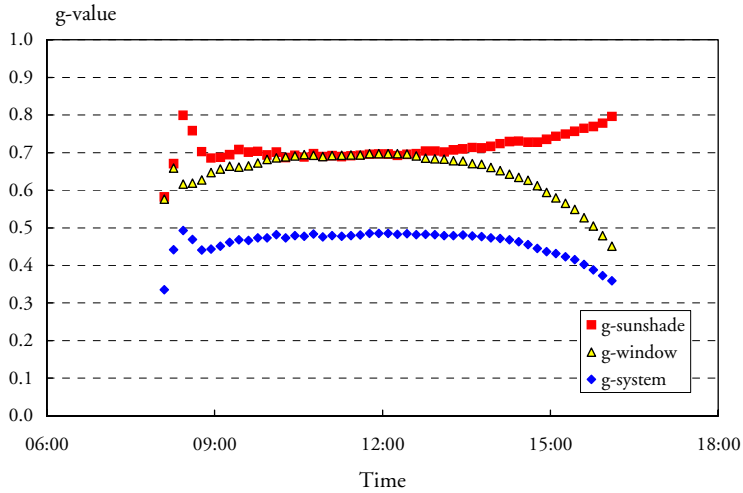

Figure 6.26.a g-values of "Sun Stop Bronze", internally mounted, measured in the twin boxes, 000328, 8:00-16:00.

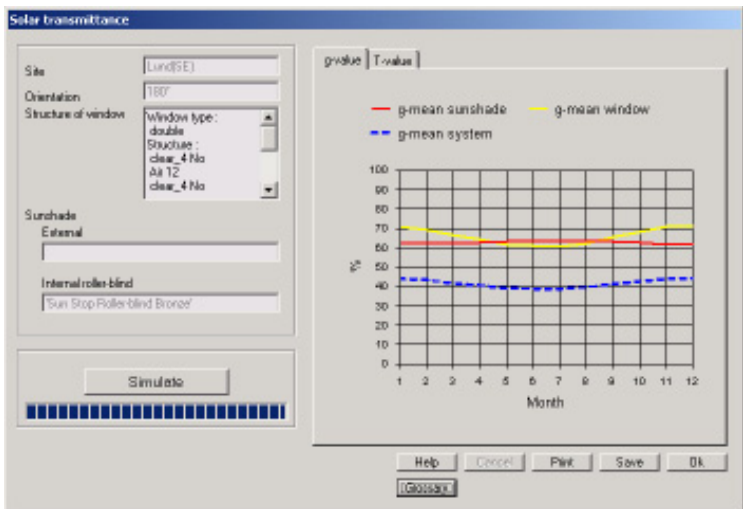

Figure 6.26.b Monthly mean g-values of "Sun Stop Bronze", internally mounted, from ParaSol simulations.

6.6 Summary and analysis of the results

The resulting $g_{sunshade}$ values from the measurements, simulations and calculations are given in Table 6.1. The difference between **outdoor** measurements and Parasol simulations are calculated in one column. The two values are not directly comparable, since the simulations are mean values for a whole month, while the outdoor measurements are mean values for a sunny day (8 hours). However, if the angle dependence of $g_{sunshade}$ is not too strong, this difference is of less importance. The results from the outdoor measurements and the ParaSol simulations for all the products are shown in Figure 6.27.a. If the two values are equal, the point is on the line $y = x$ in the diagram.

The difference between **indoor** measurements and Parasol calculations at normal incidence are calculated in another column. These two values are comparable, although the boundary conditions are not exactly the same. The results from the indoor measurements and the ParaSol calculations are compared in Figure 6.27.b.

Table 6.1 Resulting $g_{sunshade}$ values for the investigated products from outdoor / indoor measurements and ParaSol simulations / calculations. Also differences between outdoor measurements / Parasol simulations and between indoor measurements / Parasol calculations.

product	slat angle °	position	indoor g-shade %	PS calc. g-shade %	outdoor g-shade %	PS sim. g-shade %	diff. g in.-calc. %	diff. g out.-sim. %	material absorpt. %
White Texienne		interpane	18.5	17.2	14.4	16.6	1.3	-2.2	12
White Texienne		internal	26.0	29.8	30.8	29.7	-3.8	1.1	12
Ombra, white thread		internal	58.1	60.2	65.3	61.2	-2.1	4.1	11
Optic		internal	25.0	24.5	29.8	28.2	0.5	1.6	15
Blue roller blind		internal		68.4	80.9	70.8		10.1	81
White roller blind		internal		53.3	54.2	52.8		1.4	5
Silver-grey blind		internal		43.1	51.8	44.3		7.5	38
White-grey Texienne		internal		32.3	36.3	32.4		3.9	17
Ombra, black thread		internal		64.3	76.9	64.9		12.0	48
White slat 28/22	80	interpane	28.7	25.0	24.4	18.6	3.7	5.8	33
White slat 28/22	45	interpane	50.2	47.3	37.3	32.9	2.9	4.4	
White slat 28/22	0	interpane	95.5	100.0	65.6	60.9	-4.5	4.7	
White slat 28/22	-45	interpane	47.5	47.3			0.2		
Blue slat 28/22	80	interpane	42.7	43.6	42.5	38.5	-0.9	4.0	81
Blue slat 28/22	45	interpane	52.1	52.7	49.0	41.6	-0.6	7.5	
Blue slat 28/22	0	interpane	96.1	100.0	70.3	63.7	-3.9	6.6	
Blue slat 28/22	-45	interpane	54.2	52.7			1.5		
White slat 28/22	80	internal		43.4	50.5	40.3		10.2	33
White slat 28/22	45	internal		66.0	68.1	50.3		17.8	
White slat 28/22	0	internal		99.2	84.3	66.2		18.1	
Blue slat 28/22	45	internal		78.3	82.2	64.7		17.5	81
Blue slat 28/22	0	internal		99.2	95.5	82.5		13.0	
Hexcel Satine Sable		interpane		34.7	27.4	33.9		-6.5	12
Hexcel Satine Sable		internal		50.4	52.8	50.4		2.4	12
Sun Stop Gold		internal		49.2	57.6	50.1		7.5	41
Sun Stop Bronze		internal		61.7	70.8	62.3		8.5	53

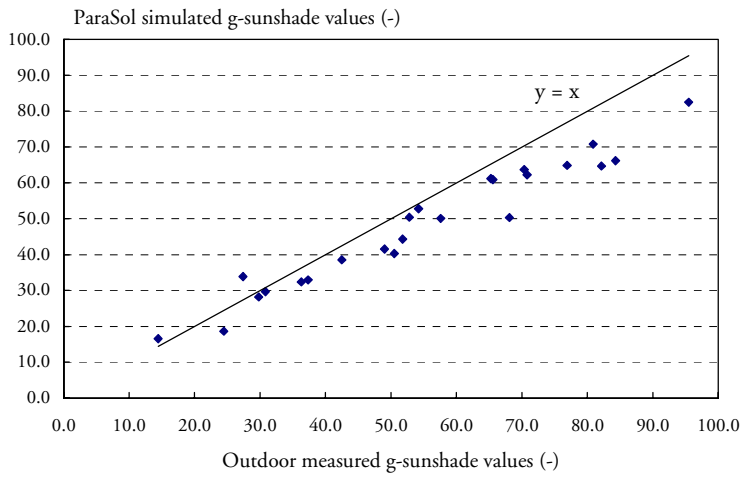

Figure 6.27.a $g_{sunshade}$ *values from ParaSol simulations vs from outdoor measurements.*

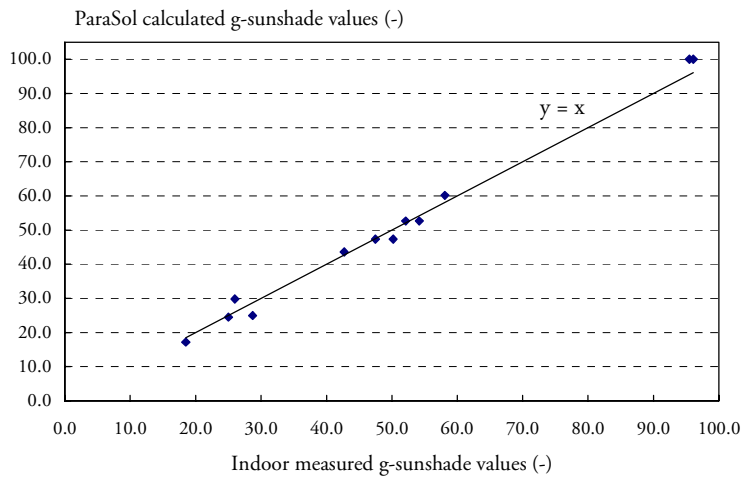

Figure 6.27.b $g_{sunshade}$ *values from ParaSol calculations vs from indoor measurements.*

The indoor measurements for normal incidence gave a $g_{sunshade}$ value 1.5% higher than the ParaSol calculated result. At higher angles of incidence the $g_{sunshade}$ value of the indoor measurements drops. For the outdoor measurements this would correspond to lower values in the morning and the late afternoon, since the angle of incidence then is larger than at noon. This is however not found, the tendency is rather the opposite. Also in the ParaSol simulation results, the mean $g_{sunshade}$ values are higher for the summer months when the average angle of incidence is higher than in the winter months.

The outdoor measurements gave an average $g_{sunshade}$ value for 990507, 8:00-16:00 which was 2.2% lower than the ParaSol simulation value for May, but the value is drifting during the day.

Neither the indoor nor the outdoor measurements are accurate enough to be used to fully validate the ParaSol results, but the comparable measurement results lie in the interval ± 3% from the ParaSol results, which at least indicates that the ParaSol results are in the right range.

6.6.1 Fabrics

Firstly, in Table 6.1 one can note that for the difference between the **outdoor** measurements and the Parasol simulations, the two negative values occur for the fabrics measured with interpane applications. For all **internal** applications, the outdoor measurements give larger $g_{sunshade}$ values than the Parasol simulations. The differences are in the range 1-12%, on average 4-5%.

However, there is a strong correlation between the difference and the absorptance of the material, as can be seen in Figure 6.27.c. For instance, for the blue roller blind with A = 0.81, the measured result is 10.1 % higher than the simulated one, while for the white roller blind with A = 0.05, the difference is 1.4%, see Table 6.1. Two of the sunshades in Figure 6.27.c have an open, air permeable structure and are therefore marked differently in the diagram. They have the same tendency as the rest but the differences between the outdoor measurements and the Parasol simulations are somewhat larger. For one product, “Hexcel Satine Sable”, the difference is somewhat lower (2.4% for A = 0.36) than for products with comparable absorptance, see Table 6.1.

A theoretical explanation for this correlation is that if the convective heat transfer coefficient on the inside is larger than expected, a larger proportion of the heat from the solar radiation absorbed by the sunshade will be transferred to the room and thereby increase the g-value. Also if the air gap between the sunshade and the inner pane is not fully closed,

air change between the gap and the inside could increase the *g*-value. Both these explanations could have contributed to the larger $g_{sunshade}$ values for the outdoor measurements.

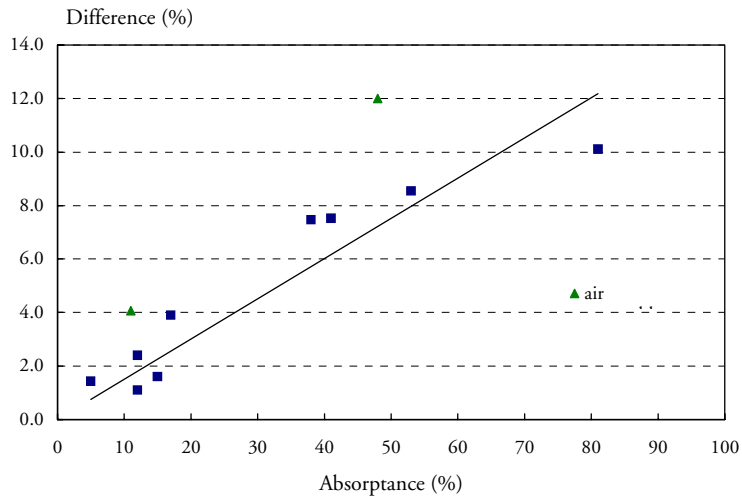

Figure 6.27.c Difference between outdoor measured and ParaSol simulated $g_{sunshade}$ vs the material absorptance for internally mounted fabrics + a linear fit.

Two of the products, "Optic" and "White Texienne" were measured several times. For "White Texienne" the results were about the same as given in Table 6.1, with $g_{sunshade}$ values around 30%. For "Optic", the other measurements gave larger $g_{sunshade}$ values, 30-40%, depending strongly on the season when the measurement was made . It seems that the high specular reflectance of this product (compared with others with mostly diffuse reflectance) makes it more sensitive to the angle of incidence and therefore to the season. During summer with direct insolation of high average angle of incidence, the $g_{sunshade}$ values were larger than in spring and autumn. This could possibly be an edge effect.

Only two fabrics were measured outdoors with **interpane** mounting, "White Texienne" with the difference value –2.2% and "Hexcel Satine Sable" with –6.5%. One possible contributing reason for the low values is that the products, for mounting reasons, were placed closer to the outer than to the inner pane. The reason for the very low value for "Hexcel Satine Sable" is unknown, but the difference for the internal mounting of this product is also comparatively low.

Three fabrics were measured **indoors**: "Optic", "Ombra" and "White Texienne". With **internal** application they were all measured several times. The results for a product given in Table 6.1 are from only one measurement. For "Optic" the difference between the measurements and the ParaSol calculations varied between –1.5% and +4.5%. For "White Texienne" the difference varied between –6% and 0%. For "Ombra", which is an air permeable fabric, the difference varied between –2% and +6%. The variations in the results were partly due to different attempts to make the sunshade layer airtight and to make the edges specularly reflecting to minimize edge effects, but also due to unsatisfactory repeatability of the measurement results.

The dependence of "Optic" on differences in angle of incidence, noticed for the outdoor measurements, could also be noticed for the indoor measurements. The product was the only fabric which showed increasing $g_{sunshade}$ values with increasing angle of incidence. The other fabrics had more or less decreasing values at large angles of incidence in the indoor measurements. This tendency for the other fabrics could however not be seen in the outdoor measurements, nor in the ParaSol simulations where the angle dependence was negligible or slightly reversed.

Only one of the products, "White Texienne", was measured indoors with **interpane** mounting. The difference between measurements and calculations was then +1.3%. This means that the difference was positive for the interpane application and negative for the internal application. For the outdoor measurements, these relations were reversed.

6.6.2 Slats

The difference between the **outdoor** measurements and the Parasol simulations for slats are for the **interpane** application between 4-7.5%. For the **internal** application, the differences are in the range 10-18%, on average 15-16%. A possible explanation for at least part of these differences is that the inside convective heat transfer coefficient is larger than what the correlation used in ParaSol gives, due to the fact that a fan blows the air along the absorber in the twin boxes. This would mostly affect the internal blinds, especially since the blinds are air permeable.

The difference between the **indoor** measurements and the Parasol calculations at normal incidence for the slats (only **interpane** mounted measured) is for **0°** slat angle around –4%. One explanation for this is that in ParaSol the calculations are made for perfectly parallel light and non-curved, infinitely thin slats. A lower measured $g_{sunshade}$ can therefore

be expected. For the other slat angles (**–45°**, **+45°**, **80°**), the difference for the **blue** slat is within ± 1.5%, on average 0%. For the **white** slat the difference is 0-4%, on average 2%.

6.7 Conclusions

The products that were measured indoors (three fabrics and two interpane venetian blinds with different slat angles) showed reasonable agreement with the ParaSol calculations at normal incidence. The differences were in general within ± 4 %. The repeatability of the solar simulator measurements was however not good enough to validate the ParaSol results in detail.

The agreement between the outdoor measurements and the Parasol simulations was not equally good. The measured results for all the products, except the internally mounted venetian blinds, gave $g_{sunshade}$ values 1-12% (on average 4-5%) larger than the ParaSol simulated values. The differences for the internally mounted fabrics were seen to have a strong correlation with the absorptance of the fabric material. A theoretical explanation for this is that the convective heat transfer coefficient on the inside is large due to fan induced air movement.

For the internally mounted venetian blinds, the resulting outdoor measured $g_{sunshade}$ values are 10-18% (on average 15-16%) larger than the ParaSol simulated values. The reason for this could be the same as suggested for the fabrics, namely a high convective heat transfer coefficient on the inside. This effect would be enhanced for an air permeable structure like the venetian blinds.

The results indicate that the optical calculations of ParaSol are correctly performed, except that the dependence of the optical properties of the products on angle of incidence is disregarded. The $g_{sunshade}$ values are however also dependent on the magnitude of the heat transfer coefficients between the sunshade, the window panes and the inside and outside surroundings, since they determine how much of the energy absorbed by the glass panes and the sunshade will be transferred to the room. The magnitude of the heat transfer coefficients is therefore important both for the measurements and for the ParaSol calculations/ simulations.

In ParaSol v2.0, all interpane or internal sunshades are assumed to be mounted with closed air gaps to the adjacent glass pane(s). Especially for internal sunshades, the combination of open air gaps and high absorptance would give larger $g_{sunshade}$ values.

The outdoor measurements of internal sunshades gave values larger than the simulated ones. This is assumed to be at least partly caused by a large inside convective heat transfer coefficient. However, one should not take for granted that the convective heat transfer coefficients used in the program are the true ones.

6.8 Future developments

The disagreements between the measurements and the Parasol simulations/ calculations should be further investigated, especially concerning the effect of different heat transfer coefficients.

The solar simulator needs to be further developed to give better repeatability of the results and thereafter calibrated in order to compare and validate the ParaSol results in detail. In IEA, Task 27, work has started to compare measurements from different laboratories and to develop an international standard for measurements using solar simulators. It would be of great importance to participate in such international cooperation.

The outdoor measurements also need to be further developed in order to give results which can be used to more accurately compare and validate the ParaSol results. The influence of the fan on the inside convective heat transfer coefficient needs to be further investigated. The influence of the different external conditions, like the solar altitude, outdoor temperature and the wind speed, also needs to be investigated.

6.9 Symbols

R = reflectance
R_{diff} = diffuse reflectance
R_{spec} = specular reflectance
T = transmittance
T_{diff} = diffuse transmittance
T_{dir} = direct transmittance
A = absorptance
E = emittance
g_{system} = total solar transmittance for the window - sunshade system
g_{window} = total solar transmittance for the window
$g_{sunshade}$ = g_{system} divided by g_{window}

7 Discussion and Conclusions

The project comprises both theoretical and applied work. The main parts consist of

- outdoor measurements of solar transmittance,
- development of the solar simulator,
- measurements of solar transmittance in the solar simulator,
- development of calculation models,
- development of a user-friendly software tool, ParaSol and
- studies of the effect on daylight quality.

The daylight studies are reported earlier and will therefore not be discussed here.

7.1 Outdoor measurements

The outdoor measurements using a double hot-box arrangement continued during this second part of the project. In addition to the earlier measured external products, now products between panes and internal products were also studied. The total solar energy transmittance (g-value) was measured. As expected, external shading devices are in general more efficient in reducing solar gains than interpane and internal devices. Internal devices are least efficient, although the variation within each group is large.

The performance varies depending on position in relation to the window, reflectance of shading material, colour, slat angle position, geometry etc. For internal products it is essential that they reflect the short wave solar radiation, since the heat absorbed in the sunshade contributes

to room overheating. However, for external shading devices, dark products (with low reflectance and high absorptance) provide lower g-values than light ones.

The average g-value for each group of measured shading devices was 0.3 for external products, 0.5 for interpane products and 0.6 for internal products. Thus, on average, external products are twice as good as internal products in reducing peak cooling loads. However, note that other aspects, such as daylight, also are very important. Some products yielding low g-values admit almost no daylight into the room, and totally obstruct the view out, two of the main reasons for having a window.

7.2 Solar laboratory

A solar simulator has been constructed so that solar transmission for sunshades, windows and solar heating components may be measured in a more standardized and consistent manner. It is a special feature of this solar simulator that the beam of light is as parallel as possible. One of the reasons for this is to make it feasible for measurements to be made on sunshades with marked angular dependent characteristics like awnings and venetian blinds.

One of the obvious advantages of a solar simulator with a movable light source is that it can produce the desired solar altitudes on a window kept in the normal vertical position and at any time of the year. This is especially valuable for angle dependent sunshades e.g. venetian blinds. For such a sunshade a complete set of tests for different angles can be performed on one occasion. For those distinctly angle dependent measurements a parallel light source is vital. This solar simulator has very good qualities in this respect.

Another valuable advantage of a solar simulator is that the convective conditions for the exterior can be repeatedly produced and also altered. This is especially important for several types of exterior sunshades that for instance are dark and absorbing and have a tendency to build up a hot air pocket.

Extensive developments have been carried out regarding the measuring method. No standardized method exists yet and therefore tests and comparisons with outdoor measurements and theoretical models have been made.

Results show that the reflector arrangement used for the lamps gives good divergence quality with very little stray light. The distribution over the area of the object of measurement is however rather uneven. A modification to improve the light distribution is suggested with probably only

a moderate degradation of the divergence. Also for the calorimeter plate improvements are recommended. It is suggested that the front sheet should be made of metal to improve heat transfer to the water. The current calorimeter plate is made of glass for its non-corrosive and stability properties.

Measurements in the solar simulator were carried out on awnings, Italian awnings and exterior screens. Different fabrics and positions of the shadings were tested. Venetian blinds, pleated curtains and one flat curtain have been tested in the interpane position. Variations included different colours and slat angles. A few measurements were also made on internal sunshades.

Measurements of internal products have been limited to sunshades with flat inner surface. The radiative and convective heat transfers between the sunshade and the room have been simulated by using an air gap. Measurements on other internal sunshades, and especially for the situation with natural convection that occurs when the volume between the inner pane and the sunshade is not closed, are more complex. In that case the calorimeter box should be designed with a substantial volume behind the window to reasonably reproduce the conditions for the natural convection of a whole room.

7.3 Calculation models

Calculation models for interpane and internal shading devices have been developed and implemented into the program ParaSol. Screens, roller blinds and venetian blinds are examples of interpane and internal shadings. Calculation models for external devices were developed during the first part of the project and reported earlier.

New developments include the treatment of long wave transparent layers (shading devices) in combination with long wave opaque glass panes. Short wave transmittance, reflectance and absorptance as well as long wave radiation exchange are calculated in detail. Direct and diffuse transmittance and direct (specular) and diffuse reflection and absorption are treated.

Plane solar shading devices are defined as plane layers, parallel with the glass panes. Although some plane shadings are air permeable, all internal and interpane plane sunshades are calculated as non-permeable. All air gaps/layers are also treated as closed (non-vented). Especially for internal sunshades, which are often mounted with an air gap, this is an important limitation. In reality, an open air gap will cause a larger heat

transfer to the room by air movements. The calculation results will therefore show the lower limit of the g-value, such as a theoretical optimal performance.

The venetian blind slats are also simplified as plane, although in reality they are usually slightly curved. An improvement of the model could be to also consider the curvature of the slats. This work has been partly carried out, but has not yet been implemented in the model. The results should also be compared with measurements to show that this really improves the model, before it is implemented.

International standards for calculating venetian blinds are being developed but are not yet approved. However, it seems from the drafts that these models will consider only diffusely reflected and transmitted radiation.

7.4 ParaSol

A design tool with the name ParaSol v2.0 has been completed during this phase of the project. The main purpose of the design tool is to be a simple but still accurate design aid for architects, building services consultants and other engineers. It can be used to study the solar protection potential of different types of sunshades and also their influence on the building energy performance at an early design phase.

Apart from annual cooling and heating loads for a room with or without sunshades, the ParaSol program also gives monthly average values of direct and total transmittance for the window, the sunshade(s) and the system. It is possible to have two sunshades if one internal or interpane sunshade is combined with one external shade. Thermal comfort can also be studied.

A new feature is introduced in ParaSol, where U, T and g-values are calculated under standardized conditions and normal incidence of the solar radiation for a window or for a system of a window and an internal/interpane sunshade. However, external sunshades are not yet part of this calculation.

Different strategies for controlling sunshades as well as an air conditioning unit to heat or cool the inlet air have also been added to this version of ParaSol.

Future work regarding ParaSol could include a number of improvements, depending on funding possibilities. Some examples are:

- Additional strategies for controlling sunshades should be added

- A new structure and interface for the window, glass, and gas libraries is desirable
- A function to change the boundary conditions for the calculations. The current calculations are based on a draft international standard (ISO/DIS 15099) and will be upgraded as soon as a final standard is available
- A more detailed description of the available types of wall and frame constructions is desired
- Simulation models for sunshades in ventilated cavities need to be developed
- A more homogeneous documentation of input data and results for a simulation is needed, to save or print out as a product information sheet
- Functions for comparisons between different simulations need to be implemented
- Presentation of statistics for the energy demand of the air conditioning unit could be added
- It should be possible to combine external, interpane and internal sunshades in one system

7.5 Comparison of ParaSol results with measurements

The products measured in the solar simulator showed reasonable agreement with the ParaSol calculations at normal incidence. The differences were in general within ± 4%.

Nevertheless, the solar simulator needs to be further developed to give better repeatability of the results and thereafter calibrated in order to compare and validate the calculation results and models in detail. In IEA, Task 27, work has started to compare measurements from different laboratories and to develop an international standard for measurements using solar simulators. It would be of great importance to participate in such international cooperation.

The agreement between the outdoor measurements and the Parasol simulations was not equally good. The measured results for all the products, except the internally mounted venetian blinds, gave $g_{sunshade}$ values on average 4-5% larger than the ParaSol simulated ones. The differences for the internally mounted fabrics were found to have a strong correla-

tion with the absorptance of the fabric material. An explanation is that the convective heat transfer coefficient on the inside is large due to fan induced air movement. However, it should not be taken for granted that the convective heat transfer coefficients used in the program are the true ones.

For the internally mounted venetian blinds, the resulting outdoor measured $g_{sunshade}$ values are 10-18 % (on average 15-16%) larger than the ParaSol simulated ones. The reason for this could be the same as suggested for the fabrics, namely a high convective heat transfer coefficient on the inside. This effect could be mainly due to the air permeable structure of the venetian blinds.

The results show that the optical calculations of ParaSol are correctly performed, except that the dependence of the optical properties of the products on the angle of incidence is disregarded. The $g_{sunshade}$ values are however also dependent on the heat transfer coefficients between the sunshade, the window panes and the inside and outside surroundings, since it is these that determine how much of the energy absorbed by the glass panes and the sunshade that will be transferred to the room. The heat transfer coefficients are therefore important both for the measurements and for the ParaSol calculations/simulations.

In ParaSol, all interpane or internal sunshades are assumed to be mounted with closed air gaps to the adjacent glass pane(s). Especially for internal sunshades, the combination of open air gaps and high absorptance would give larger $g_{sunshade}$ values.

The disagreements between outdoor and indoor measurements and the Parasol calculations should be further investigated, especially concerning the effect of heat transfer coefficients.

7.6 Further studies

Further studies would include standardization work regarding measurement methods and analyses. Models for internal shading devices mounted with a ventilated air gap should be developed. In addition, it would be very advantageous to develop more sophisticated models for control of sunshades and to implement these into ParaSol.

Studies on *how* to control shading devices are also important. Apart from enabling the users to manually adjust the shading devices, different types of automatic control would be useful in order to ensure a good indoor climate and low energy use. However, there are many important aspects to be considered regarding control of the shading devices, such as

air temperature, operative temperature, daylight level and glare. Further research is needed to find the most important parameters that could be used to automatically control shading devices.

Further developments regarding ParaSol would also be to include a simple daylight-linked control of shading devices and to include a daylight module so that both daylight and thermal comfort may be studied for different combinations of shading devices and windows.

8 Summary

Commercial buildings with large glazed surfaces may easily suffer from overheating problems or large peak cooling loads. Solar shading devices can significantly reduce these cooling loads, improve thermal comfort and also reduce potential glare problems. Also in moderately glazed buildings, shading devices may to a great extent improve conditions. Due to lack of relevant data as to how well sunshades protect buildings against unwanted insolation, the Solar Shading Project at Lund University was initiated in 1997.

Phase 1 of the project focused on exterior shading devices, and was completed in 1999. Now phase 2 is completed and includes both interpane and interior devices. This report constitutes the final report on the whole project.

The work consists of a number of "work packages" which are: measurements of the performance of sunshades; development of calculation models; development of a user-friendly software tool, ParaSol; parametric studies of energy use in offices; and studies of the effect on daylight quality. The daylight studies were reported earlier.

The developed calculation models include both interpane and internal shading devices. Screens, roller blinds and venetian blinds are examples of such devices. Calculation models for external shading devices were developed during the first phase of the project.

One goal of the project was to measure the solar transmission properties of a large selection of solar shadings available on today's market, in order to provide comparable g-values measured under similar conditions. The project has specifically targeted common types of shading devices which are applicable both in new construction and in refurbishing. The products have been divided into three groups: external shading devices, devices between panes (interpane products), and internal shading devices.

Measurements on external shading devices included awning, Italian awning, venetian blind, screen, solar control film (on glass) and horizontal slatted baffle. Interpane products included venetian blind, pleated

curtain and roller blind. Internal shading devices included venetian blind, pleated curtain, roller blind (fabric and film) and solar control film (on glass).

Results from the outdoor measurements in Lund showed on average 4-5% higher total energy transmittance (g-value) than results from the developed calculation models. However, for internally mounted venetian blinds, the outdoor measurements were on average 15-16% higher than simulated values. This is assumed to be due at least partly to the air permeable structure of venetian blinds and to forced convection induced with a fan. However, further developments and validations need to be carried out especially regarding convective heat transfer, which could have a large influence on both measurements and calculation results for internal shading devices.

The average g-value for each group of shading devices measured outdoors was 0.3 for external products, 0.5 for interpane products and 0.6 for internal products. Thus, on average, external products are twice as good as internal products in reducing peak cooling loads. However, note that other aspects, such as daylight, are also very important. Some products yielding low g-values admit almost no daylight into the room, and totally obstruct the view out, two of the main reasons for having a window.

A solar simulator for measurements under standard conditions has also been developed. This enables work to be performed during both day and night, and the facility to study conditions different from those at the latitude of Lund, such as angles of incidence, is especially important. For sunshades such as venetian blinds, a complete set of tests for different angles can be performed on one occasion. For those distinctly angle dependent measurements a parallel light source is vital. The solar simulator has very high qualities in this respect.

Another valuable advantage of a solar simulator is that the convective conditions for the exterior can be repeatedly produced and also altered. This is especially important for several types of exterior sunshades that for instance are dark and absorbing and have a tendency to build up a hot air pocket.

Measurements in the solar simulator have been carried out for external, interpane and interior shading devices. In addition, extensive developments have been carried out in order to achieve a reliable measuring method. The products measured in the solar laboratory showed reasonable agreement with the developed calculation models. The differences were in general within ± 4%.

In order to disseminate the knowledge gained to a broader audience, e.g. architects, HVAC-engineers and the solar shading industry, the computer tool ParaSol has been developed. With this tool it is possible to determine the solar transmittance properties of arbitrary combinations of glazing systems and shading devices. It also enables the user to simulate peak heating and cooling loads and annual heating and cooling demands for an office module with one wall and one window facing the external climate. Thermal comfort can also be studied. The program can handle exterior shading devices in combination with internal or interpane sunshades. Different strategies for controlling sunshades as well as an air conditioning unit to heat or cool the inlet air have also been added to this version of ParaSol.

Guidelines in Swedish will be developed as a separate project during 2003, in collaboration with architects and consultants.

References

Bülow-Hübe, H. (2001). Energy-Efficient Window Systems. *Effects on Energy Use and Daylight in Buildings.* Report TABK--01/1022. PhD-thesis. Lund, Sweden: Dept. of Construction & Architecture. Lund University, Lund Institute of Technology.

Bülow-Hübe, H., & Lundh, U. (2002). Outdoor measurements of g-values for external, interpane and internal sunshades. *Proc. of EPIC 2002 AIVC*, Energy Efficient and Healthy Buildings in Sustainable Cities, Lyon 23-26 Oct 2002, Vol. III, pp. 795-800. ISBN: 2-86834-118-7.

Dubois, M-C. (2001a). *Solar Shading for Low Energy Use and Daylight Quality in Offices. Simulations, Measurements and Design Tools*. Report TABK--01/1023 PhD-thesis. Lund, Sweden: Dept. of Construction & Architecture. Lund University, Lund Institute of Technology.

Dubois, M-C. (2001b). *Impact of Solar Shading Devices on Daylight Quality: Measurements in Experimental Office Rooms.* Report TABK--01/3061. Lund, Sweden: Dept. of Construction & Architecture. Lund University, Lund Institute of Technology.

Dubois, M-C. (2001c). *Impact of Shading Devices on Daylight Quality in Offices. Simulations with Radiance*. Report TABK--01/3062. Lund, Sweden: Dept. of Construction & Architecture. Lund University, Lund Institute of Technology.

ElSherbiny, S. M., Raithby, G. D. and Hollands, K. G. T. Heat transfer by natural convection across vertical and inclined air layers. *J. Heat Transfer*, *Trans*. *ASME*, Vol. 104, p. 96-102, 1982.

ISO, *Draft International Standard ISO/DIS 15099*, 2000.

Min, T. C. et al. Natural convection and radiation in a panel heated room. *Trans*. *ASHRAE*, Vol. 62, p. 337-358, 1956.

Rosenfeld, J. L. J., Platzer, W. J., van Dijk, H. and Maccari, A. Modelling the optical and thermal properties of advanced glazing. Overview of recent developments. *Proc. Eurosun 2000*, Copenhagen, Denmark, 2000.

Siegel, R. and Howell J. R. *Thermal Radiation Heat Transfer*, Taylor and Francis, London/New York, 4:th edition, 2002.

Wall, M., & Bülow-Hübe, H. (2001). *Solar Protection in Buildings*. (Report TABK--01/3060). Lund, Sweden: Energy and Building Design, Lund University, Lund Institute of Technology.

Additional Project Publications, 2000 - 2002

Dubois M-C. (2003). Shading Devices and Daylight Quality: An Assessment Using Simple Performance Indicators. Accepted for publication in *Lighting Research and Technology*, Vol. 35(1), 2003.

Bülow-Hübe H. (2000). Office Worker Preferences of Exterior Shading Devices: A Pilot Study. Proc. of the *EuroSun 2000 Conference*, June 19-22 June, Copenhagen (Denmark).

Dubois M.-C. (2000). A Complementary Chart to Mazria's Sunpath Diagram to Design Shading Devices Considering the Window Angular Properties. Proc. of the *ISREE (International Symposium on Renewable Energy Education) Conference 2000*, 14-17 June, Oslo.

Dubois M.-C. (2000). A Simple Chart to Design Shading Devices Considering the Window Solar Angle Dependent Properties. Proc. of the *Eurosun 2000 Conference*, 18-22 June, Copenhagen.

Dubois M.-C. (2000). A Method to Define Shading Devices Considering the Ideal Total Solar Energy Transmittance. Proc. of the *Eurosun Conference 2000*, 18-22 June, Copenhagen.

Wallentén P., Kvist, H. & Dubois M.-C. (2000). ParaSol-LTH: A Userfriendly Computer Tool to Predict the Energy Performance of Shading Devices. Proc. of *the International Building Physics Conference*, September, Eindhoven (Holland).

Research project home page

http://www.byggark.lth.se/shade/shade_home.htm

LUND INSTITUTE OF TECHNOLOGY
Lund University

ISSN 1651-8128
ISBN 91-85147-00-1